12-17-2004

Biomimetics and Host-Guest Chemistry

Jiachang Gong
University of New Orleans

BIOMIMETICS AND HOST-GUEST CHEMISTRY

A Dissertation

Submitted to the Graduate Faculty of the
University of New Orleans
in partial fulfillment of the
requirement for the degree of

Doctor of Philosophy
in
The Department of Chemistry

by

Jiachang Gong

B.S., Ningbo University, 1993
M.S., Chinese Academy of Sciences, 1996

December 2004

ACKNOWLEDGEMENTS

I would like to express my greatest gratitude to my advisor, Professor Bruce C. Gibb, for his patient guidance, support and encouragement throughout the course of this work. My gratitude also goes to the members of my research advisory committee, Professor Mark L. Trudell, Professor Steven P. Nolan, Professor Paul Hanson and Professor Branko S. Jursic. They have given me helpful discussions and fresh ideas.

I would like to acknowledge all the past and present members in our group, especially to Corrine Gibb, who has generously assisted me in the physical studies and analytical instruments. This work would have been impossible for me to finish without their contributions. I also want to thank Professor John B. Wiley for his help on my presentation preparation, Professor Richard B. Cole and Dr. Chau-weu Chou for mass spectroscopy analysis, and Professor Matthew A. Tarr for ICP analysis.

Great appreciation also goes to my dear wife, Li Chen, for her love, patience and understanding, and to my beloved daughters, Katherine Gong and Melinda Gong.

TABLE OF CONTENTS

LIST OF TABLES vi

LIST OF FIGURES vii

LIST OF SCHEMES xiii

ABBREVIATIONS xiv

ABSTRACT xv

I. Introduction 1

1.1 Supramolecular Chemistry 1

1.2 Molecular Recognition and Host-Guest Chemistry 2

1.3 Zinc Enzymes 3

1.4 Carbonic Anhydrase 5

1.5 Carbonic Anhydrase Mimics 7

1.6 Cation Binding Receptors 15

1.6.1 Crown Ethers 15

1.6.2 Cryptands 19

1.6.3 Calixarences 21

1.7 Anion Receptors 24

1.7.1 Positively Charged Anion Receptors 24

1.7.2 Neutral Amide Based Receptors 26

1.7.3 Neutral Pyrrole Based Receptors 29

1.7.4 Urea Based Receptors 31

1.8 Dipotic Receptors 33

1.8.1 Simultaneous Complexation of Inorganic Ion Pairs 33

1.8.2 Simultaneous Complexation of Organic Pairs 38

1.8.2.1 Carboxylate Salts and Zwitterionic Amino Acids 38

1.8.2.2 Tetraalkylammonium Salts 40

1.9 Enantioselective Receptors 42

1.9.1 Through Ammonium Cation Binding 43

1.9.2 Through Carboxylate Binding 46

1.9.3 Recognition of Zwitterionic Amino Acids 49

II. Toward the Mimicry of Carbonic Anhydrase 52

2.1 Synthesis and Binding Studies of First Generation Ligands 55

2.2 Synthesis and Binding Studies of Second Generation Ligands 60

2.3 Synthesis and Binding Studies of Third Generation Ligands 63

2.4 Kinetics Studies: Towards the Hydrolysis of *p*-nitrophenyl Acetate and Phosphate Esters 68

III. Investigation of the Ditopic Properties of Novel Tris(pyridyl)macrocycles 70

3.1 Synthesis of Macrocycle **105** 74

3.2 Optimized Synthesis of Diacid **112** 79

3.3 Anion Binding Studies 81

3.4 Primary Ammonium Salt Binding Studies 85

IV. Enantioselective Recognition of Amino Acid Derivatives by chiral ditopic macrocycles 89

4.1 Macrocycle Synthesis 91

4.2 Enantioselective Binding Studies of Macrocycles 93

4.3 Investigation of the Ditopic Properties of Macrocycles 97

V. Conclusions 99

VI. Experimental Section 100

6.1 General 100

6.2 Synthesized Compounds 100

6.3 Zinc Binding Studies of *Tris*(2-pyridyl)methanol Derivatives 124

6.4 Kinetics Studies of Zinc Complexes of *Tris*(2-pyridyl)methanol Derivatives in D_2O 125

6.5 Kinetics of *p*-nitrophenyl Acetate Hydrolysis 128

6.6 COSY and NOESY ^{1}H NMR of Macrocycle **105** 131

6.7 IR studies 134

6.8 ^{1}H NMR Titration Experiments of Macrocycle **105** 135

6.9 Job's Plot of Macrocycle **105** 142

6.10 ^{1}H NMR Titration Experiment of Macrocycles **124** and **125** 143

VII. References 156

VITA 167

LIST OF TABLES

Table 1.1 Binding constants of ligands **33**, **34** with alkali cations 23

Table 2.1 Equilibrium distribution for 1:1 mixtures of Zn^{2+} and the 'first generation' ligands 59

Table 2.2 Equilibrium distribution for 1:1 mixtures of Zn^{2+} and the 'second generation' ligands 62

Table 2.3 Equilibrium distribution for 1:1 mixtures of Zn^{2+} and the 'third generation' ligands 64

Table 3.1 The yield of the cyclization reaction at different concentration of **119** 77

Table 3.2 Associate constants for macrocycle **105** with anions in $CDCl_3$ 84

Table 3.3 Associate constants for macrocycle **105** with ammonium salts in $CDCl_3$ 87

Table 4.1 Associate constants for macrocycles **124** and **125** with nitrate salt of amino acid methyl esters 95

Table 4.2 Associate constants for macrocycles **124** and **125** with nitrate salt of methionine and threinine methyl esters 97

Table 4.3 Associate constants for macrocycles **124** and **125** with various ammonium salts of phenylalanine methyl esters 98

LIST OF FIGURES

Figure 1.1 Common structure feature of zinc enzymes 4

Figure 1.2 Cartoon of the active site of CAII 6

Figure 1.3 The mechanism of hydration of CO_2 by CAII 7

Figure 1.4 Facial binding of a tripodal ligand 8

Figure 1.5 Structures of common tri-podal ligands 9

Figure 1.6 Reaction between the zinc hydroxide complex of **5** (R, R' = *t*-Butyl) with CO_2 10

Figure 1.7 Synthesis of the novel biomimetic calix[6]arene-based zinc complexes 11

Figure 1.8 Formation of $[ML_2]^{2+}$ complex of tris(pyridyl)methanol ligand 12

Figure 1.9 Catalytic mechanism of complex **13** 14

Figure 1.10 Synthesis of bis[2-(O-hydrxyphenoxy)ether] ether **14** and dibenzo 18-crown-6 **15** 15

Figure 1.11 Binding of K^+ by dibenzo-18-crown-6 **15** 16

Figure 1.12 Templated synthesis of crown ether **16** 16

Figure 1.13 Metal complexation of N-substituted crown ethers 18

Figure 1.14 Complexation of Cl^- by protonated forms of ligands **37** and **38** 25

Figure 1.15 The synthesis of bipyrrole based macrocycles **46**, **47** 30

Figure 1.16 Simultaneous complexation of NaCl by calix[4]arene **60** 37

Figure 1.17 Simultaneous complexation of NaCl by ligand **62** 38

Figure 1.18 Simultaneous complexation of NaCl by ligand **63**. 39

Figure 1.19 Complexation of *p*-nitrobenzoate with ligand **64** 39

Figure 1.20 Complexation of phenylalanine with ligand **65** 40

Figure 1.21 Enantiomeric recognition of amino acid derivatives by receptor **73** 47

Figure 1.22 Binding model between guanidinium salts and carboxylate 48

Figure 2.1 Deprotonation of bound water 53

Figure 2.2 Formation of $[ZnL_2]^{2+}$ sandwich complexes 54

Figure 2.3 Formation of tetrahedral zinc complex with tris(pyrazolyl)borate **5** 55

Figure 2.4 ^{1}H NMR of a 1:1 mixture (1 mM) of ligand **84** and zinc perchlorate in DMSO 58

Figure 2.5 ^{1}H NMR COSY spectrum of a 1:1 mixture (1 mM) of ligand **84** and zinc perchlorate in DMSO. 59

Figure 2.6 ^{1}H NMR EXSY spectrum of a 1:1 mixture (1 mM) of ligand **84** and zinc perchlorate in DMSO 60

Figure 2.7 Schematic represent of two major causes of weak binding 60

Figure 2.8 Formation of oxygen-bridged zinc complex 63

Figure 2.9 ES mass spectrum of a 1:1 mixture (1 mM) of ligand **91** and zinc perchlorate in H_2O 63

Figure 2.10 Change of the percentages of $[ZnL]^{2+}$ in aqueous solution as a function of time 66

Figure 3.1 Schematic represent of counteranion affect on cation binding 71

Figure 3.2 The structures of macrocycle **105** and the guest molecule 73

Figure 3.3 The structures of coupling reagents 78

Figure 3.4 Noesy signals of receptor **105** 81

Figure 3.5 Proposed binding model of receptor **105** with anions 82

Figure 3.6 Binding isotherm for the complexation of macrocycle **105** and TBA-Cl 83

Figure 3.7 The job's plot of macrocycle **105** with phenylalanine HBr salt 83

Figure 3.8 The structure of the guest molecule **123** 85

Figure 3.9 Binding isotherm for the complexation of macrocycle **105** and phenylalanine HNO_3 salt 86

Figure 3.10 The Job's plot of macrocycle **105** with phenylalanine HBr salt 86

Figure 3.11 Proposed binding model of receptor **105** with ammonium salt 87

Figure 4.1 The structures of macrocycles **124**, **125** and the guest molecules 90

Figure 4.2 The structures of the guest molecule **133** 93

Figure 4.3 Binding isotherm for the complexation of macrocycle **124** and S-phenylalanine HNO_3 salt 94

Figure 6.1 ^{1}H NMR of a 1:1 mixture of ligand **91** and zinc perchlorate in D_2O 126

Figure 6.2 Change of the percentages of $[ZnL]^{2+}$ and $[ZnL_2]^{2+}$ of ligand **91** as a function of time 127

Figure 6.3 Change of the percentages of $[ZnL]^{2+}$ and $[ZnL_2]^{2+}$ of ligand **100** as a function of time 128

Figure 6.4 Change of the percentages of $[ZnL]^{2+}$ and $[ZnL_2]^{2+}$ of ligand **103** as a function of time 128

Figure 6.5 Change of the percentages of $[ZnL]^{2+}$ and $[ZnL_2]^{2+}$ of ligand **104** as a function of time 129

Figure 6.6 The kinetics of *p*-nitrophenyl acetate hydrolysis in the presence of 1 mM zinc complex of ligand **100** at 298 K and pH = 8.4 131

Figure 6.7 The kinetics of *p*-nitrophenyl acetate hydrolysis in the presence of 2 mM zinc complex of ligand **100** at 298 K and pH = 8.4 132

Figure 6.8 The kinetics of *p*-nitrophenyl acetate hydrolysis in absence complexes at 298 K and pH = 8.4 132

Figure 6.9 The structure of the macrocycle **105** 133

Figure 6.10 ^{1}H NMR of macrocycle **105** in $CDCl_3$ 133

Figure 6.11 ^{1}H NMR COSY spectrum of macrocycle **105** in $CDCl_3$ 134

Figure 6.12 ^{1}H NMR of macrocycle **105** in DMSO 134

Figure 6.13 ^{1}H NMR NOESY spectrum of macrocycle **105** in DMSO 135

Figure 6.14 NH stretching region of the FT-IR spectra of macrocycle **105** in $CDCl_3$ .. 136

Figure 6.15 Binding isotherm for the complexation of macrocycle **105** and TBA-Br 138

Figure 6.16 Binding isotherm for the complexation of macrocycle **105** and TBA-F .. 138

Figure 6.17 Binding isotherm for the complexation of macrocycle **105** and TBA-I 139

Figure 6.18 Binding isotherm for the complexation of macrocycle **105** and TBA-NO_3 139

Figure 6.19 Binding isotherm for the complexation of macrocycle **105** and TBA-TFA 140

Figure 6.20 Binding isotherm for the complexation of macrocycle **105** and TBA-TsO 140

Figure 6.21 Binding isotherm for the complexation of macrocycle **105** and phenylalanine HNO_3 salt 141

Figure 6.22 Binding isotherm for the complexation of macrocycle **105** and phenylalanine HCl salt 141

Figure 6.23 Binding isotherm for the complexation of macrocycle **105** and phenylalanine TFA salt 142

Figure 6.24 Binding isotherm for the complexation of macrocycle **105** and phenylalanine HBr salt 142

Figure 6.25 Binding isotherm for the complexation of macrocycle **105** and phenylalanine TsOH salt 143

Figure 6.26 Binding isotherm for the complexation of macrocycle **105** and phenylalanine HI salt 143

Figure 6.27 The job's plot of macrocycle **105** with phenylalanine HBr salt 144

Figure 6.28 The job's plot of macrocycle **105** with TBA-B 144

Figure 6.29 The structure of macrocycle **123** and **124** 145

Figure 6.30 Binding isotherm for the complexation of macrocycle **124** and S-phenylglycine HNO_3 salt 146

Figure 6.31 Binding isotherm for the complexation of macrocycle **124** and R-phenylglycine HNO_3 salt 146

Figure 6.32 Binding isotherm for the complexation of macrocycle **124** and S-phenylalanine HNO_3 salt 147

Figure 6.33 Binding isotherm for the complexation of macrocycle **124** and R-phenylalanine HNO_3 salt 147

Figure 6.34 Binding isotherm for the complexation of macrocycle **124** and S-valine HNO_3 salt 148

Figure 6.35 Binding isotherm for the complexation of macrocycle **124** and R-valine HNO_3 salt 148

Figure 6.36 Binding isotherm for the complexation of macrocycle **124** and S-alanine HNO_3 salt 149

Figure 6.37 Binding isotherm for the complexation of macrocycle **124** and R-alanine HNO_3 salt 149

Figure 6.38 Binding isotherm for the complexation of macrocycle **125** and S-phenylalanine HNO_3 salt 150

Figure 6.39 Binding isotherm for the complexation of macrocycle **125** and R-phenylalanine HNO_3 salt 150

Figure 6.40 Binding isotherm for the complexation of macrocycle **125** and S-phenylglycine HNO_3 salt 151

Figure 6.41 Binding isotherm for the complexation of macrocycle **125** and R-phenylglycine HNO_3 salt 151

Figure 6.42 Binding isotherm for the complexation of macrocycle **125** and S-alanine HNO_3 salt 152

Figure 6.43 Binding isotherm for the complexation of macrocycle **125** and R-alanine HNO_3 salt 152

Figure 6.44 Binding isotherm for the complexation of macrocycle **125** and S-valine HNO_3 salt 153

Figure 6.45 Binding isotherm for the complexation of macrocycle **125** and R-valine HNO_3 salt 153

Figure 6.46 Binding isotherm for the complexation of macrocycle **124** and S-methionine HNO_3 salt 154

Figure 6.47 Binding isotherm for the complexation of macrocycle **124** and R-methionine HNO_3 salt 154

Figure 6.48 Binding isotherm for the complexation of macrocycle **124** and S-threonine HNO_3 salt 155

Figure 6.49 Binding isotherm for the complexation of macrocycle **124** and R-threonine HNO_3 salt 155

Figure 6.50 Binding isotherm for the complexation of macrocycle **125** and S-methionine HNO_3 salt 156

Figure 6.51 Binding isotherm for the complexation of macrocycle **125** and R-methionine HNO_3 salt 156

Figure 6.52 Binding isotherm for the complexation of macrocycle **125** and S-threonine HNO_3 salt 157

Figure 6.53 Binding isotherm for the complexation of macrocycle **125** and R-threonine HNO_3 salt 157

LIST OF SCHEMES

Scheme 2.1 Synthesis of *Tris*-(2-nicotinic acid)methanol methyl ether **85** 56

Scheme 2.2 The synthesis of ligands **86**-**88**..... 57

Scheme 2.3 The synthesis of ligands **91**-**93**..... 61

Scheme 2.4 The synthesis of ligands **100**, **102** and **103** 65

Scheme 2.5 The synthesis of ligand **104**..... 67

Scheme 2.6 Catalytic hydrolysis of esters by CA..... 68

Scheme 3.1 The synthesis of macrocycle **105** 75

Scheme 3.2 The synthesis of macrocycle **105** (continued)..... 76

Scheme 3.3 Side reaction from synthesizing **110** 76

Scheme 3.4 Formation of guaridinated by-products..... 78

Scheme 3.5 Optimized synthesis of diacid **112** 80

Scheme 4.1 The synthesis of macrocycles **124, 125**..... 92

ABBREVIATIONS

BOP	Benzotriazole-1-yl-oxy-tris-(dimethylamino)-phosphoniumhexa-fluorophosphate
n-BuLi	*n*-Butyllithium
DMF	N,N'-Dimethylformamide
DMSO	Dimethylsulfoxide
DPPA	Diphenylphosphoryl azide
HOBt	N-hydroxylbenzotriazole
HBTU	2-(1H-benzotriazole-1-yl)-1, 1, 3, 3-tetramethyluronium hexaflorophosphate
MOE	Ethoxymethyl
MOM	Methoxymethyl
PyBOP	Benzotriazole-1-yl-oxy-tris-pyrrolidino-phosphonium hexafluorophosphate
rt	Room temperature
THF	Tetrahydrofuran
TLC	Thin layer chromatography
Ts	Tosyl (*p*-Toluenesulfonyl)

ABSTRACT

In an effort to produce the tetrahedrally coordinated, catalytically active zinc center, three families of *tris*(2-pyridyl)methanol derivatives were synthesized and characterized. Zinc binding studies revealed that the binding behaviors of the ligands depended on the steric and electronic properties of the substituents on the pyridyl rings, as well as the functional group on the tertiary alcohol.

A novel *tris*-pyridyl macrocyclic receptor was synthesized. The receptor possesses both hydrogen bond donors and acceptors. NMR titration experiments revealed that the receptor simultaneously bound both ammonium cation and the counter anion. The counter anion significantly influences the association between the receptor and the ammonium cation.

Chiral ditopic macrocycles, which enantioselectively bind chiral ammonium cations, have also been synthesized. Their enantioselective binding properties, as well as the ditopic recognition properties were investigated.

I. Introduction

1.1 Supramolecular Chemistry

Chemistry can be divided into two broad areas: molecular and supramolecular.[1] Traditional chemistry, or molecular chemistry, deals mainly with the synthesis of complex molecules. Its power arises through the manipulation of the covalent bonds between atoms. However, most biological processes do not involve the making or breaking of covalent bonds, but rather non-covalent, intermolecular interactions. These non-covalent, intermolecular interactions are the basis of supramolecular chemistry.

As defined by Jean-Marie Lehn, supramolecular chemistry is "chemistry beyond the molecule".[2] The field of supramolecular chemistry started with the selective binding of alkali metals by artificial receptors: crown ethers and cryptands, and then moved to consider intermolecular interactions between neutral species and anions. In the past several decades, supramolecular chemistry has undergone enormous development. It is one of the most popular and fastest growing areas of chemistry now. This highly interdisciplinary field of science has brought about wide-ranging collaborations between chemical, physical and biological researchers.

1.2 Molecular Recognition and Host-Guest Chemistry

Molecular recognition is defined by the energy and the information involved in the binding and selection of substrate by a given receptor or host molecule.[3] The term "host" describes the ability of a molecule to bind another one with preference over all others, and with greater strength than is commonly found in unspecific molecular interactions. The chemical nature of the "guest" to be specifically bound mutually complements the host. These include geometry and electronics.[4] In general, molecular recognition relies on the factor that there is a molecular interaction between host and guest, leading to an assembly of two or more species into a well-defined structure. These non-covalent interactions could be: ion-ion, ion-dipole, dipole-dipole, hydrogen bonding, cation-π, π-π stacking, van der waals forces, close packing in the solid-state, the hydrophobic effect or the combination of those interactions.

Generally, molecular recognition is restricted to certain conditions. Changing one or more condition may lead to no binding or reduced selectivity. For example, a compound qualifying as a host for one particular guest species in one solvent may completely fail to bind the same guest under different solvent conditions.

The design of a synthetic host requires a careful consideration of the nature of the guest. This leads to conclusions about the general properties of the new host system. There must be a good match or complementary between host and guest: Lewis acids must match Lewis bases; hydrogen bond donors must match acceptors. Another very important concept in host design is pre-organization. A pre-organized ligand means there is less unfavorable conformational rearrangement to take place in order to adopt the optimum complex geometry. Although the natural receptors do not follow the concept of

rigid host design, it is widely accepted that a rigid host having all of its anchor groups preorganized complementary to the respective guest function should show strong binding.

Nature's enzymes are complex host-guest systems that bring about reactions essential to life. Enzymes recognize and respond to specific substrates, as part of the control mechanism of the cell.

1.3 Zinc Enzymes

Zinc is known to be an essential trace element. There are 2 to 3 g of zinc in adult humans, making it one of the most important trace elements.[5] However, no specific biological role for zinc was established until 1940, when it was shown to be required for the catalytic activity of the enzyme Carbonic Anhydrase (CA). In the following five decades, more than 300 enzymes have been found to contain zinc. The influence of zinc derives from its roles in enzymes, with functions that are both structural and catalytic. In a few enzymes, zinc plays a purely structural role, in which zinc stabilizes the enzyme folding. However, in most of the enzymes, zinc is directly involved in catalysis, interacting with substrate molecules undergoing transformation.[6]

The active sites of catalytic zinc enzymes feature a tetrahedrally coordinated zinc center that is attached to the protein backbone by three amino acid resides, with the fourth being occupied by a water molecule.[7] The water molecule is activated by zinc through ionization and polarization and is a critical component of a catalytic reaction. Deprotonation of the bound water molecule occurs at physiological condition and the resulting zinc hydroxide species is active toward hydration reactions (Figure 1.1).

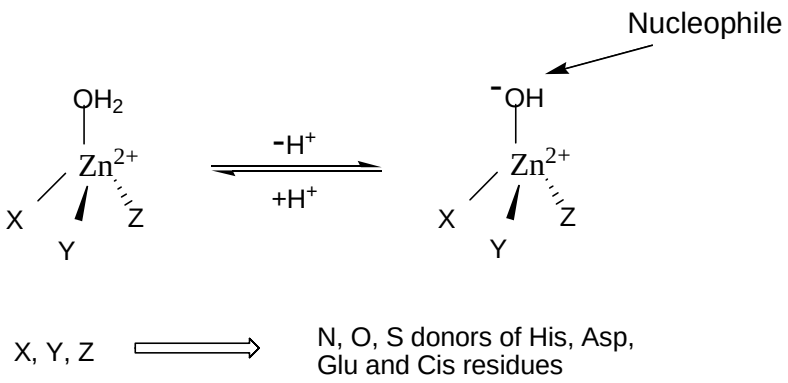

Figure 1.1 Common structure feature of zinc enzymes

The specific function performed by each of these enzymes is dictated by the nature of the residues with which zinc is bound to the protein. The residues that zinc bind to are typically a combination of histidine, glutamic acid, aspartic acid and cysteine, which provide nitrogen, oxygen, and sulfur donors. Histidine is the most commonly encountered. The most important function of the zinc enzymes is the cleavage of amide bonds and hydrolysis of phosphates with high regio- and enantio-selectivities. The importance of zinc enzymes is not, however, restricted to their role in cleaving amide and phosphate bonds. Another important family of zinc enzyme is Carbonic Anhydrase which performs the reversible hydration of CO_2.[8]

1.4 Carbonic Anhydrase (CA)

Of all the zinc enzymes, Carbonic Anhydrase is probably the most extensively studied.[9] It is the first enzyme recognized to contain zinc and has played the most pivotal role in the development of enzymology. The essential physiological function of Carbonic Anhydrase is to catalyze the reversible hydration of CO_2 and thus plays an important role in respiration and intracellular CO_2/HCO_3^- equilibration.[10] In addition to its physiological function, Carbonic Anhydrase also catalyzes non-physiological reactions such as hydration of aldehydes and hydrolysis of esters.[11-14]

The three-dimensional structure of Carbonic Anhydrase II (CAII), an isozyme found in human red blood cells,[15] revealed the active site as shown in Figure 1.2. Zinc is located at the bottom of the cavity (ca. 15 Å deep) and is coordinated to three histidine residues (His 94, His 96, and His 119), with the remaining tetrahedral site being occupied by a water molecule. The water molecule is also involved in a hydrogen-bonding interaction with a threonine residue. The most striking feature of this active site is that the pK_a of this bound water molecule is 7.3 which is much more acidic than free water molecule (pK_a = 15.6).[15,16] At physiological pH, the water molecule is deprotonated and nucleophilically attacks electron deficient carbon atoms, such as those in carbon dioxide and carboxylate esters, resulting in the hydration or cleavage of the respective molecules.[18,19]

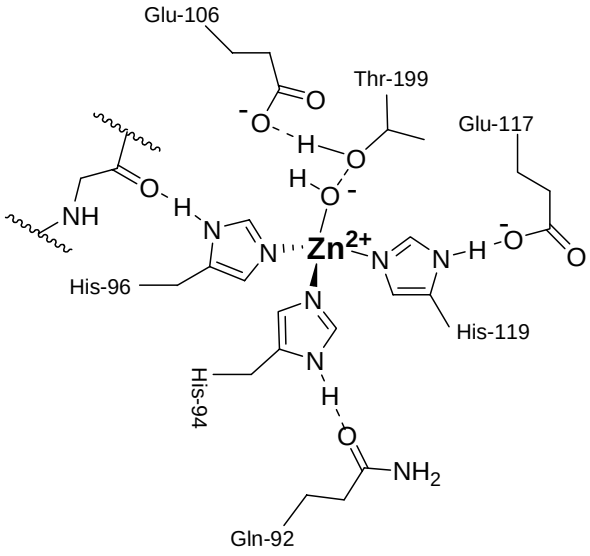

Figure 1.2 Cartoon of the active site of Carbonic Anhydrase II.

Figure 1.3 illustrates the currently accepted mechanism of hydration of CO_2 by Carbonic Anhydrase II.[10] The mechanism comprises the following steps: (i) deprotonation of the zinc bound water molecule (via a His-64 shuttle) to give the active zinc hydroxide derivative $[(His)_3Zn\text{-}OH]^+$, (ii) nucleophilic attack of the zinc-bound hydroxide at the carbon dioxide substrate to give a hydrogen carbonate intermediate $[(His)_3Zn\text{-}OCO_2H]^+$, and (iii) displacement of the bicarbonate anion by H_2O to complete the catalytic cycle. The rate-determining step of the process is the initial proton transfer.

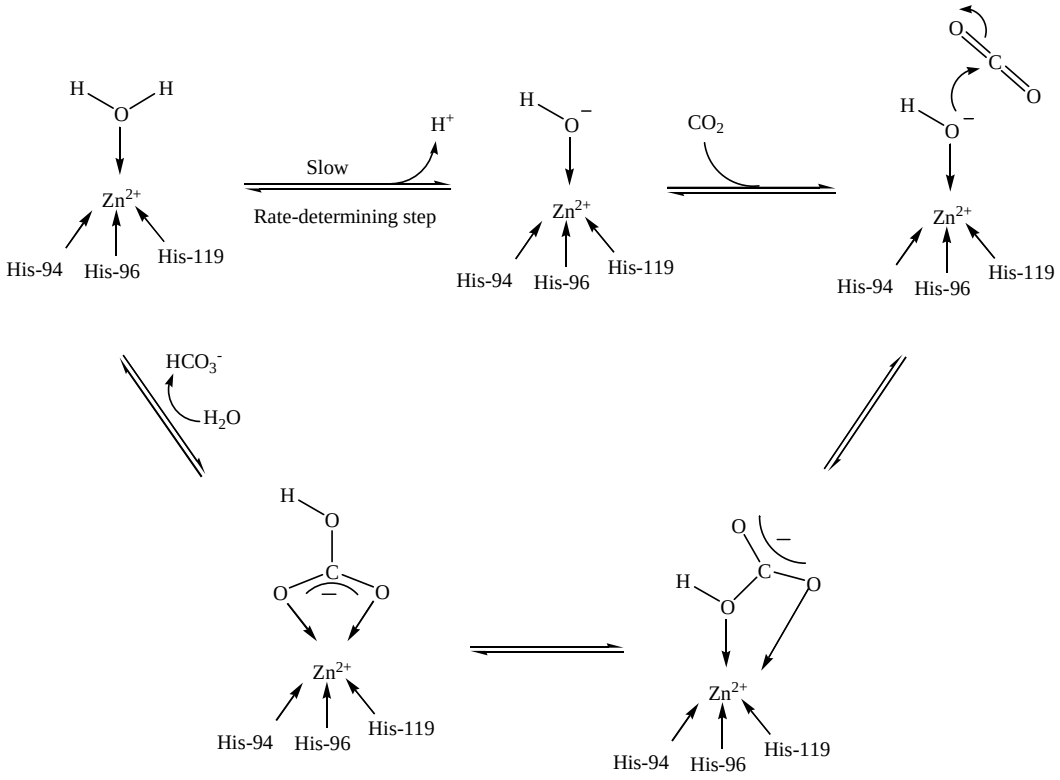

Figure 1.3 The mechanism of hydration of CO_2 by CAII

1.5 Carbonic Anhydrase Mimics

As the native enzyme contains a zinc ion in its active site, zinc complexes were extensively studied in order to detect model compounds that would mimic the function of enzyme. One of the first models was reported in 1975 by Wooley.[20,21] Although this model was intriguing and very convincing about the essential role of zinc ions, the "fatal" drawbacks of **1** are that zinc is tetra-coordinated, and relatively high pK_a value (8.7) of the bound water molecule (against 7.3 in Carbonic Anhydrase). Consequently, complex **1** was not an active catalyst for CO_2 hydration.

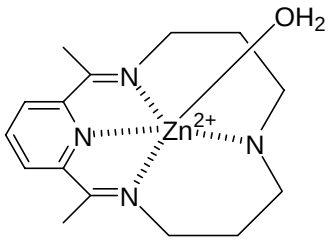

1

Thus, it appeared of considerable interest to design tridental ligands which incorporate the requisite three donor groups to mimic the three protein residues that bind zinc at the catalytic center. The fact that tridental ligands enforce facial binding with single relevant binding conformation provides them the ideal environment as Carbonic Anhydrase mimics (Figure 1.4). The possibility of incorporation substituents that directly influence the steric environment about the metal center makes them even more attractive.

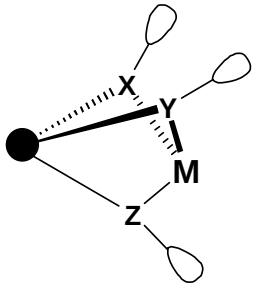

Figure 1.4 Facial binding of a tripodal ligand.

Figure 1.5 shows the common tripodal ligands **2-5** which were synthesized and studied as synthetic analogues of Carbonic Anhydrase. However, none of them possess Carbonic Anhydrase -like properties. Without bulky subsitituents on the heteratomatic rings, these ligands tend to form inactive 2:1 sandwich complexes even if an excess of zinc is used.[23-26]

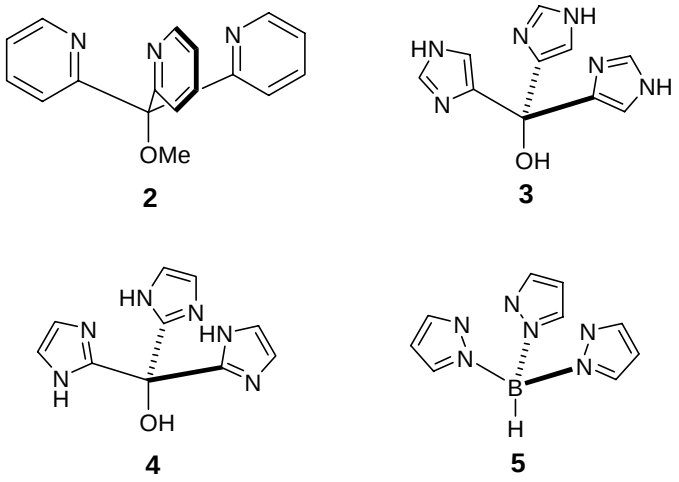

Figure 1.5 Structures of common tri-podal ligands

Structural modifications of these tripodal ligands were extensively studied to inhibit the formation of 2:1 complexes.[27-31] A successful synthetic analogue of Carbonic Anhydrase was obtained by Gerard Parkin through modifying the structure of tris(pyrazolyl)borate **5**. Thus, with bulky *tert*-butyl substituents on the 3-position of the pyrazolyl groups, the ligand has the tendency to favor a tetrahedral coordination (Figure 1.6).[32] A tetrahedral zinc hydroxide complex of tris(pyrazolyl)borate was also isolated by reaction of monomeric zinc complex with KOH in methanol. This active species which can hydrate CO_2 to bicarbonate bound to zinc. However, the zinc hydroxide species does not act as a catalyst since it can't be regenerated during the reaction.

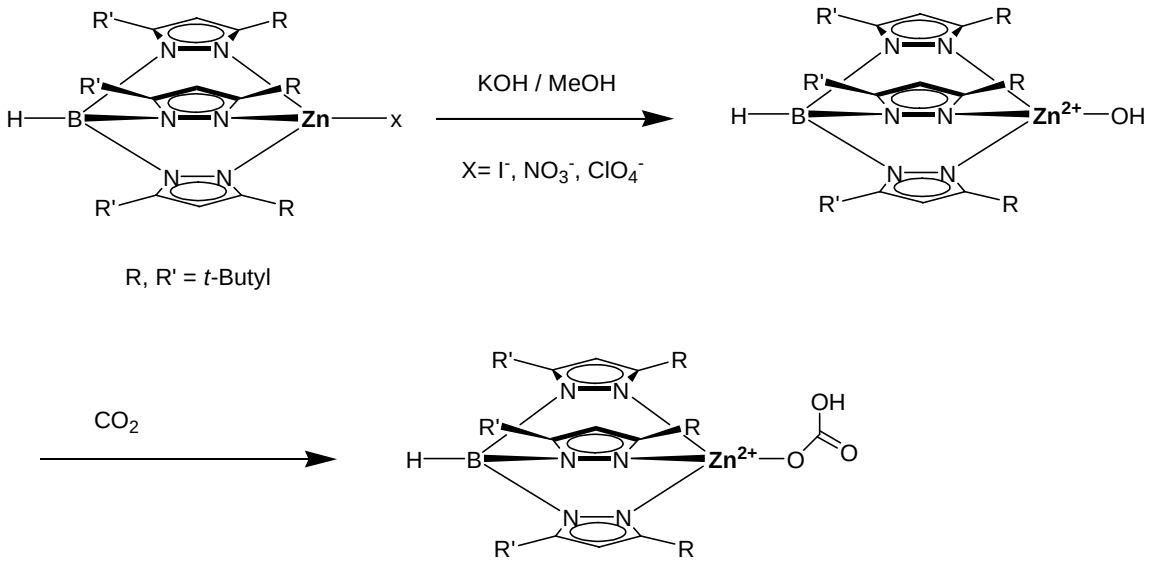

Figure 1.6 Reaction between the zinc hydroxide complex of **5** (R, R' = *t*-Butyl) with CO_2.

A benzene platform with three histidine side chains **6** has been synthesized in Vahrenkamp's group.[33] The results from potentiometric titration demonstrated the formation of tetrahedrally coordinated zinc complex $[L\text{-}Zn\text{-}OH_2]^{2+}$, with the p$K_a$ of the bound water molecule 6.2.

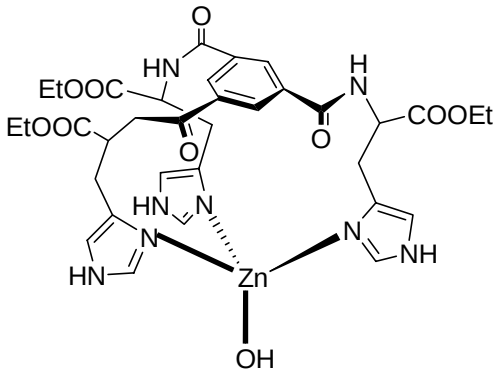

6

By incorporating three imidazole groups on the lower rim of calix[6]arene, Reinaud and co-workers generated a novel supramolecular system as Carbonic Anhydrase mimics.[34,35] Upon reaction with zinc ion, an air-stable dicationic zinc-aqua complex $[Zn(X_6Me_3Imme_3)(H_2O)](ClO_4)_2$ was obtained (Figure 1.7). The highly acidic Zn^{2+} center was constrained in a tetrahedral environment with a labile site oriented toward the inside of the calix[6]arene structure. The hydrophobic pocket acted as a selective molecular funnel for neutral molecules. ^{1}H NMR spectroscopy studies showed the easy exchange of the bound water for amines, alcohols, amides, or nitriles.

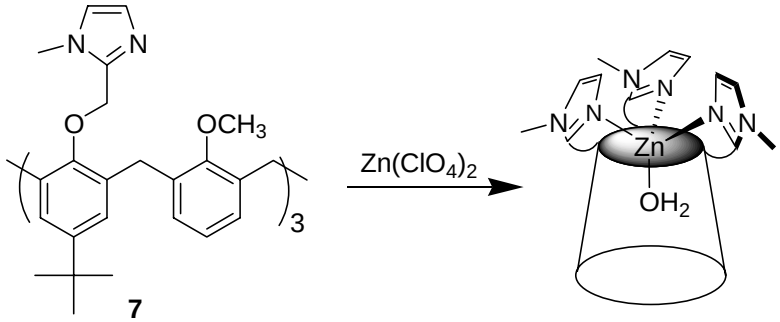

Figure 1.7 Synthesis of the novel biomimetic calix[6]arene-based zinc complexes

In an approach to mimic Carbonic Anhydrase in both tetrahedral zinc coordination geometry and a hydrophobic cavity around metal center, Walton and co-workers reported the synthesis and metal binding studies of a family of 1,3,5-tris(acrylideneamino)cyclohexane-based ligands **8**-**9**.[36,37] Upon addition of zinc ion, the ligand adopted a face-capping imine-N_3 coordination geometry with the metal cation situated in the bottom of a rigid hydrophobic cavity.

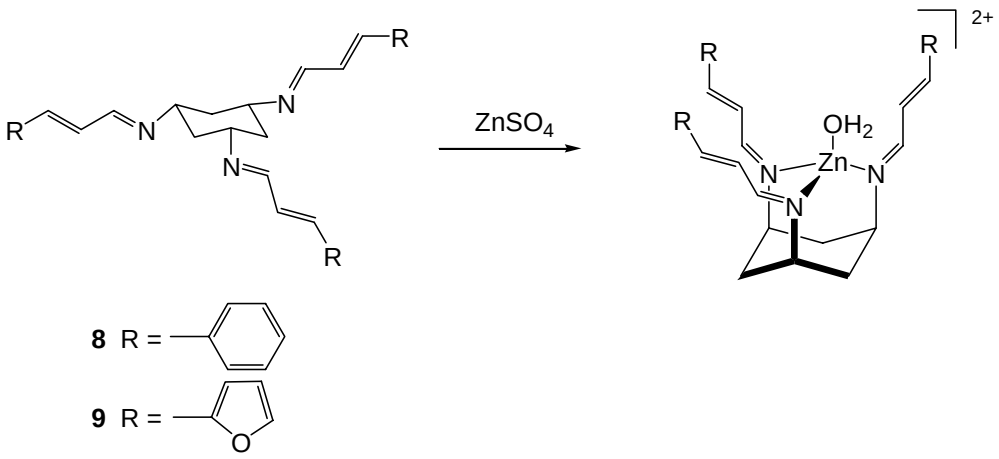

Another easily synthesized family of tripodal ligands that may act as Carbonic Anhydrase mimics are the tris(2-pyridyl)methanols e.g. **10**. Previous investigations of zinc complexation reveal a strong tendency to form inactive $[ZnL_2]^{2+}$ sandwich-type complex instead of a tetrahedral coordinated species (Figure 1.8).[38,39]

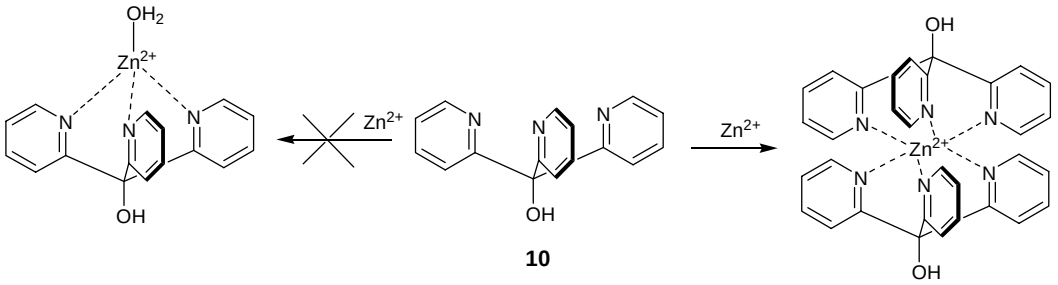

Figure 1.8 Formation of $[ML_2]^{2+}$ complex of tris(pyridyl)methanol ligand

One approach to modify and control the metal binding behavior of the tris(2-pyridyl)methanol ligand is to generate a cavity around the metal complex. Thus, by tailoring a hydrophobic dendimeric cleft around tris-(2-pyridyl) methanol ligands, it is possible to form $[ZnL]^{2+}$ species such as **11** that cannot undergo sandwich complex formation.[40]

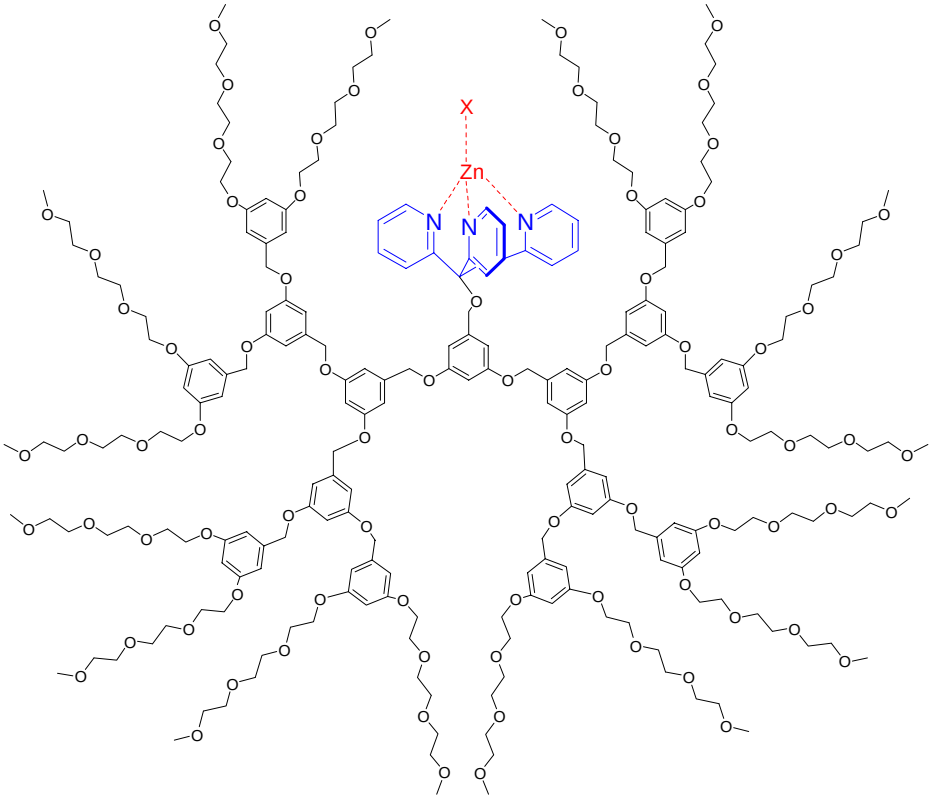

11

A recently reported zinc complex of the macrocyclic triamine (**[12]ane N_3**) is one of the simplest models for the Carbonic Anhydrase active site.[41,42] The zinc ion is coordinated to the three nitrogen atoms of the macrocyclic ligand, and a water molecule, as shown by X-ray crystallographic and NMR studies. The complex possesses a pK_a value of 7.3, very similar to CA.[43]

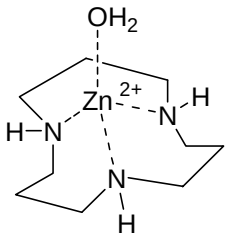

12

Complex **12** has been proven to be an efficient catalyst for hydration of aldehydes and to a similar extent for the hydrolysis of esters.[44] Kinetic studies of the hydrolysis of

4-nitro-phenylacetate at pH 8.5 reveal a second order reaction catalyzed by zinc complex, and the rate constant was determined to be 4.1×10^{-2} $M^{-1} \cdot s^{-1}$, compared to 4×10^{2} $M^{-1} \cdot s^{-1}$ of Carbonic Anhydrase II.

An alcohol-pendant cyclen **13** was synthesized later by the same group.[45] Its zinc complex has the pK_a value similar to complex **12**. However, complex **13a** is a more efficient catalyst for the hydrolysis of esters. The enhancement of the catalytic activity is due to the assistant from the tethered alcohol during the reaction. Detailed mechanical studies have shown that the tethered alcoholic OH of **13a** deprotonated and then directly attacked the electrophilic ester carboxyl group of 4-nitrophenyl acetate, to yield an acyl-intermediate **13b**. It was then quickly hydrolyzed, to complete the hydrolysis and regenerate the initial alkoxide complex **13a** (Figure 1.9). The second rate constant was determined to be 0.14 $M^{-1} \cdot s^{-1}$ at pH 9.3 and 25 °C, which was four times faster than the corresponding value of **12**.

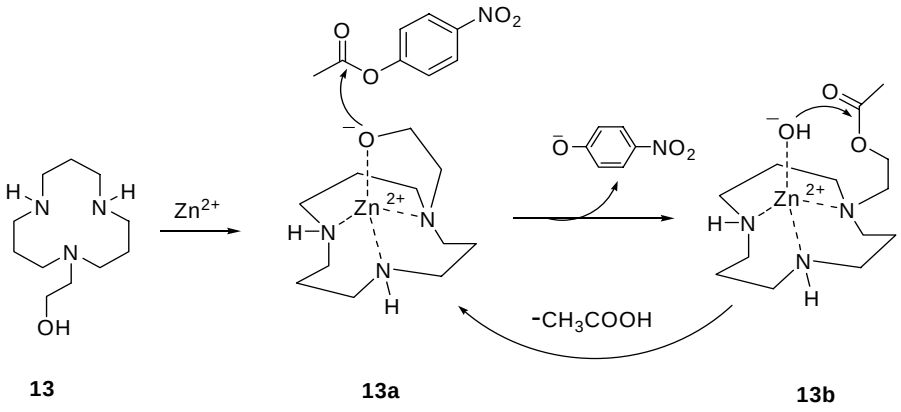

Figure 1.9 Catalytic mechanism of complex **13**

1.6 Cation Binding Receptors

1.6.1 Crown Ethers

The first crown-ether dibenzo-18-crown-6 **15**, was synthesized by Nobel Prize winner Charles Petersen in 1967 (Figure 1.10).[46] The product was formed as an unexpected by-product during a preparation of bis[2-(O-hydroxyphenoxy)ether] ether **14**. Small amount of catechol as impunities in the starting material led to the discovery of a new family of compounds – the crown ethers.

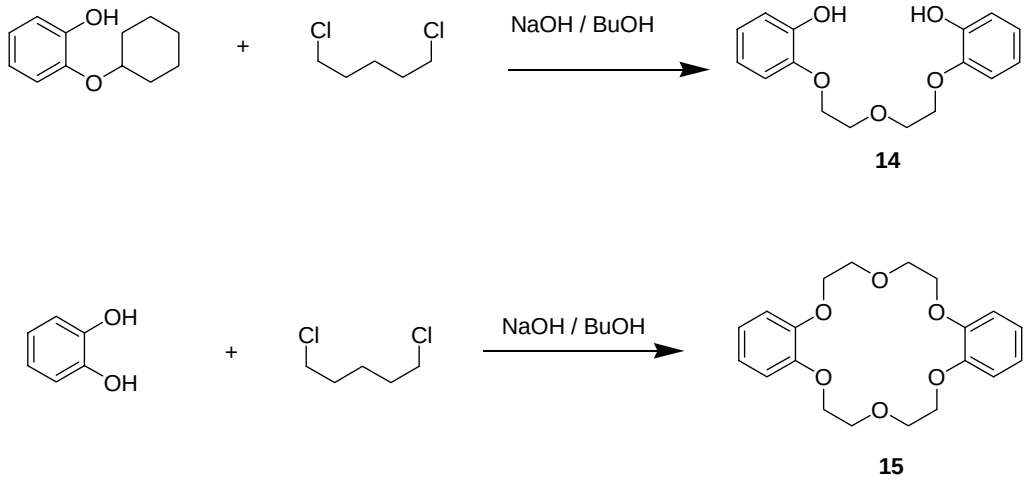

Figure 1.10 Synthesis of bis[2-(O-hydrxyphenoxy)ether] ether **14** and dibenzo 18-crown-6 **15**

Its complexation properties with metal ions were quickly discovered (Figure 1.11). This initial result rapidly led to the synthesis of other crown ethers with different size or different donor atoms. Methods of evaluating their metal complexation properties were established.

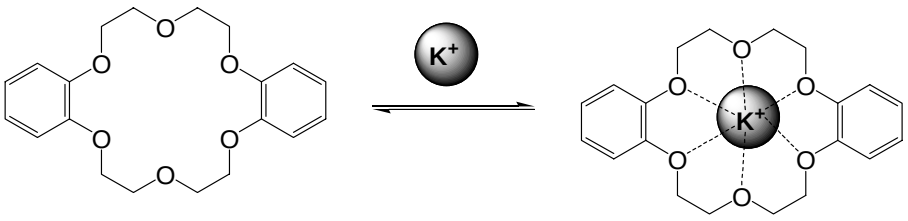

15

Figure 1.11 Binding of K^+ by dibenzo-18-crown-6 **15**

The synthesis of crown ethers generally utilizes Williamson ether reaction.[47,48] The use of alkali and alkali earth cations as template greatly facilitates their formation. The template effect arises from complexation of the crown ether's precursor around the metal ion. The efficiency of metal ions is closely related to the strength of interaction between metal ions and the product. Mandolini and co-workers have investigated the effect of metal ions on the synthesis of benzo-18-crown-6 **16** in methanol and dimethylsulfoxide. It was found that K^+ was 1500 times more efficient than Na^+ as a template because the potassium ion pre-organizes the linear backbone in a position favorable for the nucleophilic attack to occur (Figure 1.12).

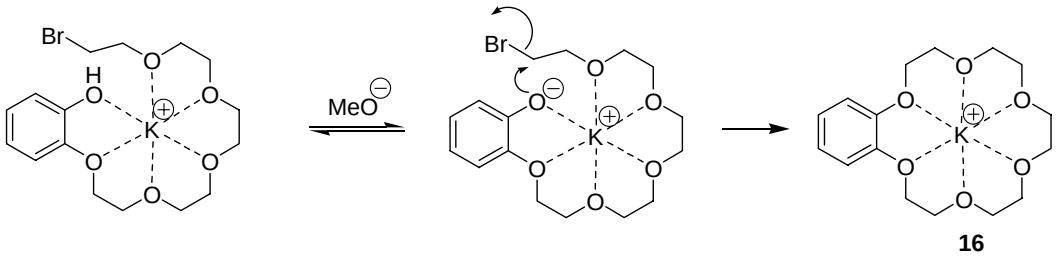

16

Figure 1.12 Templated synthesis of crown ether **16**

The ability of selective cation binding is the most remarkable property of crown ethers.[49-52] In order to distinguish different cations from one another, ligands must

display differences in their complexation abilities. Izatt and co-workers have made a detailed study of the effect of the crown size on the binding stabilities with a variety of univalent and bivalent cations.[53] Comparison of these binding stabilities revealed that log *K* values for complexes with 15-crown-5 **17** were much lower that those with the ligand 18-crown-6 **18** for all cations studied, except for those of small cations, such as Na^+, Li^+, and NH_4^+. The maximum stability for complexes with **18** occurs when the dimension of the metal ion best matches the ligand cavity.

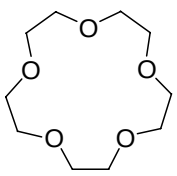

17

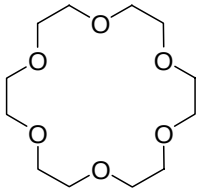

18

On the other hand, the larger crown ethers dicyclohexyl-21-crown-7 **19** and dicyclohexyl-24-crown-8 **20** bind Cs^+ more strongly than those of smaller macrocycles and are generally selective for Cs^+ over all other cations.[54-56]

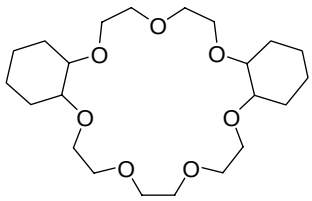

19

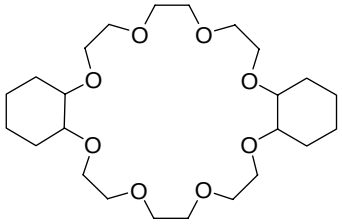

20

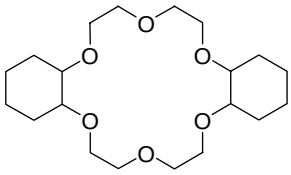

21

Solvents also have a significant effect on selective binding of cations. Agostiano and coworkers have noted that the complexation ability of dicyclohexyl-18-crown-6 **21** shows the order: $K^+ > Na^+ > Cs^+$ in water, but the selectivity between Na^+ and Cs^+ is

reversed in alcoholic solvents.[47] The complexation constants of **21** in protic solvents increase regularly for all alkali cations in the order: water < methanol < ethanol < 1-propanol.

The replacement of one or more oxygen atoms in crown ether by other donors such as nitrogen and sulfur dramatically changes the complexation properties of the ligands.[47] Frensdorf has studied the effect of nitrogen substituents on the complexation stabilities of **18** (Figure 1.13). Substitution of one oxygen by nitrogen results in macrocycle **22** which has less affinity for K^+. Dinitrogen substituted macrocycle **23** binds K^+ even weaker. However, replacing oxygen with nitrogen atoms results in increased binding constants for Ag^+. Similar results were obtained with crown ethers containing sulfur donor atom.

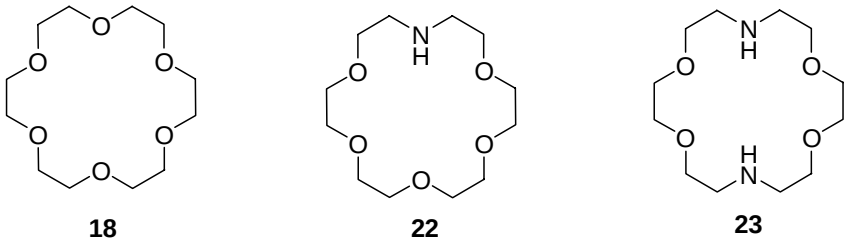

18 **22** **23**

log K for K^+:	6.1	3.9	2.0
log K for Ag^+:	1.6	3.3	7.8

Figure 1.13 Metal complexation of N-substituted crown ethers

1.6.2 Cryptands

Cryptands are macrobicycles capable of ion encapsulation due to their cage-like three dimensional structures. Their macrobicyclic cavities are more rigid and restricted than crown ethers, and thus, have higher selectivity for cations. Generally, the metal ion whose ionic radius best matches the size of the cryptand cavity will form the most stable complex.

Because of their rigidity, cryptands are pre-organized for cation binding. Consequently, cryptand binds cation much more strongly than corresponding crown ethers.[58-61] For example, ligand **23** and **24** have the same number of the donor atoms, while ligand **24** binds K^+ 10^3 times stronger than ligand **23** (log K = 2.0 and 5.4 for ligand **23** and **24** respectively).[58]

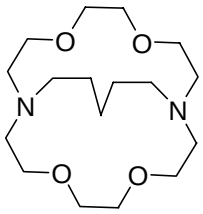

24

Micheloni and co-workers have synthezied a variety of new small aza cages and have studied their ligation properties.[62-64] Small aza cages are highly preorganized molecules that possess three dimensional cavities of fixed sizes. These preorganized small cavities allow selective encapsulation of metal ions of appropriate sizes. Especially strong and selective Li^+ binding is a remarkable feature of these compounds. For example, in water ligands **25** and **26** bind Li^+ with log K values of 5.5 and 3.0 respectively. This compares to log K value for binding Na^+ of 2.0 and 1.2 respectively. The relatively lower binding constant of **26** is due to the high steric hinderance of the benzyl group.

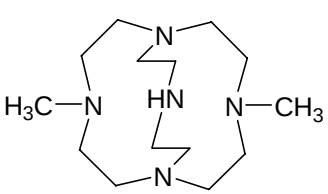

25

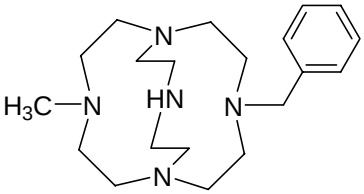

26

Bradshaw and co-workers have synthesized a series of new cryptands.[65,66] Binding studies with a variety of cations demonstrated that these ligands had high selectivity of K^+ over Na^+. The highest selectivity was observed on ligand **27** which had selectivity factor of 6.17.

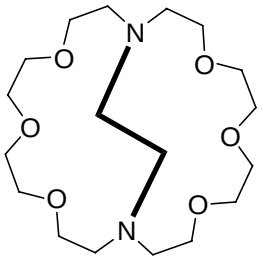

27

More recently, Bradshaw and co-workers reported novel benzene-bridged macro-bicyclic and macro-tricyclic polyethers.[67,68] Both ligands **28** and **29** are highly selective for Cs^+ over Na^+ and Pd^+, with log K = 2.20 and 3.50 respectively for cesium binding. Macrotricyclic ligand **29**, with an additional bridge, shows a stronger interaction with Cs^+ than does macrobicyclic ligand **28** due to the increased number of donor atoms. Little or no interaction was found for these ligands with Na^+ and Pd^+.

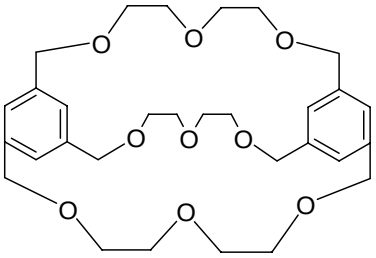

28

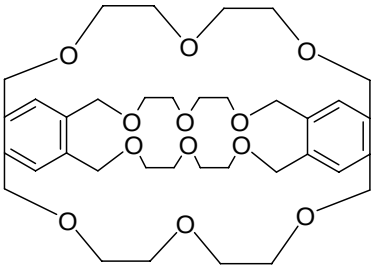

29

1.6.3 Calixarenes

Calixarenes are cavity-shaped cyclic oligomers made up of phenol units. Their easily synthized and versatile host frameworks make them very attractive in supramolecular chemistry.[69,70] Calixarenes offer many interesting possibilities in host-guest chemistry, particularly in ion complexation. The upper and lower rims of calixarenes can be easily functionalized to be the host of a variety of guest molecules. As hosts for cations, the phenolic oxygen atoms at the lower rim of calixarenes can complex to cations, either in hydroxyl form, or as alkyl ether derivatives.

The selectivity of calixarenes toward cations is mainly a function of the cavity dimensions and the nature of the binding groups. Arnaud-Neu and co-workers have studied cation complexing properties of lower rim modified calix[4]arenes.[71] Their binding studies with alkali and alkali earth metal ions demonstrated that the acid derivative **32** was a much stronger binder than the ester **31** or original hydroxyl derivative **30**. The stepwise substitution of the phenonlic hydrogen in **30** or ester function in **31** by a carboxyl acid led to an enhancement of the stability of the resulting complex, but a decrease of Na^+ / K^+ selectivity.

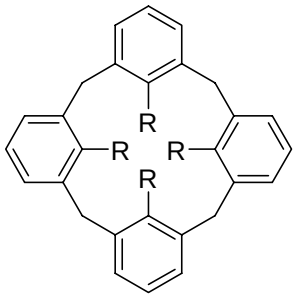

30 R = OH

31 R = $OCH_2CO_2CH_2CH_3$

32 R = OCH_2CO_2H

The cavity size of calixarenes has a significant effect on the selectivity of metal ions. In general, calix[4]arenes show a high selectivity for Na^+ over the other alkali metal cations. Barrett and co-workers extensively studied the effect of cavity size on the cation selectivity.[72]

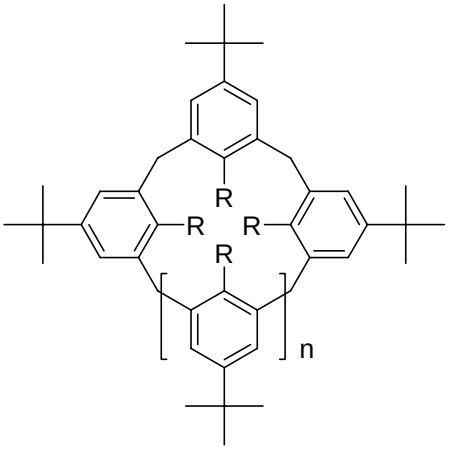

33 n = 1 R = $OCH_2CO_2CH_2CH_3$

34 n = 2 R = $OCH_2CO2CH_2CH_3$

Their results have shown that the pentamer **34** with its big cavity prefers larger cations. The binding constants with alkali metal ions are listed in Table 1.1.

Table 1.1 Binding constants (M^{-1}) of ligands **33**, **34** with alkali cations

Ligands	Li^+	Na^+	K^+	Rb^+	Cs^+
33	1.0	4.4	5.3	5.6	5.5
34	2.6	5.0	2.4	3.1	2.7

Further modification of calixarenes resulted in diooxocalix[4]arene **35**[73] and homocalixarene **36**[74], both of which exhibit selectivity for larger cations over small ones. For example, ligand **35** has log *K* value of 2.70 and 0 for Sr^{2+} and Ca^{2+} respectively. Ligand **36** has the similar selectivity of Sr^{2+} over Ca^{2+} (log *K* = 1.22 and 0 respectively).

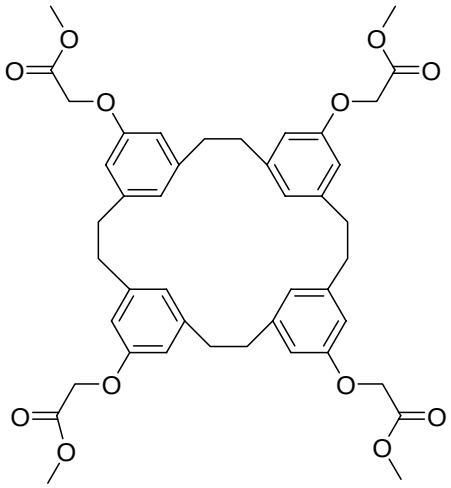

35

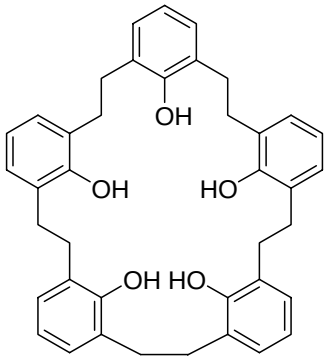

36

1.7 Anion Receptors

Synthetic anion receptors were developed much later then cation receptors.[75-79] The most prominent property of anions distinguishing them from any other guest species is their negative charges. Correspondingly, anions have a relative large radius and high free energies of salvation. Furthermore, anions occur in a range of shapes and geometries. For example, halides are spherical, NO_3^- is planar, SCN^- and N_3^- are linear.[1] The intrinsic properties of anions make it difficulty in designing multidentate receptors with appropriately situated Lewis acidic or other acceptor sites. However, due to its important biological role, considerable attention has been focused on supramolecular anion complexation in recent years.

1.7.1 Positively Charged Anion Receptors

The first synthetic anion receptor was reported by C. H. Park and H. E. Simmonds in 1968.[80,81] They found that the macrocycles **37** and **38**, when protonated at the bridgehead nitrogen atom, were able to bind halide anions within the cavity (Figure 1.14). The penetration of the halides anions into the macrocyclic structure was later confirmed by X-ray crystallography. This sharply observed result of the noncovalent encapsulation of anion opened the door of anion receptors and had a lasting effect on future development of host-guest chemistry with anions.

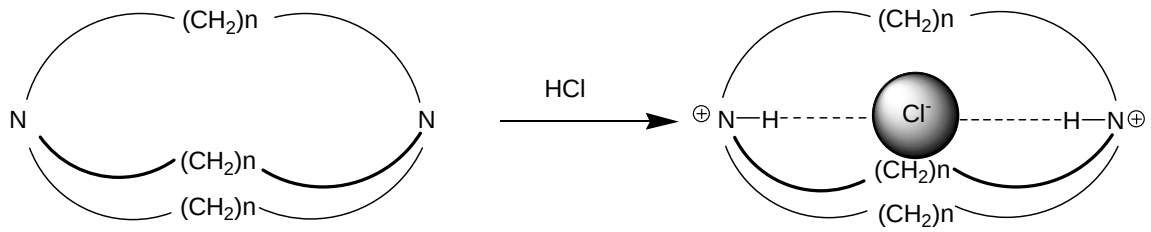

37 n = 9
38 n = 10

Figure 1.14 Complexation of Cl^- by protonated forms of ligands **37** and **38**

Due to the easy synthesis of azamacrocycles that were widely used as cation complexing agents, positively charged azamacrocycles as anion receptors were quickly developed.[82-84] Host-guest binding in these molecules depends on the relative proton affinities in interconnected multiple equilibria. In water as a solvent, protonation equilibria are readily established and the corresponding pK_a values of the individual proton can be determined by potentiometric titrations. It is no surprise, therefore, that water is the solvent of choice to study anion binding of most of the protonated azamacrocycles.

An aesthetically pleasing macrotricyclic ligand **39** was synthesized by Graf and Lehn.[85,86] Compound **39** may be regarded as arising from four fused triaza 18 crown-6 rings. This spherical molecule is a highly versatile example for both cation and anion receptor, depending on the pH of the medium. At neutral pH, compound **39** has basic properties that enable it to bind strongly to cations. Once the four nitrogen atoms are protonated, it becomes an anion binder. The tetra-protonated species has a remarkable Cl^- / Br^- selectivity($>10^3$). The crystal structure of Cl^- complex shows the enclosed Cl^- is bond by a tetrahedral array of $N\text{-}H^+ \ldots Cl^-$ hydrogen bonds.

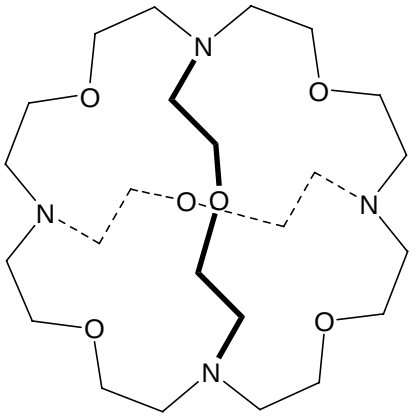

39

1.7.2 Neutral Amide Based Receptors

The hydrogen-bonding amide groups have been employed to produce a wide range of receptors capable of binding anions. Choi and Hamilton have recently reported the synthesis and anion binding properties of a new family of cyclic triamides.[87]

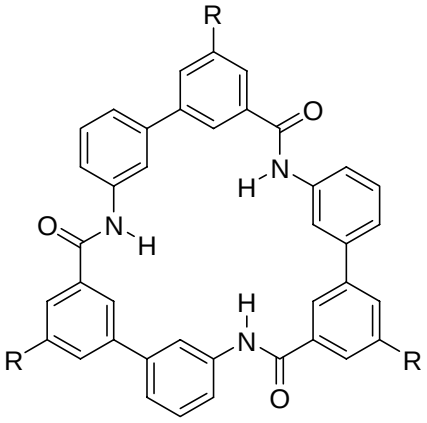

40 R = CO_2Et

41 R = NHBoc

The triamide macrocycles **40** and **41** have rigid structures in which three amide groups are projected into the central cavity. The convergent arrangement of dipoles enables the macrocyle to bind anions with size and shape selectivity. NMR evidence suggested that the receptors bound I^-, in a 2:1 mode of M_2I at low I^- concentration,

switching to a 1:1 binding mode at higher I^- concentration. The peak of amide proton had an initial up-field shift followed by a down-field shift in the ^1H NMR spectra.

The binding behaviors of the macrocycles were solvent-dependent. Increasing the polarity of solvent by increasing the percentage of DMSO-d_6 in $CDCl_3$, diminished binding. The effect was so great with halides that at 50% DMSO-d_6 / $CDCl_3$, the M_2I complex formation could not be observed.

A three-dimensional polyamide **42** has been reported by Brown-James and co-workers.[88] Strong bindings of ligand **42** with anions were observed in $CDCl_3$ (log $K > 10^5$). However, in more polar solvent DMSO-*d6*, ^1H NMR titrations revealed a 1:1 binding model between **42** and anions and quantitative binding results were able to obtain. The highest binding constant was observed with anion F^- (log K = 5.0), followed by Cl^- (log K = 3.47), CH_3COO^- (log K = 3.38) and $H_2PO_4^-$ (log K = 3.30). The crystal structure analysis of its F^- complex demonstrated that F^- was centered in the cryptand cavity with hydrogen bonds to all six amide protons.

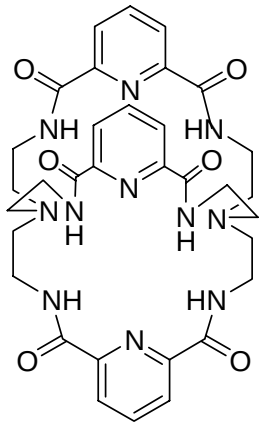

42

Stefan Kubik and co-worker have used cyclic peptide **43** as an anion receptor.[89] Electrospray mass spectrometry and NMR investigations suggested that **43** forms

sandwich type 2:1 complexes with many anions. According to crystal structure analysis, the guest resides in a cavity formed by the aggregation of two perfectly-shape-complementary molecules of **43**. A quantitative determination of binding stabilities of anions revealed that complex formation was cooperative. K_1, the stability constant of the 1:1 complex, was in every case significantly smaller than K_2, the equilibrium constant from the 1:1 to the 2:1 complex.

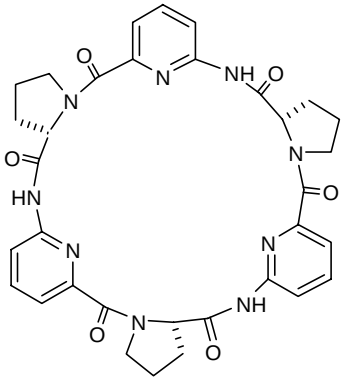

43

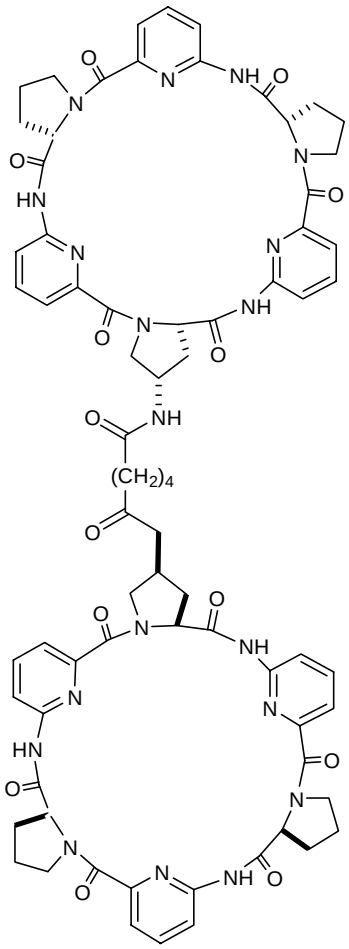

44

To further investigate their cooperative effect, a bis(cyclopeptide) **44** was synthesized.[90] Binding investigations showed that the **44** formed 1:1 complexes with halides, sulfate and nitrate, with the stability constants decreased in the order $SO_4^{2-} > I^- >$

$Cl^- > NO_3^-$. A comparison of the complexation stabilities of **44** with these of cyclopeptide **30** that forms 1:1 anion complexes showed that the presence of the second binding site increased complexation stability by a factor of 100-350.

1.7.3 Neutral Pyrrole Based Receptors

The calixpyrrole (named because of its resemblance to calixarenes) was first reported in the 1880's. However, its anion binding properties were not studied until 1996. Although, calix[4]pyrrole **45** possesses only a very small cavity, it can form four hydrogen bonds with anions, and was found to be able to bind small anions, such as F^- and Cl^-.[91]

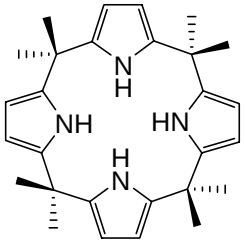

45

The compound is attractive because it is readily obtained in one step from the condensation of pyrrole and formaldehyde. However, its relatively small cavity prevents it from binding large anions effectively. To explore the area of pyrrole based anion receptors, Sessler and co-workers reported the synthesis and anion binding properties of the two bipyrrole-based marocycles **46** and **47** (Figure 1.15).[92]

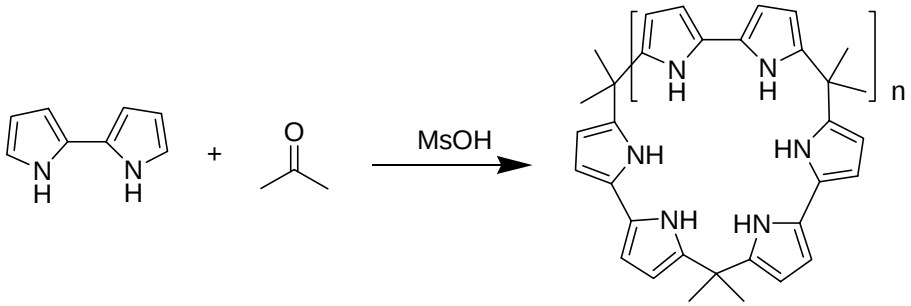

46 n = 1
47 n = 2

Figure 1.15 The synthesis of bipyrrole based macrocycles **46**, **47**.

Macrocycles **46** and **47** were synthesized in one step by the condensation of bipyrrole with acetone in the presence of a catalytic amount of methanesulfonic acid. Binding studies revealed that macrocycle **46** bound large halide anions in a 1:1 binding model, with affinities that were substantially enhanced compared to those of calix[4]pyrrole **45**.

Expanding pyrrolic anion receptors into the third dimension, Sessler and co-workers have reported the synthesis and binding studies of a family of calix[4]pyrroles bearing a single side diether straps **48**-**50**.[93] The straps were expected to provide additional hydrogen bonding sites and thus allow specific modulation of the inherent anion affinity. The results of NMR titrations revealed enchanced affinity for Cl^- and Br^- relative to calix[4]pyrrole. The anion binding ability of strapped calix[4]pyrrole can be effectively tuned by modifying the length of the straps. The largest Cl^- affinity was seen with the shortest strap, whereas the largest affinity for Br^- anion was recorded in the case of the longest strap.

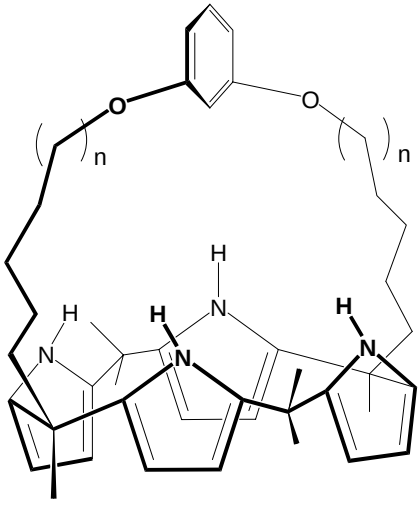

48 n = 1
49 n = 2
50 n = 3

1.7.4 Urea Based Receptors

Ureas are excellent hydrogen bond donors, and, thus, widely used in the design of synthetic receptors for anions. Gunnlangsson has employed anthracene derivatives **51**-**53** with aromatic or aliphatic thiourea moieties as fluorescent photo-electron transfer chemsensor for anions.[94]

A titration experiment using fluorescence spectroscopy demonstrated that the fluorescence of **51** was quenched upon addition of AcO^- in a solvent such as DMSO, $CHCl_3$ or CH_3CN. The highest degree of quenching was observed in DMSO. However, no binding was observed in the highly competitive hydrogen bonding solvent EtOH. Titration of **51** with common anions demonstrated that compound **51** selectively bound AcO^-, F^-, $H_2PO_4^-$. Thus, the fluorescence of **51** was quenched by AcO^-, F^- and $H_2PO_4^-$, but not Cl^- or Br^-. Similar results were obtained using ligands **52**, **53**.

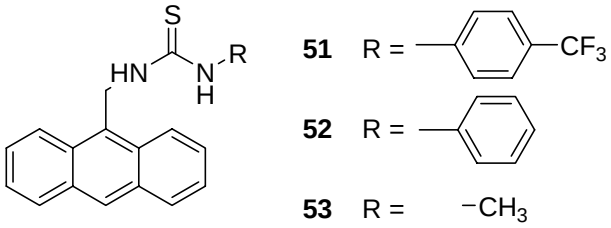

Another family of chemsensors based on thioureas were reported by Hong and co-workers.[95] The UV-Vis absorption of **54** in chloroform undergoes a red shift upon addition of $H_2PO_4^-$ anion. Clear isosbestic were observed on UV-Vis spectra, which demonstrated a 1:1 complexation. Compound **54**, with both azophenyl and nitrophenyl chemophores, has high selectivity of $H_2PO_4^-$ over other common anions. The degree of a red shift was determined to be $H_2PO_4^-$ >> AcO^- ≅ F^- > Br^- ≅ Cl^- > I^-. In the case of compound **55** with only an azophenyl group as the chromophore, the red shift upon complexation with $H_2PO_4^-$, F^- and AcO^- were similar, and thus no discrimination of anions was obtained.

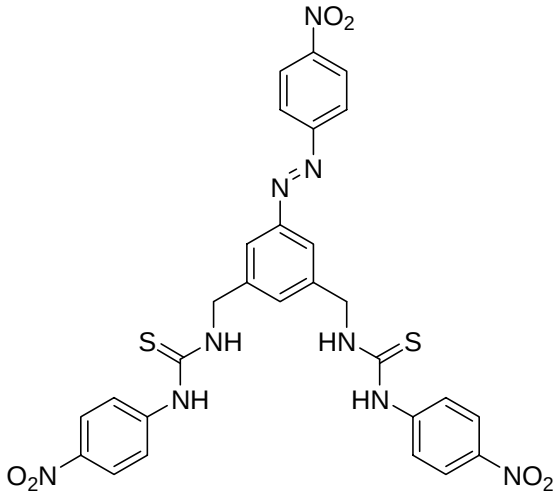

54

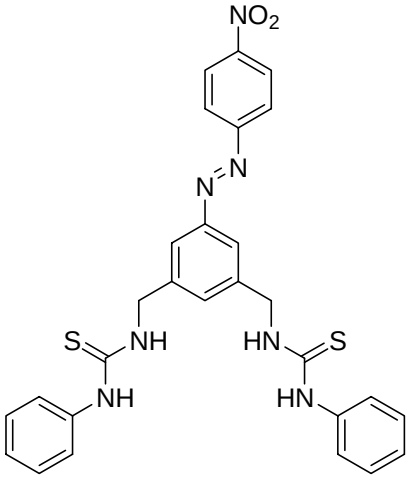

55

Hong and co-workers have continued to synthesize anion selective receptors.[96] Macrocycles **56**, **57** contain three thiourea units as linkers between aromatic groups. Both ligands displayed high affinities with anions. Macrocycle **57**, with extra ethyl groups, is conformationally more rigid. The binding results demonstrated that **57** had higher affinities with anions then **56**, with higher selectivity of AcO^- (K = 5300 M^{-1}) over $H_2PO_4^-$ (K = 1600 M^{-1}).

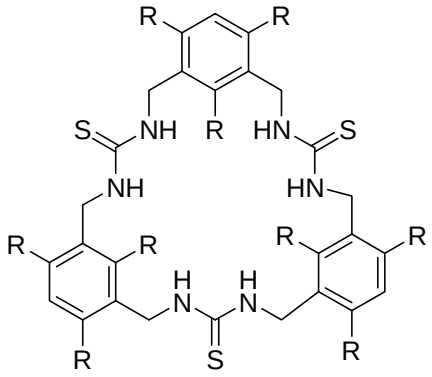

56 R = H
57 R = Et

1.8 Ditopic Receptors

The concept of ditopic receptor is relatively new in supramolecular chemistry. Those receptors simultaneously bind cation and anion, and thus often exhibit cooperative and allosteric effects whereby the association of one influence the binding affinity of the counter ion.[97-101] Such systems have potential as new selective extraction and transportation reagents for ion pair species of environmental importance and for zwitterion recognition.

1.8.1 Simultaneous Complexation of Inorganic Ion Pairs

To date, the design of ion-pair receptors have been based on hydrogen bonding, positively charged groups or Lewis acids to coordinate the anion, and crown ether or modified calixarenes to bind the cation. One early example of ditopic receptors was provided by Reetz and coworkers, who linked a Lewis acidic boron center to a crown ether.[102,103]

Compound **58** is capable of coordinating $K^+ \cdot F^-$ simultaneously. The crystal structure of the KF complex showed that K^+ was bound by the crown ether moiety, while the F^- was held by a combination of orbital overlap with the Lewis acidic boron atom and an electrostatic interaction with K^+.

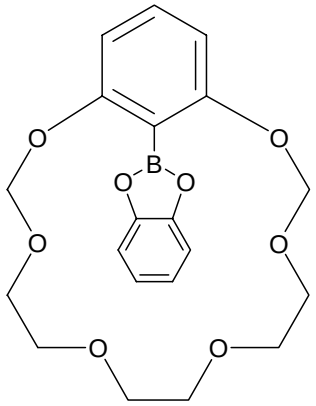

58

Beer and coworkers have synthesized a series of calixarenes-based ditopic receptors.[104-106] Calix[4]arene **59**, which was substituted at the lower rim by two benzo-15-crown-5, had very low affinity for anions alone. However, in the presence of K^+ or NH_4^+ cations, a sandwich complex is formed by the two crown ether units. This resulted in the amide groups being held close together, that along with the electrostatic attraction

of the cation, preorganized **59** to bind anions. Tetrahedrally shaped $H_2PO_4^-$ and HSO_4^- were found to be particularly strongly bound.[107]

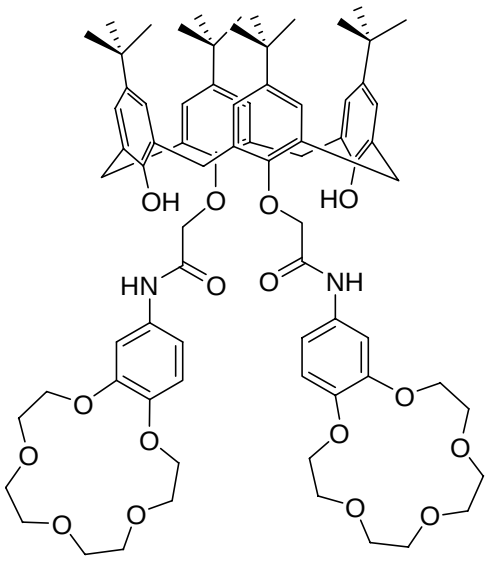

59

Another calixerene-based ditopic receptor was synthesized by Reinhoudt and co-workers.[108] Receptor **60** consists of a calix[4]arene with cation-binding ester groups at the lower rim and anion-binding urea groups at the upper rim. In chloroform, compound **60** adopts a pinched conformation due to intramolecular hydrogen binding between two urea groups. However, when sodium ion are added, cation binding to the ester groups of the calixarene alters the calix conformation, thereby breaks the hydrogen bond between two urea groups. This makes the urea groups available for anion guests, such as Cl^- and Br^- (Figure 1.16).

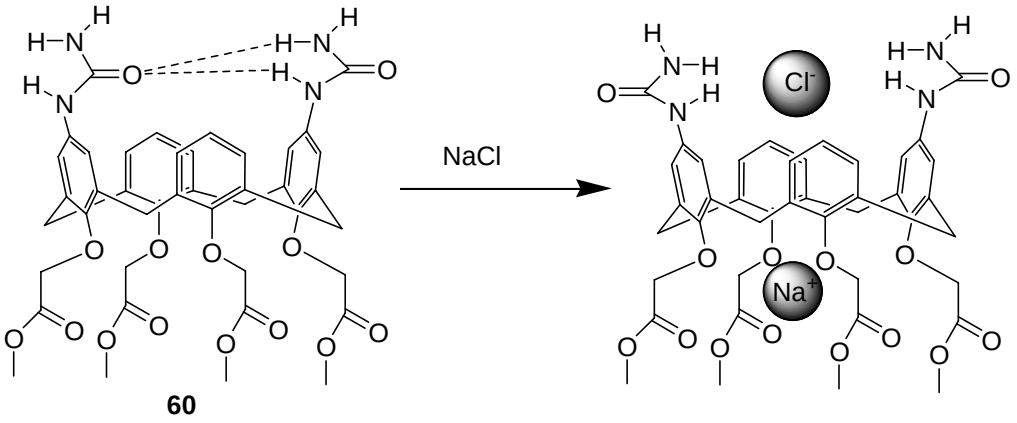

60

Figure 1.16 Simultaneous complexation of NaCl by calix[4]arene **60**

In another approach to the problem of ditopic receptor preparation, Beer and coworkers generated a di-calix[4]arene compound **61** connected by ethyl linkers, with two urea groups on one of the upper rims.[109]

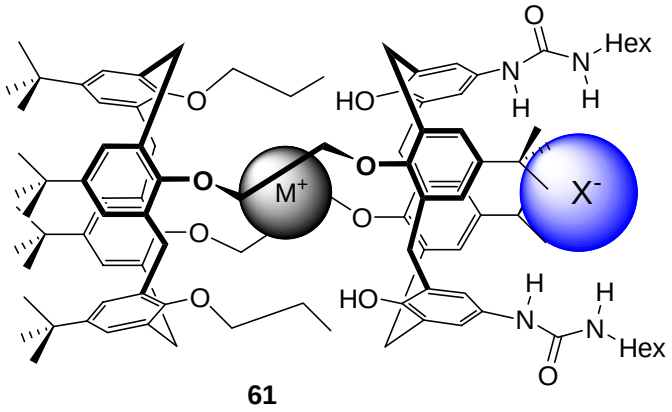

61

The receptor displays a remarkable selectivity for K^+ over all other alkali metal cations. Whereas **61** generally only binds halide and acetate anions very weakly, the Na^+ and K^+ complexes of **61** form much more stable complexes with these anions, with anion binding enhancements of over 30 fold in the case of Br^- ion.

Smith and coworkers have synthesized a pre-organised macrobicyclic receptor **62** with crown ether as metal binding site and bridging amide groups for anion bindings.[110] Binding studies of compound **62** revealed a weak binding with halide ions in a solvent system DMSO/CD_3CN (3:1). However, in the presence of one molar of Na^+ or K^+, halide affinities were significantly increased. The crystal structure of NaCl complex showed that in the solid state compound **62** bound NaCl as a solvent separated ion pair, with Na^+ bound within the crown unit, while Cl^- was hydrogen-bonded to the two amide residues (Figure 1.17).

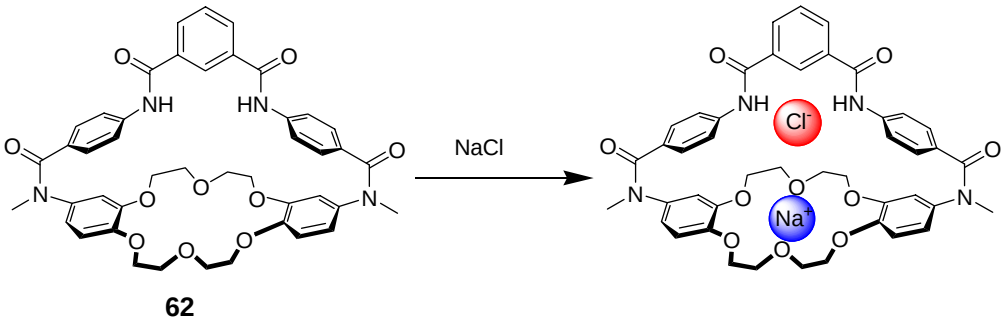

62

Figure 1.17 Simultaneous complexation of NaCl by ligand **62**

A more rigid macrobicyclic receptor **63** was prepared from the same group. The structure of compound **63** is very similar to **62**, but with a smaller distance between the anion and cation binding sites.[111] Results of ^1H NMR titration experiments demonstrated that Cl^- ion affinity normally displayed by **63** was significantly increased in the presence of K^+ (Figure 1.18). However, the more closely coordinated Na^+ had little effect.

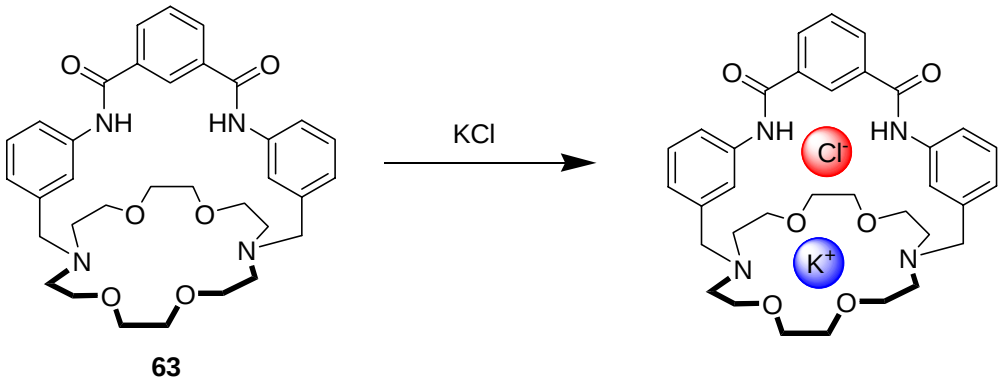

63

Figure 1.18 Simultaneous complexation of KCl by ligand **63**

1.8.2 Simultaneous Complexation of Organic-pairs

1.8.2.1 Carboxyl Salts and Zwitterionic Amino Acids.

Mendoza and coworkers have synthesized a carboxylate receptor **64** containing a guanidinium group (Figure 1.19).[112]

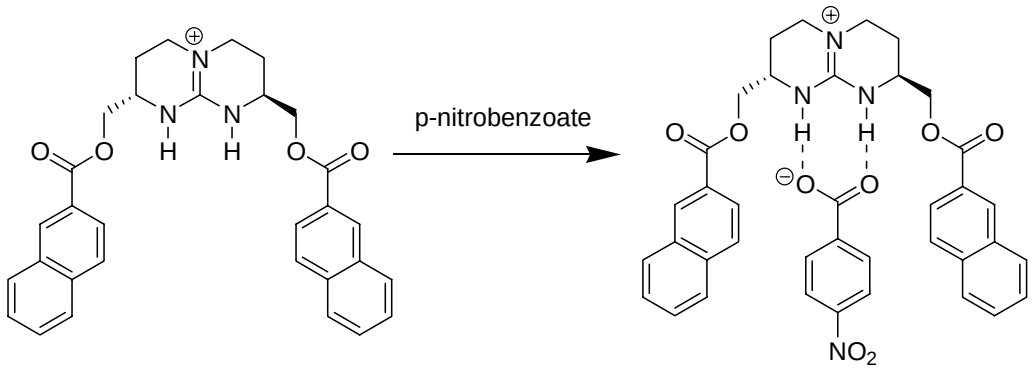

64

Figure 1.19 Complexation of *p*-nitrobenzoate with ligand **64**

Receptor **64** shows a preference for extracting sodium p-nitrobenzoate and Boc protected amino acids with aromatic side chains from water into chloroform. The gauanidium-carboxylate interaction is further enhanced by π-π stacking. However, free amino acids in zwitterionic form were not extracted from aqueous solutions by **64**. A

structure modification of **64** was then undertaken by incorporating a crown ether unit as a binding site for ammonium cation.[113] The results of extraction experiments revealed that receptor **65** had much higher affinities of amino acids. Thus, amino acids were extracted from aqueous solution into chloroform phase containing 1 equivalent of ligand **65**, with strong preference for amino acid with aromatic side chain, such as phenylalanine and tryptophan.

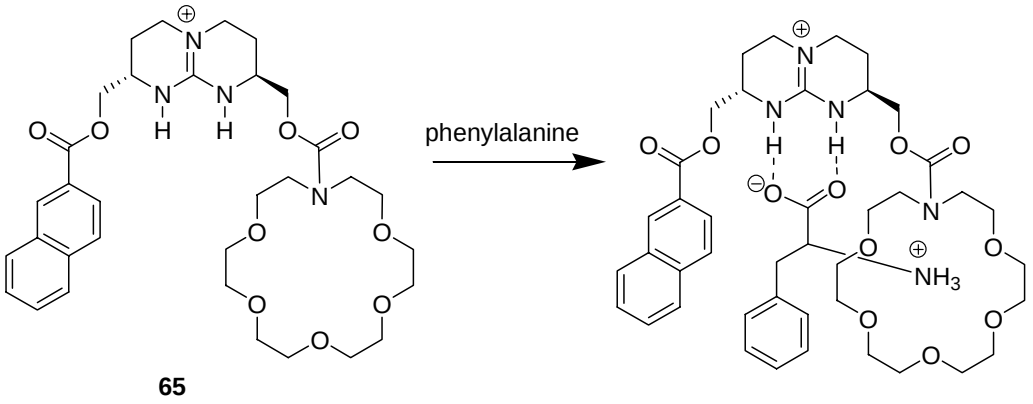

65

Figure 1.20 Complexation of phenylalanine with ligand **65**

A three–point binding mode has been proposed (Figure 1.20), with carboxylate bound by the guanidinium unit, ammonium cation by the crown, and π-π interaction between the phenyl side chain of the amino acid and receptor's naphthalene unit enchancing the strength of complex formation.

More recently, Sessler's group has synthesized two ditopic receptors based on the structure of sapphyrin and porphyrin.[114-116] The sapphyrin-lasalocid conjugate was found to be able to selectively transport aromatic amino acids. In direct competition experiments, L-phenylalanine was transported 4 times faster than L-tryptophan and 1000

times faster than L-tyrosine. On the other hand, none of the amino acids under investigation was transported efficiently by the porphyrin-lasalocid conjugate.

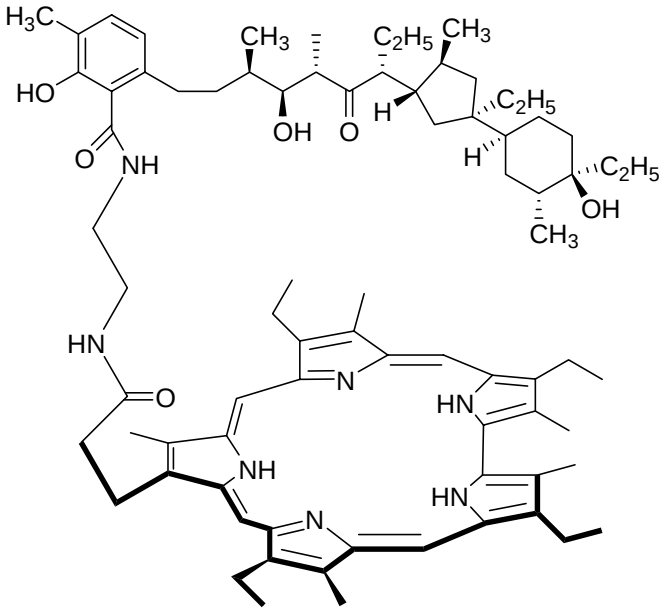

66

1.8.2.2 Tetraalkylammonium Cations

Among the various weak noncovalent forces that provide the basis for molecular recognition, the cation-π interaction between quaternary ammonium cations and aromatic hosts is receiving attention in recent years.[117-122] The synthetic receptors for binding quaternary ammoniums studies as far are mostly cyclic molecules, such as cyclophanes, crytophanes, calixarenes.

The binding between quaternary ammonium cations and host molecules generally occurs in organic solvents of low polarity. The nature of the counter anion is expected to influence host-guest association, either by cation-anion association or active participation in binding.

One approach to the design of receptors for quaternary ammonium cations employs cyclic peptides.[123] Stefan Kubik demonstrated that cyclopeptide **67** was able to bind ammonium cations by cation-π interactions. For the n-butyltrimethylammonium iodide complex, an associate constant of 300 M^{-1} has been determined in chloroform. Besides cations, cyclopeptide also binds anions via peptide N-H hydrogen bonds. Anion complexation results in an increase of the cation affinity by a factor of 10^3-10^4. Thus, cyclopepetide binds n-butyltrimethylammonium tosylate with $K_a = 3.88 \times 10^6\ M^{-1}$. The positive coorperativity of counter anions could be correlated with the preorganization of the cyclic-peptide by the anion as well as electrostatic interactions between anionic and cationic substrates in the final complex.

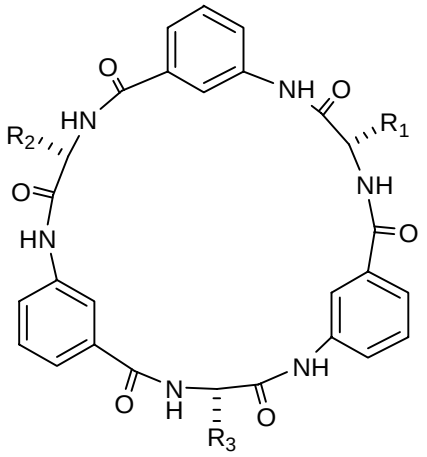

$R_1 = R_2 = R_3 = CH_2CH_2COOCH(CH_3)_2$

67

Roelens and coworkers have extensively studied the binding properties of macrocycle **68** with tetramethyl ammomium.[124] The results from ^1H NMR titrations in $CDCl_3$ revealed a dramatic variation of binding constants for the same complex with different counter anions. The author hypothesized that the anion effect could be correlated to the charge dispersion instead of the anion size.

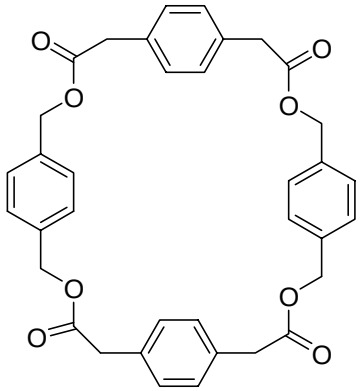

68

1.9 Enantioselective Receptors

The development of enantioselective receptors continues to be a challenging endeavor for supramolecular chemists.[125-127] As a special case of molecular recognition, enantioselective recognition involves discrimination between enantiomers of a guest by a chiral receptor or a chiral matrix.

The formation of the stable complex between host and guest molecules is a primary requirement for enantiomeric recognition. No recognition is observed if complexes are not formed. Interaction between host and guest species results in a proper conformation of the diastereomeric complexes, creating an appropriate environment for enantiomeric recognition. In principal, enantiomeric recognition stems from the steric repulsion between the substitutes at the chiral portions of the host and guest species. A reasonably large steric repulsion results in good enantiomeric recognition.

To date, most of the enantiomeric recognitions are based on hydrogen bonding.[128-133] The most studied host systems are the macrocylic crown ethers and cryptands. Other host molecules include: calixarenes, spherands and urea or guanidinium-based receptors.

Amino acids and their derivatives are the most studied guest molecules, due to their significance in biology and readily availability of pure enantiomers.

1.9.1 Enantiomeric Recognition of Amino Acid Derivatives through Ammomium Cation Binding.

The first chiral macrocyclic compounds were reported by Cram and co-workers in 1973.[144] Compound **69** has no specific chiral carbon atom. However, the relative orientation of the two binapthyl groups result in a twisted, chiral conformation. Ligand **69** was found to be able to recognize D-enantiomer assessed by two phase liquid-liquid extraction experiments. The chiral recognition factors range from 3 for $C_6H_5CH(CO_2Me)NH_3^+$, down to 1 for $C_6H_5CH(CO_2H)NH_3^+$.

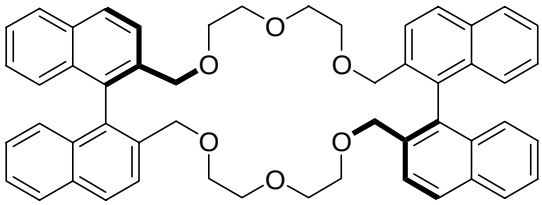

69

Since then, many binapthyl containing macrocycles have been synthesized and their chiral recognition properties studied.[145-150] A dramatic increase in chiral recognition provided by attachment of two methyl groups onto the binapthyl group of compound **69** has been observed. Compound **70** has the chiral recognition factor of 31 for $C_6H_5CH(CO_2Me)NH_3^+$, compare to a chiral recognition factor of 3 with host **69**.[146] The dramatic increase in chiral recognition is due to a greater steric repulsion of the methyl

groups with one enantiomer of ammonium cations in the less stable diastereomeric complexes.

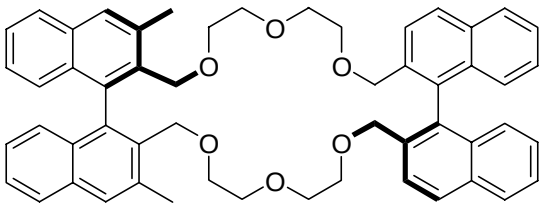

70

A C_3-symmetrical macrocycle **71** as selector of amino acid derivatives was recently reported by Shinkai and co-workers.[143] A 1:1 complexation mode between compound **71** and primary ammonium cations was determined by ^{1}H NMR titration experiments. The association constants for the L-configured guest were greater than S-isomers. The largest chiral discrimination (74% ee) was observed for the picrate salt of phenylalanine ethyl esters. The results proved their molecular design concept that a C_3-symmetrical skeleton would be very effective for chiral recognition of optically active alkyl ammonium ions.

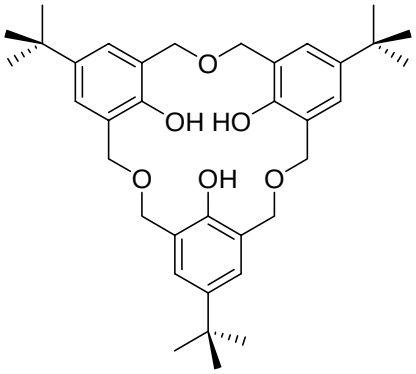

71

By incorporating a terpyridine unit into a crown ether macrocycle, Kwong and co-workers have synthesized a novel macrocyclic fluorescent sensor **72** for enantiomeric recongnition of amino acid derivatives.[151] The results obtained from fluorometric

titration demonstrated that compound **72** bound primary ammonium salts in a 1:2 binding model, with stronger binding with S-enantiomers than R-enantiomers (K_{Obs} = 4.2 × 10^{10} and 1.2 ×10^{10} M^{-1} for the S and R phenyl glycine respectively).

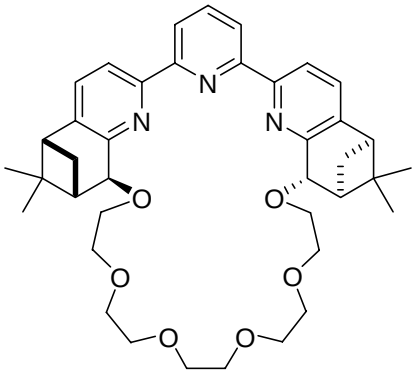

72

Although numerous synthetic receptors have developed for recognition of α-amino acid derivatives, little progress has been made for the enantiomeric recognition of β-amino acid.[152] To this contribution, Ahn and coworkers reported a rational approach to the recognition of β-chiral primary ammonium ions through bifurcated hydrogen bonding. The C_3-symmertric tripodal oxazoline receptor **73** was found to be able to enantioselectively bind ammonium salts of β-chiral amines (Figure 1.21). The chiral recognition factors of a variety of guests studied ranged from a high of 5 down to a low of 1. A hydrogen bond donor group in the β position of the guest molecule plays a critical role in the chiral discrimination, by forming the bifurcated hydrogen bond.

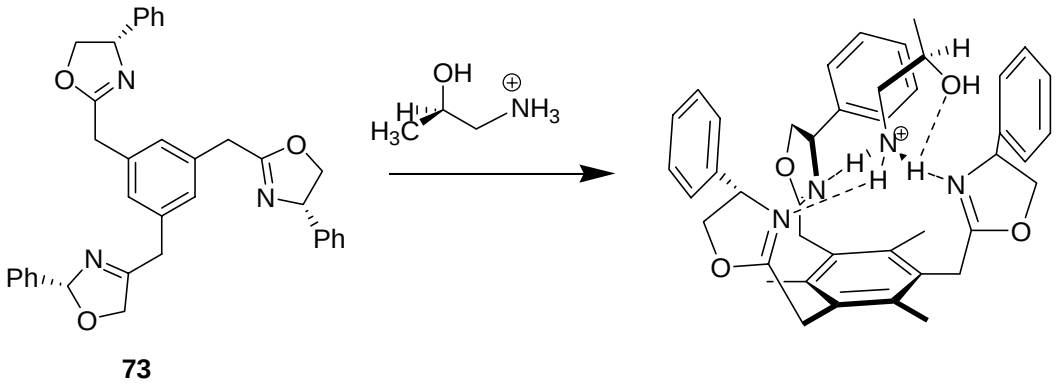

Figure 1.21 Enantiomeric recognition of amino acid derivatives by receptor **73**

1.9.2 Enantiomeric Recognition of Amino Acid Derivatives through Carboxylate Binding.

In general, the molecular recognition of caboxylate anions has been based on the multi-hydrogen bond interactions between host and guest.[153,154] One approach to design a receptor of carboxylates is by incorporating a guanidinium moiety. Guanidinium salts remain protonated over a wide pH range (pK_a = 13.5), and the binding of carboxylate combines an electrostatic interaction with a bidentate hydrogen binding pattern (Figure 1.22).

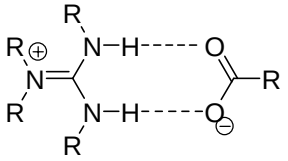

Figure 1.22 Binding model between guanidinium salts and carboxylate

Davis and coworker have described enantioselective carboxylate receptors **74**, **75** created by attachment of a monocyclic guanidinium salt to a cholic acid scaffold.[155-157]

Solutions of **74** and **75** were able to extract N-Ac-α-amino acids from neutral or basic aqueous solution via exchange of chloride for carboxylate. Receptor **74** proved remarkably consistant in its ability to differentiate between enantiomers of the N-Ac-α-amino acids (L:D=7:1) in all cases, regardless of side chain bulkness. Receptor **75** was more sensitive to side chain structure with L:D selectivities between 5:2 and 9:1, the greatest selectively being observed with phenylalanine.

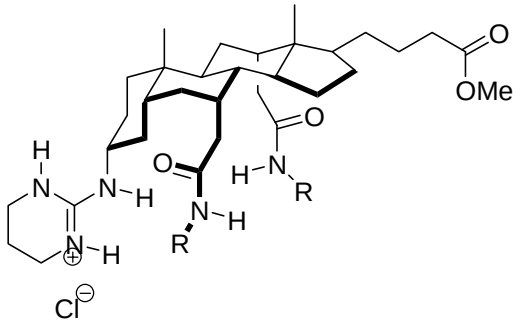

74 R =

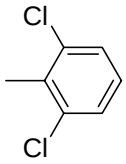

75 R =

To increase binding of guanidinium salts to carboxylates by incorporating additional hydrogen bonding functionality, Schmmck has recently described guanidinio-carbonyl pyrrole receptor such as **76**.[158,159] Receptor **76** bound N-Ac-α-amino acid carboxylates in 40% H_2O / DMSO (K_a = 3.5×10^2 to 5.3×10^3 M^{-1}) with enantioselectivity of L-isomers over D-isomers.

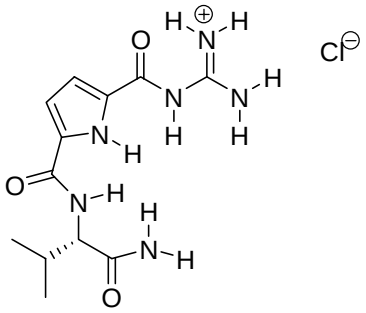

76

Despite lacking the electrostatic complementarity offered by guanidinium salt, ureas and thioureas have been shown to provide a binding site for carboxylates. Kilburn and coworkers have described the enantioselective binding of N-protected amino acid by an acylic thiourea receptor **77**.[160] Results from NMR titration with a range of amino acid carboxylates demonstrated that receptor **77** bound selectively with amino acids which have electron rich aromatic side chains. Receptor **77** also exhibited enantioseletivities with a general preference for L-amino acids, e.g. for N-Ac-Gln-CO_2^- (L:D ≈ 2:1).

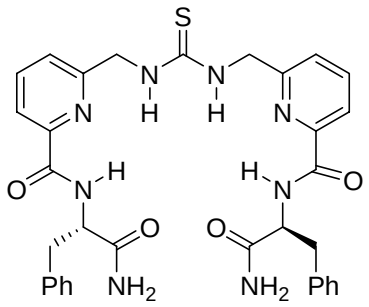

77

More recently, Kilburn has synthesized a macrocyclic receptor **78**, which features two thiourea moieties flanked by carboxyl pyridines and separated by a chiral diamine.[161] Receptor **78** was designed to bind amino acids containing two carboxylates, such as Glutamate, by forming up to eight hydrogen-bonding interaction with carboxylate oxygen atoms. The intramolecular hydrogen bonding between pyridine unit and thiourea or amide hydrogen helps preorganize the receptor. NMR titration in CH_3CN indicates that the macrocycle exhibits remarkable enantioselective 1:1 binding of N-Boc-glutamate (K_a = 2.8 ×10^4 for L-isomer and 2.2×10^3 M^{-1} for D-isomer).

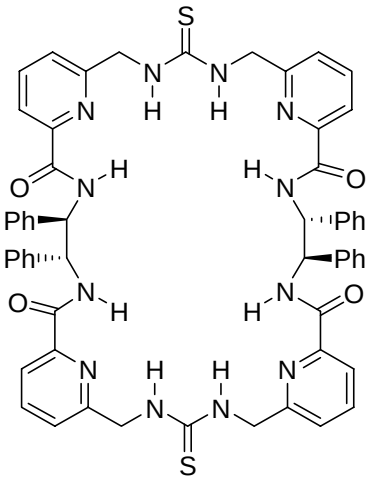

78

1.9.3 Enantiomeric Recognition of Zwitterionic Amino Acids.

The design of a synthetic receptor for amino acids in zwitterionic form remains challenging in supramolecular chemistry. In neutral aqueous solution, zwitterionic amino acids are highly hydrophilic and strongly solvated. The electronic densities at the carboxylate and ammomium functions are greatly affected by their mutual vicinity, causing the binding forces of complementary groups of the receptor to be less effective for the complexation. When extracting zwitterionic amino acids selectively from aqueous environment into some less polar organic phase, the salvation shells around the carboxylate and ammonium moieties must be replaced by dedicated ligands with specifically interact with these epitopes and compensate for the energetic cost of desolvation.

An elegant example of enantioselective receptor for zwitterionic amino acids was provided by Meneloza and coworkers. Receptor **65** was found to be able to extract amino acids from aqueous solution into chloroform. Its chiral recognition was also confirmed by the observation that the corresponding D-enantiomers were not extracted.

Schmidtchen synthesized a related receptor **79** that was found to be able to extract amino acids from aqueous solution into dichloromethane.[162] The most hydrophobic guests were extracted best, and even quite hydrophilic amino acids, such as glycine and serine had respectable extraction efficiencies. The highest binding affinities (K_a = 1810 M^{-1}) were observed with L-phenylalanine. Receptor **79** was also found to favor extraction of L-phenylalanine (40% ee) into dichoromethane from a mixture of phenylalanine in an aqueous solution.

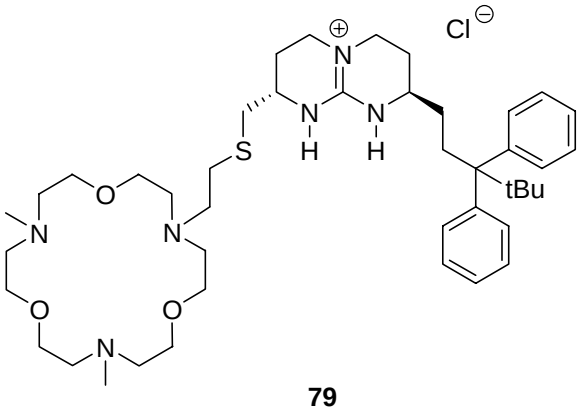

79

A chiral basket-shaped receptor for amino acids was recently reported by Escuder and coworkers.[163] Compound **80** provides a variety of interaction sites with amino acids. The binding constants with amino acids investigated were in the range of 10^3-10^5 M^{-1}. Remarkable enantioselectivity for D-tyrosine (D:L ≈ 8:1) was observed. The reverse enantioselectivity of the complex with phenylalanine as compared to tyrosine and tryptophan (which contain phenolic and indole nitrogen groups respectively,) was due to hydrogen-bonding interactions inside the cavity.

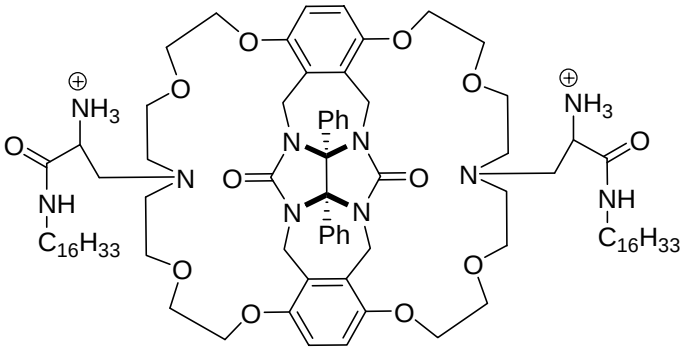

80

II Toward the Mimicry of Carbonic Anhydrase

Carbonic Anhydrase is a zinc enzyme which catalyzes the reversible hydration of CO_2. In the enzyme, the catalytically essential zinc ion is tetrahedrally coordinated to three histidine residues and a highly acidic water molecule (pK_a = 7.3). The catalytic activities of Carbonic Anhydrase are known to be dependent on the ability of zinc bound water to deprotanate at physiological pH (Figure 2.1).[10]

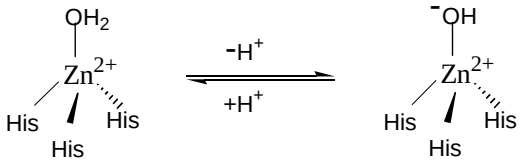

Figure 2.1 Deprotonation of bound water

Small molecules have been used extensively to mimic the active site of Carbonic Anhydrase.[5,8] These complexes have been invaluable in confirming the Lewis acid behavior of the zinc ion, and the coordination modes of substrates in the active site of Carbonic Anhydrase. Tridentate ligands possessing sp^2 nitrogen donors represent the ideal type of Carbonic Anhydrase mimic. However, despite the efforts, few studies have produced structurally characterized tetrahedral zinc complexes that mimic the active site of Carbonic Anhydrase.[28,29] The tetrahedral zinc coordination model has proven

extremely difficult to replicate in free solution due to the highly Lewis acidic zinc ion. Thus, the initially formed $[ZnL]^{2+}$ complex undergoes further reaction to form the thermodynamically more stable $[ZnL_2]^{2+}$ complex, or hydroxy-bridged dimers $[LZn\text{-}O\text{-}ZnL]^{2+}$.[22,23] For example, tris(imidozyl)methanol **3** and tris(pyridyl)methanol **10** do not give tetrahedral species, but rather form $[ZnL_2]^{2+}$ sandwich-type complexes (Figure 2.2). Without a zinc-bound hydroxide these complexes cannot act as CA mimics.

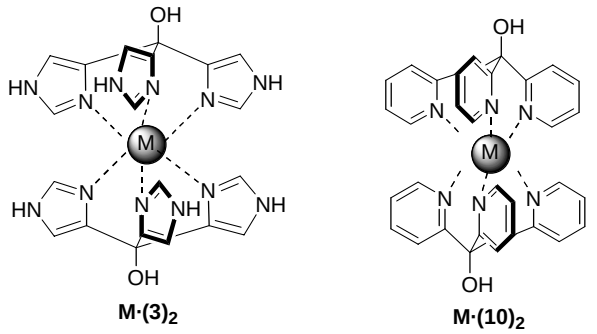

Figure 2.2 Formation of $[ZnL_2]^{2+}$ sandwich complexes

In view of these problems, it is evident that success at modeling the active site of Carbonic Anhydrase requires sufficient steric barriers around the metal center to ensure that the deleterious formation of $[ZnL_2]^{2+}$ sandwich complexes cannot occur. Thus, a tetrahedral zinc complex was obtained with tris(pyrazolyl)borate ligands when the R group was sufficiently large, e. g. R and R' = *tert*-butyl (Figure 2.3).[32]

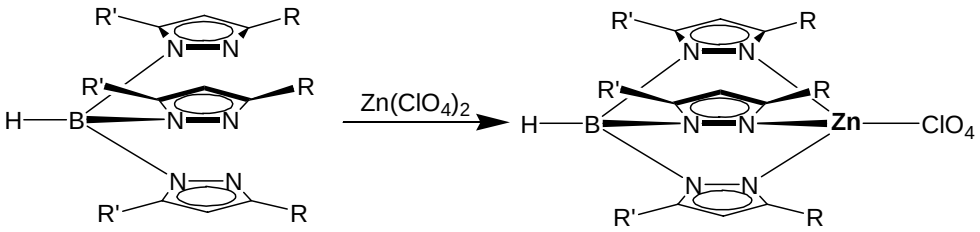

5 R, R' = *tert*-butyl

Figure 2.3 Formation of tetrahedral zinc complex with tris(pyrazolyl)borate **5**

Efforts from this laboratory towards the Carbonic Anhydrase mimicry have been focused on the synthesis of *tris*(2-pyridyl)methanol derivatives.[164] *Tris*(2-pyridyl)methanol was reported in 1951 as an analogue to triphenyl methanol.[165] The easy synthesis and facial zinc binding of the ligand provide a good model compound for Carbonic Anhydrase. However, work relating to the structural modified *tris*(2-pyridyl)methanol derivatives as potential Carbonic Anhydrase mimics is rare.[25,40] Hannon *et. al*. have recently reported an elegant approach in inhibiting the formation of $[ZnL_2]^{2+}$ complexes by generating a dendritic hydrophobic cavity around metal complex.[40] An attractive feature of this approach is the potential of systematic varying the nature of the cavity and to generate different coordination environment of the complexes. However, despite the considerable advances, there remains a dearth of information regarding what controls the interplay between the 1:1 and 2:1 complexes of *tris*(2-pryidyl)methanol ligands. We were interested in how structural and electronic features of the substituents affect the zinc binding behavior of *tris*(2-pyridyl)methanol derivatives.

2.1 Synthesis and Binding Studies of 'First Generation' Ligands

Tris-(2-nicotinic acid)methanol methyl ether **85** was previously synthesized in this laboratory in four steps, starting from 2-bromo-5-methyl pyridine **81** (Scheme 2.1).[164]

Scheme 2.**1**. Synthesis of *Tris*-(2-nicotinic acid)methanol methyl ether **85**

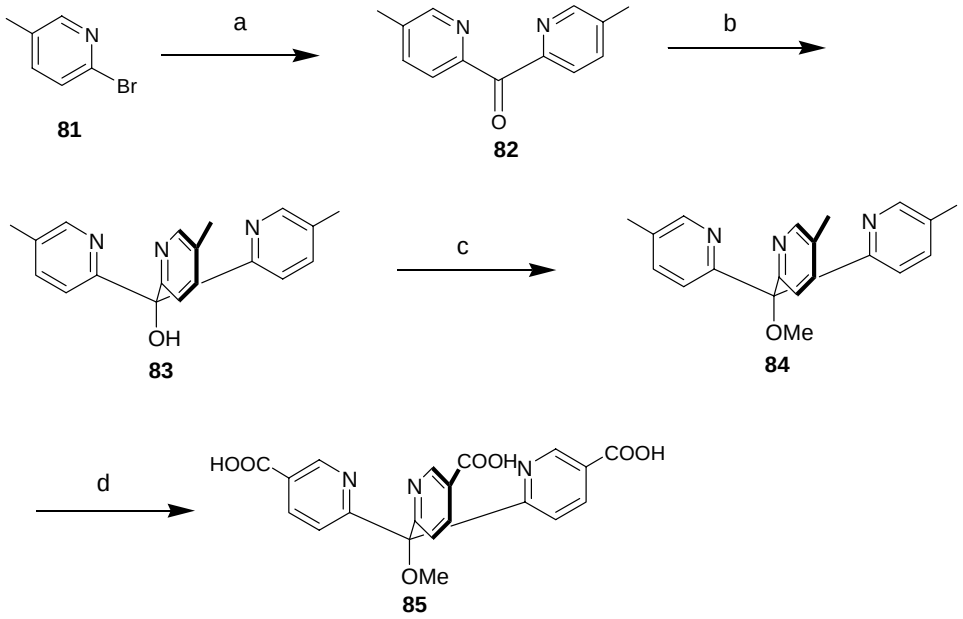

Key: (a) (i) *n*-BuLi, ether; (ii) $(EtO)_2CO$, 70%; (b) 2-lithio-5-methyl-pyridine, THF, 70%; (c) NaH, MeI, THF, 95%; (d) $KMnO_4$, water, 85%.

Our structural modification of *tris*(2-pyridyl)methanol ligands started with compound **85**, by attaching amino acid derivatives onto the pyridyl rings. Three amino acids were chosen, with different functionalities and steric properties. Using standard peptide bond forming technologies, the 'first generation' ligands **86-88** were readily obtained in good to excellent yield (Scheme 2.2). Ligands **88** offers maximal amount of steric protection against the formation of $[ZnL_2]^{2+}$ complexes, due to the bulky benzyl groups. The hydroxyl groups on ligand **87** has two opposite effects on the complex formation: it offers some steric protection, whilst also promoting the possibility of $[ZnL_2]^{2+}$ formation via

hydrogen bonding. The zinc binding studies of these ligands were carried out using ^{1}H NMR spectroscopy by examining 1:1 mixtures of ligands and zinc perchlorate, in a number of pure solvents.

Scheme 2.2 The synthesis of ligands **86-88**

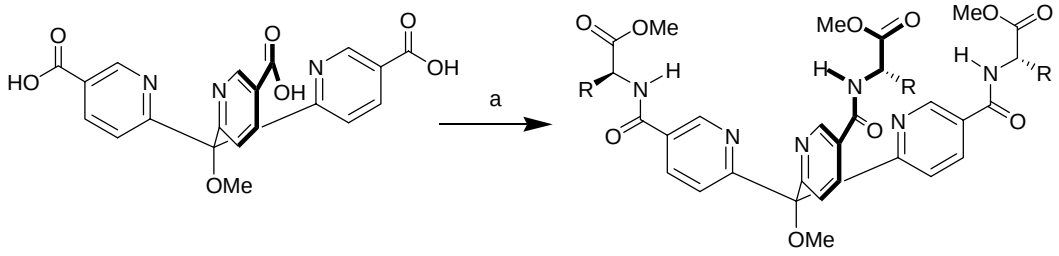

85

86 (R = H)
87 (R = CH_2OH)
88 (R = CH_2Ph)

Key:

(a) HBTU, Et_3N, DMF, respective amino acid methyl esters, 65-95%

Three species are present in the solution of a 1:1 mixture of the ligand and zinc perchlorate: free ligand L, $[ZnL]^{2+}$ and $[ZnL_2]^{2+}$. Each species gave distinguish peaks in the NMR spectrum (Figure 2.4), indicating slow exchanges between free ligands and complexes on the NMR time scale. To identify each peak, two-dimensional NMR (COSY and EXSY) experiments were carried out (Figure 2.5, 2.6). The H-6 signal (Figure 2.4) of the $[ZnL]^{2+}$ complex on the NMR spectrum underwent a 1 ppm lowfield shift upon complexation. However, it is shifted upfield to 7.34 ppm in the $[ZnL_2]^{2+}$ complex. This upfield shift probably occurs because H-6 in the $[ZnL_2]^{2+}$ complex lies very close to the plane of a pyridyl group of a second ligand and is therefore shielded by the latter's ring current.[25]

The percentages of each species were then determined by taking integrations of the corresponding peaks in NMR spectra. The results, summarized in Table 2.1, demonstrate

that a combination of electron withdrawing substituents on the pyridine rings, and strongly donating solvents such as DMSO, inhibit the binding of zinc to ligands **86**-**88**. Thus, no bindings were observed of amino acid derivatives in DMSO. In less competitive solvents such as acetonitrile, binding is stronger and no free ligand is observed. The similar complexation properties of **86** and **88** suggests that the phenylalanine side chain does not inhibit formation of the $[ZnL_2]^{2+}$ complex. Ligand **87** forms the most $[ZnL_2]^{2+}$, suggesting that in acetonitrile, the hydroxyl groups are involved in hydrogen bonding.

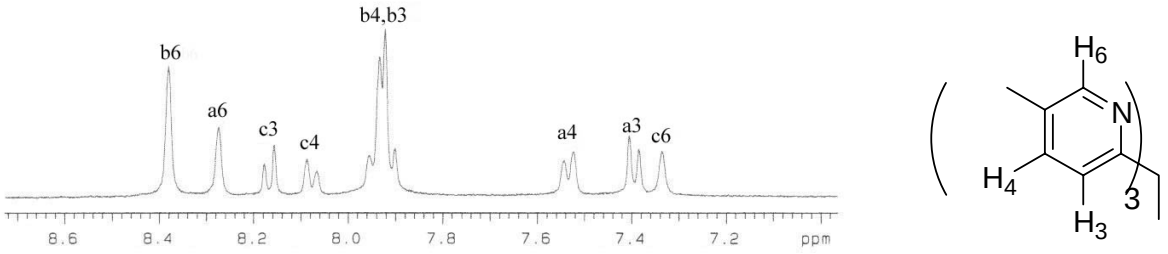

Figure 2.4 ^{1}H NMR of a 1:1 mixture (1 mM) of ligand **84** and zinc perchlorate in DMSO. The labeled signals correspond to free ligand (a), $[ZnL]^{2+}$ (b) and $[ZnL_2]^{2+}$ (c).

From an enzyme mimicking point of view, water is the most relevant of solvents. However, ligand **88** was insufficiently soluble in aqueous solution. Although ligands **86** and **87** gave a homogeneous solution in D_2O, only weak bindings were observed, with the predominant species in the mixture being free ligand.

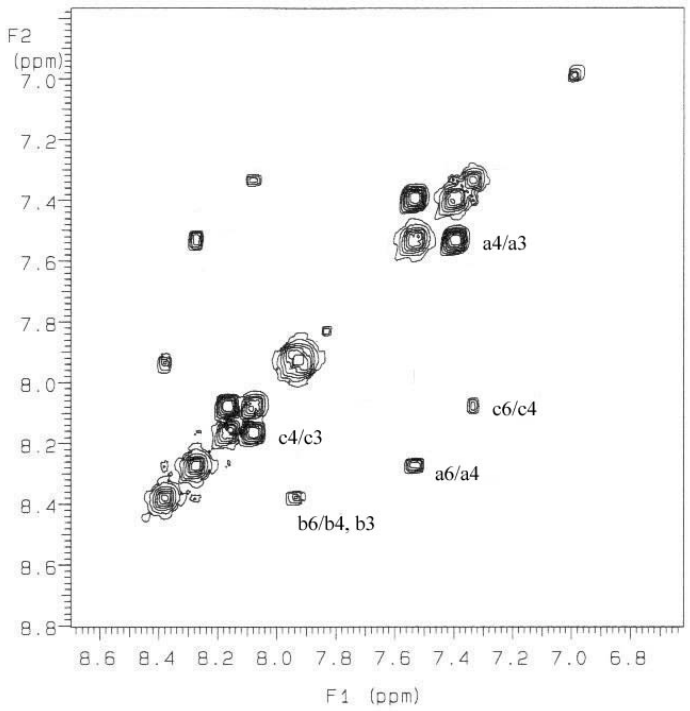

Figure 2.5 ^{1}H NMR COSY spectrum of a 1:1 mixture (1 mM) of ligand **84** and zinc perchlorate in DMSO. The labeled cross peaks correspond to the interactions between numbered protons in free ligand (a), $[ZnL]^{2+}$ (b) and $[ZnL_2]^{2+}$ (c).

Table 2.1 Equilibrium distribution[a] (25 ˚C) for 1:1 mixtures of Zn^{2+} and the 'first generation' ligands (free L : ZnL : ZnL_2)

ligand	DMSO	CD_3CN	D_2O
86	-[b]	0 : 82 : 18	70 : 30 : 0
87	-[b]	0 : 67 : 33	74 : 26 : 0
88	-[b]	0 : 85 : 15	-[c]

[a] Errors are within 5%; [b] No binding was observed. [c] Ligand was insufficiently soluble in water;

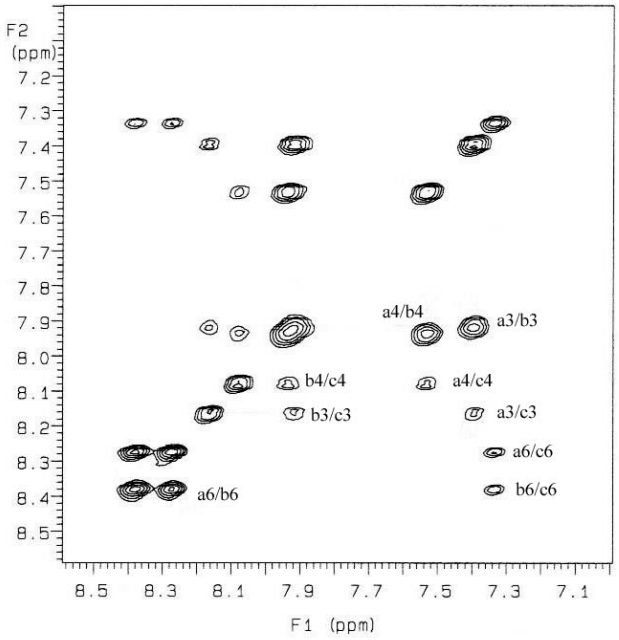

Figure 2.6 ^{1}H NMR EXSY spectrum of a 1:1 mixture (1 mM) of ligand **84** and zinc perchlorate in DMSO. The labeled cross peaks correspond to the exchange between free ligand (a), $[ZnL]^{2+}$ (b) and $[ZnL_2]^{2+}$ (c).

These results demonstrate that in water, the formation of $[ZnL_2]^{2+}$ complexes can be inhibited by limited steric shielding. Thus, both ligands **86**, **87** gave a mixture of free ligand and $[ZnL]^{2+}$ complexes, no $[ZnL_2]^{2+}$ species were detected. However, zinc binding to ligands **86, 87** is too weak to be an efficient Carbonic Anhydrase mimics. There are two possible reasons for the weak binding: 1) a steric interaction between the H-3 on each pyridine ring and the MeO methyl group, which destabilizes the complex; 2) the electron deficiency of the pyridyl nitrogen atoms due to the electron withdrawing groups on the pyridine rings (Figure 2.7).

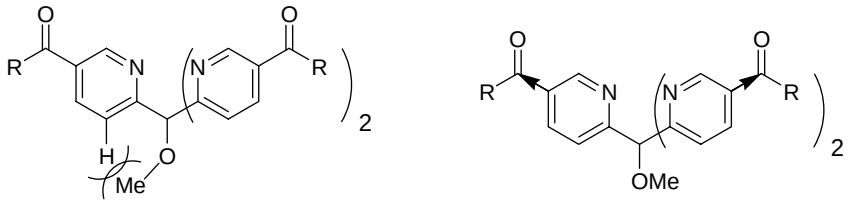

Figure 2.7 Schematic represent of two major causes of weak binding

2.2 Synthesis and Binding Studies of 'Second Generation' Ligands

CPK model of ligand **84** indicates the steric interaction between H-3 and MeO methyl group. To examine if the remote methyl group diminishes binding, we studied the zinc binding properties of ligand **84** and demethylated derivative **83** (Table 2.2). In DMSO, ligand **83** complexed Zn^{2+} more strongly. No free ligand left when a 1:1 mixture was formed. Furthermore, ligand **89**, with a larger MOM group on the tertiary alcohol, does not bind to zinc in DMSO. With these results in hand, we synthesized ligands **91**-**93** (Scheme 2.3). The required **90** could not be isolated in good yield by the oxidation of previously reported **83**. Thus, **83** was protected as its MOM ether **89**, which was oxidized with $KMnO_4$, and deprotected to yield **90**. Coupling reactions gave 'second generation' ligands **91**-**93** in good to excellent yield.

Scheme 2.3 The synthesis of ligands **91-93**

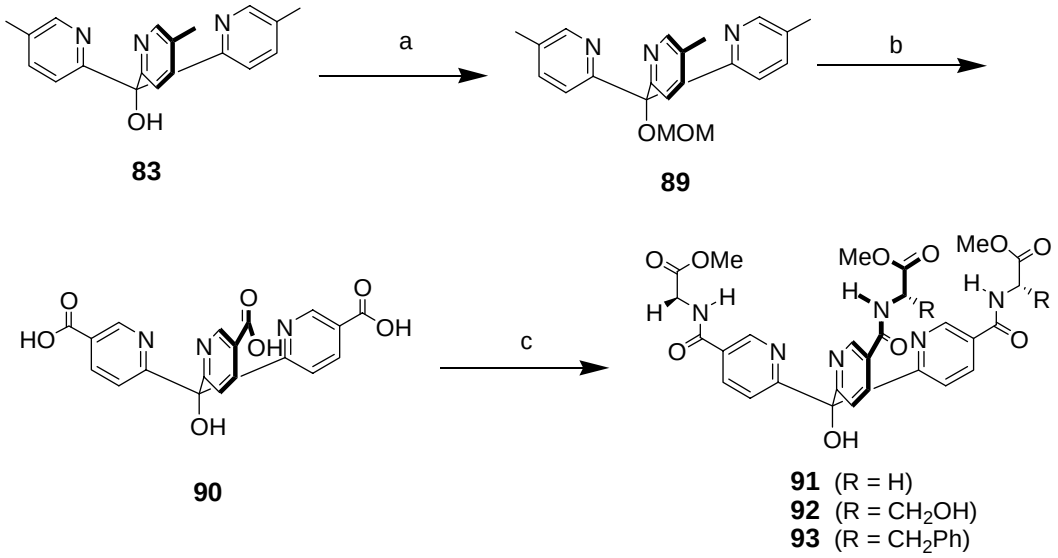

Key: (a) NaH, MOMBr, THF, 98%; (b) $KMnO_4$, NaOH, H_2O, 60°C, 16h, then 20% aq. HCl 85%; (c) HBTU, Et_3N, DMF, respective amino acid methyl esters, 60-88%.

In DMSO and acetonitrile, the binding properties of **91-93** were similar to ligands **86-88**. However in water, Zn^{2+} binding was noted to be stronger (Table 2.2). Thus, for both ligand **91** and **92**, $[ZnL]^{2+}$ complex predominates in the mixture, with small amount of free ligand and trace $[ZnL_2]^{2+}$ complex. A comparison of the binding constants for Zn^{2+} binding to **86** and **91** reveals a 40 fold increase by simply removing the methoxy methyl group ($K_a = 6.0 \times 10^2\ M^{-1}$ and $2.4 \times 10^4\ M^{-1}$ respectively).

Table 2.2 Equilibrium distribution (25 ˚C) for 1:1 mixtures of Zn^{2+} and the 'second generation' ligands (free L : ZnL : ZnL_2)

ligand	DMSO	CD_3CN	D_2O
83	0 : 80 : 20	0 : 69 : 31	0 : 0 : 100
84	77 : 23 :0	0 : 67 : 33	-[b]
91	-[a]	0 : 76 : 24	18 : 78 : 4
92	-[a]	0 : 71 : 29	22 : 72 : 6
93	-[a]	0 : 80 : 20	-[c]

[a] No binding was observed; [b] A precipitate formed upon mixing **84** and Zn^{2+}; [c] Ligand was insufficiently soluble in water.

One problem of tridentate ligands as Carbonic Anhydrase mimics is the formation of oxygen-bridged dimer.[22,23] At physiological pH, the zinc bound water deprotonates to form a highly reactive zinc bound hydroxyl species. The latter nucleophilic attacks another zinc bound water species to form catalytic inactive oxygen-bridged zinc complex (Figure 2.8).

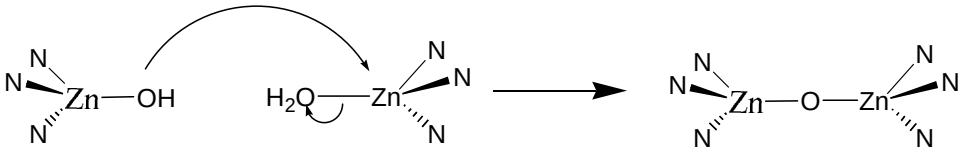

Figure 2.8 Formation of oxygen-bridged zinc complex.

To examine for the possible formation of oxygen-bridged zinc dimer, we used electrospray mass spectrometry to examine the 1:1 mixture of ligand **91** and zinc perchlorate in water. The mass spectrum exhibits signals at m/z 609, 640, 771 and 1380, corresponding to $[LH]^+$, $[ZnL_2]^{2+}$, $[ZnLClO_4]^+$ and $[ZnL_2ClO_4]^+$. No signals

corresponding to hydroxy-bridged dimer were observed (Figure 2.9). The isotopic distribution of the signals matches the theoretical calculation in all cases.

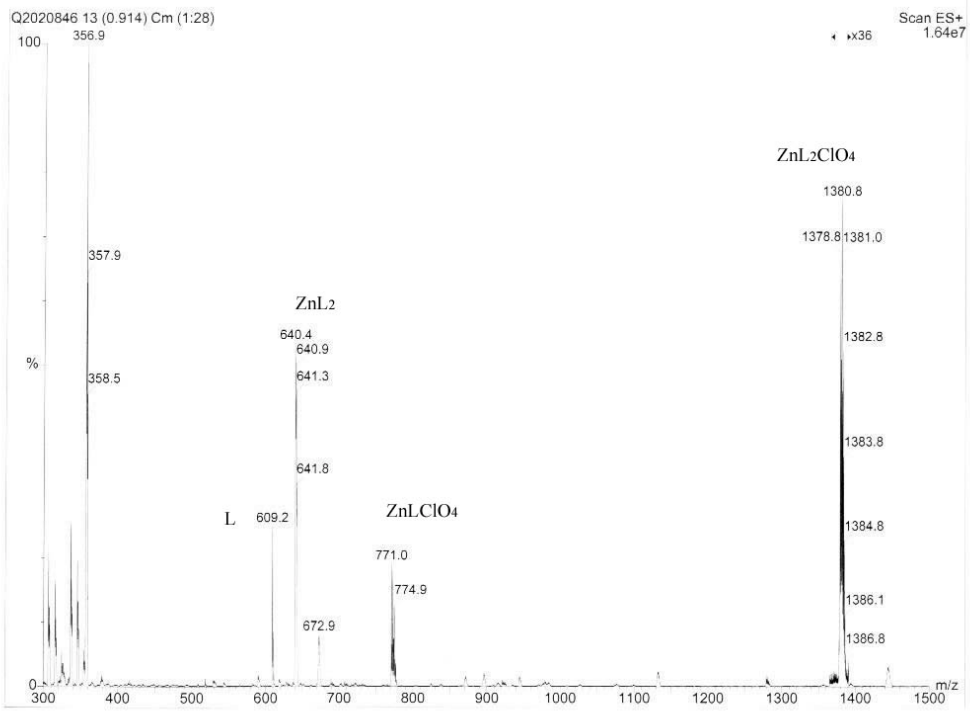

Figure 2.9 ES mass spectrum of a 1:1 mixture (1 mM) of ligand **91** and zinc perchlorate in H_2O.

2.3 Synthesis and Binding Studies of 'Third Generation' Ligands

Although the second generation ligands exhibit a significant increase in the zinc binding properties, it is still not strong enough to allow 1:1 complexes to be formed at low concentrations (the concentration at which a catalyst might be used). To further increase zinc binding, as well as investigate the electronic effects of the substituents, we designed a third family of ligands with electron donating groups on the pyridine rings (Scheme 2.4). Thus, instead of the electron-withdrawing carbonyl groups, –NH groups are connected to the pyridyl rings. The synthesis of the new 'generation' of ligands started with *tris*-acid **90**. Thus, **90** was treated with diphenylphosphoryl azide in THF to afford *tris*-azide **94**. Curtius rearrangement of **94** by refluxing in dry *t*-BuOH gave *tris*-

BOC **95** in good yield. Attempts to convert **90** to **95** directly by reflux in *t*-BuOH in the presence of DPPA were unsuccessful. Free amine **96** was then obtained in high yield by acid hydrolysis of **95**.

Table 2.3 Equilibrium distribution (25 ˚C) for 1:1 mixtures of Zn^{2+} and the 'third generation' ligands (free L : ZnL : ZnL_2)

ligand	DMSO	CD_3CN	D_2O
100	- [a]	0 : 80 : 20 [b]	0 : 53 : 47
102	- [a]	0 : 86 : 24 [b]	- [c]
103	- [a]	0 : 70 : 30 [b]	0 : 59 : 41

[a] No binding was observed; [b] 10% D_2O was added as co-solvent;
[c] Ligand was insufficiently soluble in water.

Scheme 2.4 The synthesis of ligands **100**, **102** and **103**

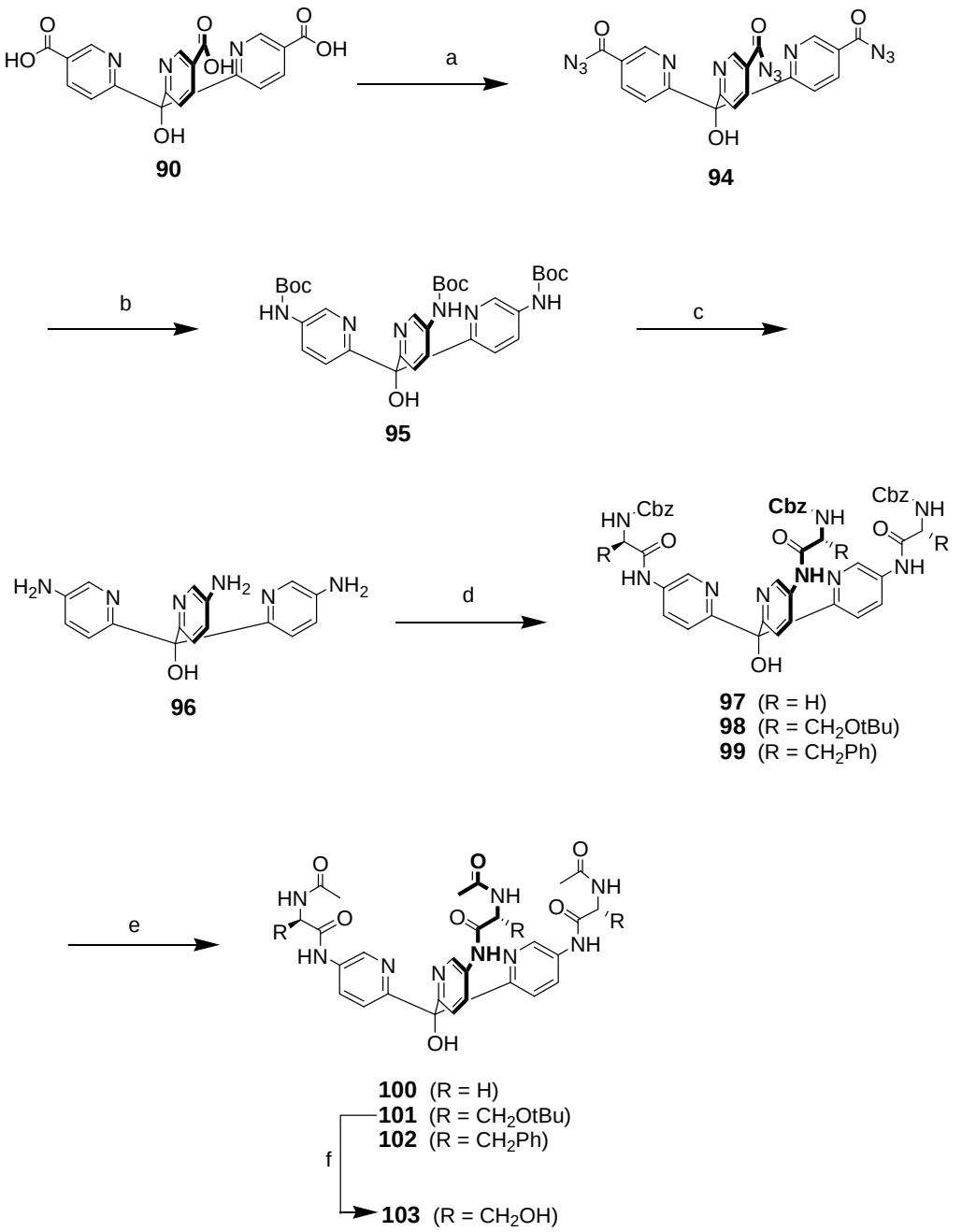

Key: (a) DPPA, Et_3N, THF, 75%; (b) *t*-BuOH, reflux, 80%; (c) 20% aq. HCl, 90%; (d) HBTU, HOBT, Et_3N, DMF, respective N-Cbz amino acids, 45°C, 70-75%; (e) H_2, Pd/C, acetic anhydride, MeOH, 80%; (f) TFA, 65%.

Attempts to couple free amine **96** and N-acetyl protected amino acids were unsuccessful, only starting materials were recovered. However, coupling with N-Cbz protected amino acids went smoothly to afford ligands **97-99** in high yield. The Cbz groups were then converted to acetates by palladium catalyzed hydrogenation in the presence of acetic anhydride to give ligands **100-102**. Removal of the *t*-Bu group on **101** with TFA afforded ligand **103**.

Zinc binding studies demonstrated that the new generation of ligands complexed zinc ion more strongly in water (Table 2.3). Thus, both **100** and **103** gave a mixture a $[ZnL]^{2+}$ and $[ZnL_2]^{2+}$compexes in solution, with no free ligand left.

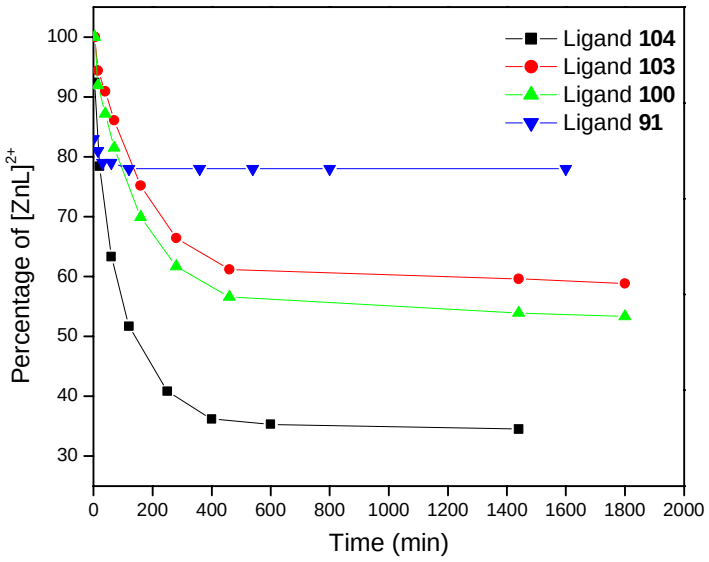

Figure 2.10 Change of the percentages of $[ZnL]^{2+}$ in aqueous solution as a function of time.

Interestingly, changing of the electronic properties of the substituents causes a significant difference of the kinetics of complex formation for these ligands. For ligands **100** and **103**, only $[ZnL]^{2+}$ complexes were present immediately after mixing the ligands and zinc perchlorate. However, the kinetically favored $[ZnL]^{2+}$ complex was unstable in the solution. Its concentration decreased slowly over a time period of nine hours to hold constant at around 50-60% (Figure 2.10). The decrease of $[ZnL]^{2+}$ complex was mirrored by a corresponding increase in the proportion of thermodynamically more stable $[ZnL_2]^{2+}$ sandwich complex. In contrast, ligands **91** and **92** gave equilibrated mixtures in a matter of minutes. To examine this kinetic phenomenon further, the less sterically hindered ligand **104** was synthesized by N-acylation of *tris*-amine **96** (Scheme 2.5). Ligand **104** has the similar kinetics to ligands **100** and **103** (Figure 2.10). However, devoid of any steric shielding, the corresponding equilibrated mixture contained a much larger proportion of the $[ZnL_2]^{2+}$ sandwich complex. Thus for these ligands, relatively small steric barriers influenced the position of the equilibrium between $[ZnL]^{2+}$ and $[ZnL_2]^{2+}$, whereas the electronic properties of the substitutents both influenced this equilibrium and the kinetics of complexation.

Scheme 2.5 The synthesis of ligand **104**

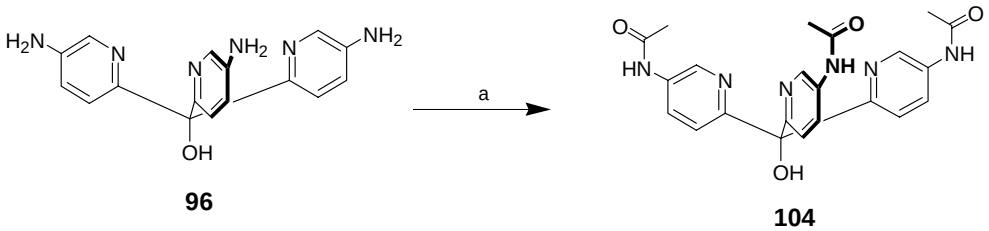

Key: (a) DMAP, acetic anhydride, DMF, 65%.

2.4 Kinetic Studies: Toward the Hydrolysis of *p*-nitrophenyl Acetate and Phosphate Esters

The essential biological function of Carbonic Anhydrase is the catalytic hydration of CO_2. However, esters have also been observed to be catalytically hydrolyzed by Carbonic Anhydrase (Scheme 2.6).[10] Model compounds which possess the same function played by Carbonic Anhydrase have constantly been interesting enzyme mimic subjects. Various types of metal complexes have been synthesized for this purpose. So far the most successful model complexes have employed Co^{3+} or Cu^{2+} ions,[166-168] which however, are not the same metal ion as in Carbonic Anhydrase. On the other hand, only a few successful models with Zn^{2+} complexes have been reported, with the most successful example being the cyclic-polyamine ligands.[42]

Scheme 2.6 Catalytic hydrolysis of esters by Carbonic Anhydrase

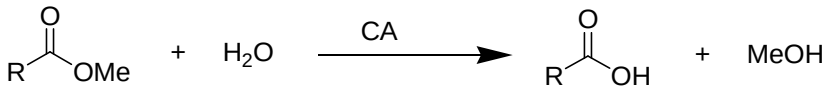

Our ultimate goal of Carbonic Anhydrase mimic is to develop efficient catalysts for ester hydrolysis. Our investigations of structurally modified *tris*(2-pyridyl)methanol derivatives have demonstrated that the binding properties of the ligands are closely related to the structural and electronic features of the substituents on the pyridyl rings. $[ZnL]^{2+}$ can be obtained with the limited steric shielding. For the 'third generation' ligands, although the initially predominated $[ZnL]^{2+}$ complex was unstable, it decreased slowly and eventually held constant at around 50-60%. This slow kinetic process will have little effect on its catalytic activity if the kinetics of ester hydrolysis is faster. With

this in mind, we carried out the catalytic studies of the metal complexes of *tris*(2-pyridyl)methanol derivatives.

The hydrolysis of *p*-nitrophenyl acetate was measured at 25 ^{o}C by an initial slope method following the increase in the 400 nm absorption on UV-spectra. The reaction followed good pseudo-first-order kinetics both in the presence and absence of the complex. Ligand **100** and **103** were used for the kinetic studies with a concentration ranges from 1.0 mM to 5.0 mM. Unfortunately, the hydrolysis rate constants in the presence of the complex are essentially the same as spontaneous hydrolysis reactions (at 25 °C, pH 8.4, the rate constants are 2.5×10^{-5} M^{-1} s^{-1} and 2.4×10^{-5} M^{-1} s^{-1} in the presence and absence of zinc complex of ligand **100** respectively), which indicates that the ligands have no catalytic activities for the hydrolysis reactions. The possible reasons are: 1) binding between ligand and zinc ion is not strong enough; 2) an catalytic inactive oxygen-bridge dimer formed in the buffered solution.

In summary, we have synthesized a series of structurally modified *tris*(2-pyridyl)methanol derivatives. Zinc binding studies reveal that both steric, electronic properties of the substituents, as well as the nature of the group on the tertiary alcohol oxygen, control the thermodynamics and kinetics of complex formation.

III Investigation of the Ditopic Properties of Novel *Tris*(pyridyl)macrocycles

The design of synthetic cation or anion receptors possessing high affinities and selectivities is an important objective in supramolecular chemistry. Particular attention has been given in recent years to studies involving neutral receptors and charged guests in organic solvents of low polarity such as chloroform.[119-121] When recognition processes occur in these solvents, the counter ion of the charged guest become problematic since extensive cation-anion associations take place in media of low polarility. The host molecule does not simply bind a charged guest. However, ion-pairs are the actual guests present in the media. The binding of anions or cations occur through the formation of the complexes between hosts and ion-pairs. Thus, the nature of counter ion is expected to strongly, and usually adversely influence the host-guest association.[106-109]

There are several ways counter ions can adversely influence host-guest association in non-polar solvents. The counter ion can competitively form a stable ion pair thus decreasing host-guest association. Alternatively, the host-guest interactions, in most cases, do not afford sufficient energy gain to separate an ionic guest from its counter ion. As a consequence, the charge presented on the ionic guest is reduced by the counter ion because of extensive electrostatic interaction.[117-122] For example, receptor **68** binds

tetramethylammonium cation through cation-π interactions (Figure 3.1).[124] The binding strongly depends on the counter anions. The weaker the cation-anion attraction, the stronger the cation-π association.

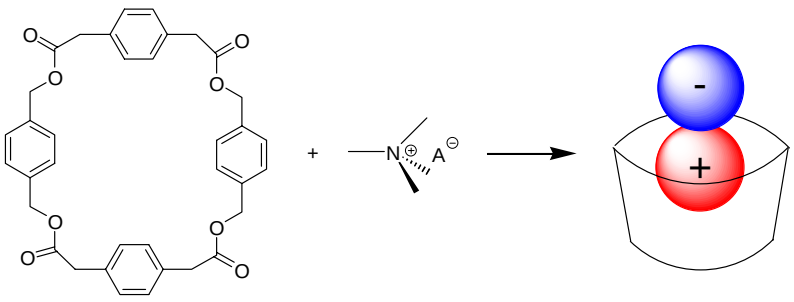

68

Figure 3.1 Schematic represent of counteranion affect on cation binding.

To minimize the affect of the counter ion, a common approach is to use a salt system with noncompetiting, low-coordinating counter ions.[97-99] For example, picrate salts are often used in cation binding studies, whilst tetrabutylammonium cation is often used as the counter ion in anion binding studies. However, the luxury of a noncompeting ion is not always available.[110,111]

More recently, thoughts have been turned to designing ditopic receptor that can simultaneously bind cationic and anionic species. In theory, ditopic receptors may exhibit coorperative and allostatic effects whereby the binding of one charged species facilitates the binding of the counter ion, giving a binding constant higher than that if only one species alone is bound.

Ditopic receptors to date have been based on hydrogen bonding, positively charged groups to coordinate anions, and crown ethers or modified calixarences to bind cations.

When both anion and cation bind to a single receptor, the electrostatic interaction between bound ion-pair usually results in a positive cooperative effect on host-guest association. High cooperativity has been seen when bound cation and anion form a tight ion-pair.[108,109]

Positive cooperativity can also be obtained from conformational changes induced by binding. The binding of anionic or cationic species preorganizes the host for the binding of counter ion, thus increasing the binding.[117]

Recent work with model systems has led to a number of ditopic receptors for inorganic salts,[169-172] zwitteronic amino acids[173-176] and tetraalkyl ammonium salts.[124] Although many examples of monoalkyl ammonium cation receptors have been reported,[125] little work has been done on the binding of salt pair.[177,178] Monoalkyl ammonium species are of significant interest since these compounds are basic building blocks of biological molecules. Studies of these compounds are important to mimic, understand and explore biological processes.

Smith *et al*. have recently reported a ditopic receptor which is capable of binding monoalkyl ammonium salts.[179] However, a systematic study of the anionic effect on the binding of monoalkylammonium cation has not been seen. Contributing to this area, we designed and synthesized a novel *tris*(pyridyl) macrocyclic receptor **105** for monoalkyl ammonium salt recognition (Figure 3.2). The dish-shaped macrocycle **105** has both hydrogen-bond receptors as well as donors, and thus, provides ideal binding sites for monoalkyl ammonium salts. The group of acceptors is comprised of three converging pyridine rings and an array of C=O groups. Two amide N-Hs function as hydrogen bond donors. The relative small ring size (16-membered), and the limited number of flexible

bonds, result in a highly rigid and preorgnized structure. We anticipate that the pyridines of receptor **105** hydrogen-bond the ammonium cation and the two amide groups coordinate the counter anion.

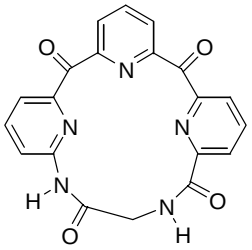

105

Figure 3.2 The structure of macrocycle **105**

3.1 Synthesis of Macrocycle 105

Our synthesis of macrocycle **105** started with the commercially available 2, 6-dibromopyridine **106** (Scheme 3.1 - 3.2). Formation of the corresponding lithiate *via* metal-halogen exchange with *n*-butyllithium followed by the slow addition of DMF gave the expected aldehyde **107** in 70% yield. Reduction of **107** with $NaBH_4$ gave alcohol **108**, which was protected as the ethoxymethyl ether **109**. The bromide **109** then served as the building block for the *tris*-pyridyl framework. Thus, formation of the corresponding lithiate of **109** and quenching with diethyl 2, 6-pyridinedicarboxylate, resulted in the expected diketone **110**. Unfortunately, the yield of this reaction is low due to the acidic proton on the 6-methylene group. The proton deprotonates in the presence of *n*-butyllithium, producing considerable amount of side products by nuclephilic attacking the diethyl 2, 6-pyridinedicarboxylate (Scheme 3.3).

The ethyoxymethyl ether protecting groups of compound **110** was then removed with dilute HCl in THF, and the resulting diol **111** was oxidized with potassium permanganate to afford desired diacid **112**. Monoester **114** was obtained in high yield by Fischer esterification of **112** to diester **113**, followed by hydrolysis with 1 equivalent of NaOH. Curtius rearrangement of **114** by refluxing in dry *t*-BuOH in the presence of 1 equivalent of diphenylphosphoryl azide (DPPA) afforded Boc protected amine **115**. The Boc group was then removed using trifluoroacetic acid and the resulting free amine **116** was coupled with N-Boc-glycine to give **117**. After the base hydrolysis of the ester group, the Boc group was removed in aqueous HCl solution to give the linear precursor **119** readily for macrocyclization. The cyclization reaction was conducted under high dilution condition with diphenylposphoryl azide as coupling reagent in 35% yield.

Scheme 3.1 The synthesis of macrocycle **105**

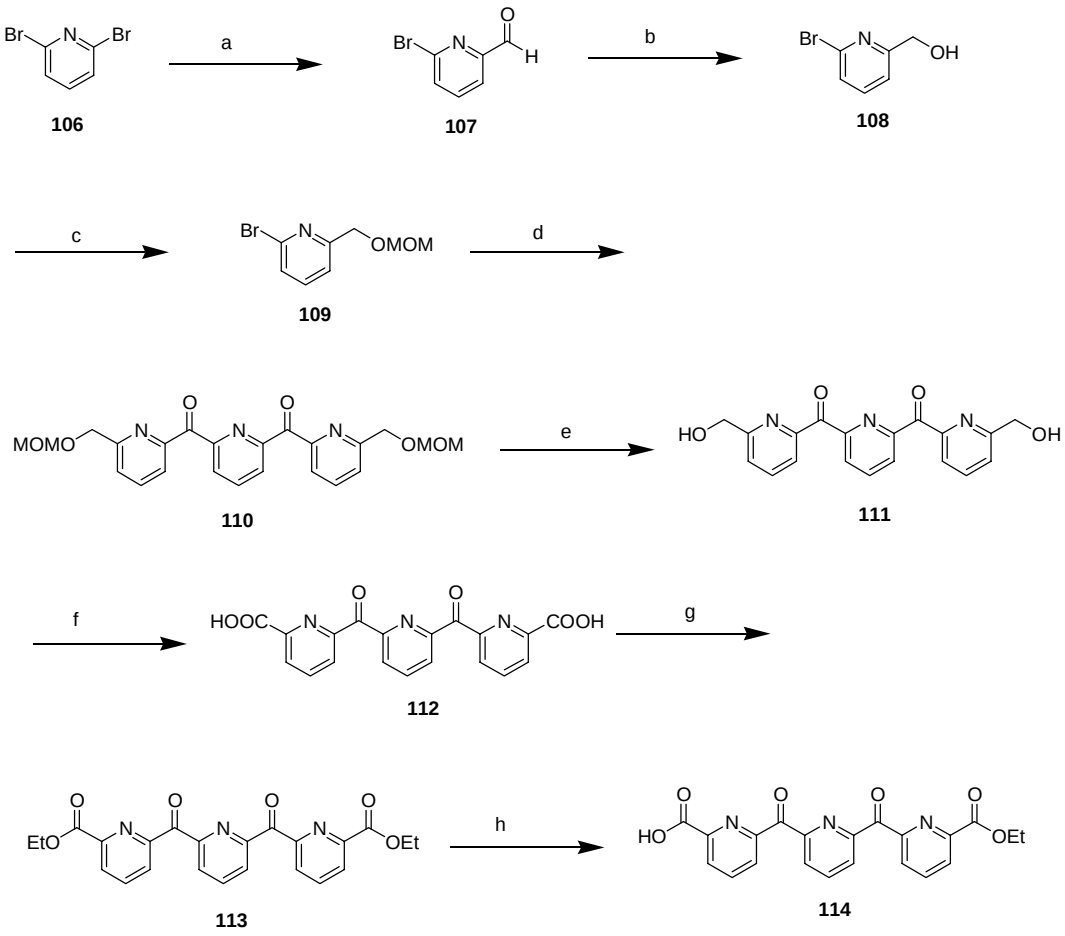

Key: a) n-BuLi, DMF, -78 °C, ether, 70%; b) $NaBH_4$, MeOH, 95%; c) $CH_3CH_2OCH_2Cl$, i-Pr_2NEt, DMF, 95%; d) *n*-BuLi, diethyl 2, 6-pyridinedicarboxylate, -78 °C, ether, 35%; e) 10% aq. HCl, THF, 90%; f) $KMnO_4$, acetone/H_2O, 80%; g) EtOH / HCl, 75%; h) 1 eq. NaOH, 65%.

Scheme 3.2 The synthesis of macrocycle **105** (continued)

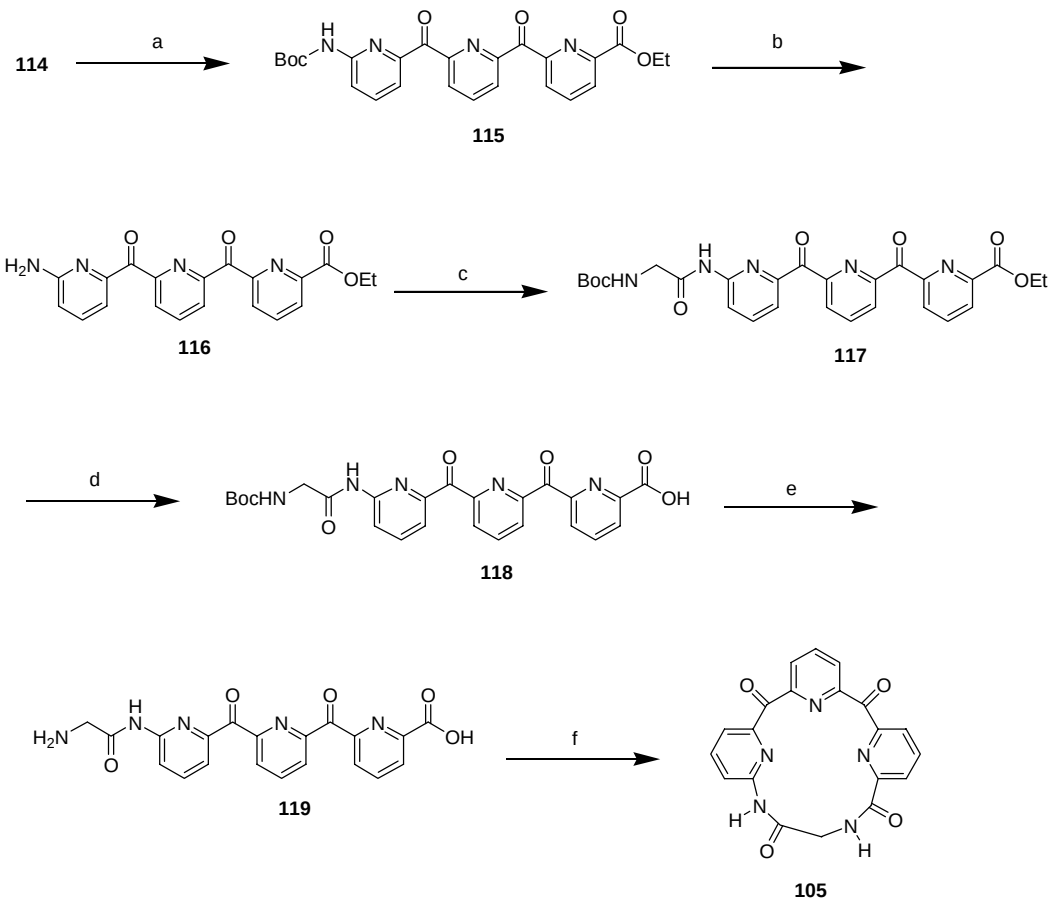

Key: a) DPPA, Et_3N, *t*-BuOH, reflux, 60%; b) TFA / CH_2Cl_2, 95%; c) Boc-glycine-OH, HBTU, HOBt, 60%; d) 1.1 eq. NaOH, 85%; e) 10% HCl, 80%; f) DPPA, DMF, 35%.

Scheme 3.3 Side reaction from synthesizing **110**

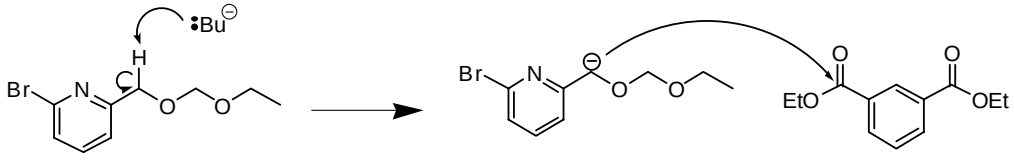

Macro-cyclizations have proven challenging in organic synthesis. Because of the formation of linear or polymeric side-products, the yield of cyclization reaction is usually low. Most of the cyclization reactions were thus carried out in high diluted condition to minimize the side reactions. In the current studies, we found the macro-cyclization was extremely sensitive to the initial concentration of the linear precursor. Thus, relatively high yield (35%) was obtained at 1 mM concentration of **119** (Table 3.1). On the other hand, no desired product was isolate at 10 mM concentration.

Table 3.1 The yield of the cyclization reaction at different concentration of **119**

Concentration (mM)	Yield (%)
1	35
2	25
5	10

Our strategy of macrocyclization is to use a coupling reagent to activate the carboxyl acid to form an active ester. The amine group then nuclephilic attacks the ester to form a new amide bond. Consequently, the yield of the cyclic reaction depends on the coupling reagents. So far, the best results were obtained when DPPA (Figure 3.3) was used as the coupling reagent. Low yields were obtained using HBTU or HATU (Figure 3.3). In addition to activate the carboxyl acid, these uronium-based reagents can also react with amine to form inactive guaridinated by-products during cyclization reaction (Scheme 3.4).

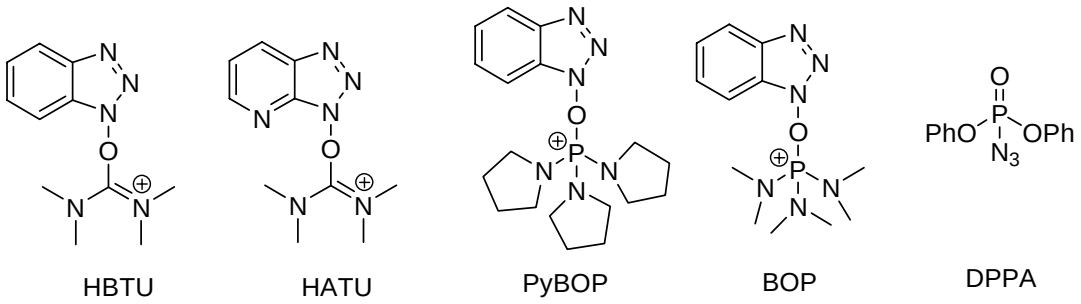

Figure 3.3 The structures of selected coupling reagents

Phosphonium-based reagents such as BOP and PyBOP generally give high yields of cyclization products. However, although there is evidence of the formation of desired product, the side product from BOP or PyBOP prevented us from isolating the desired compound.

Scheme 3.4 Formation of guaridinated by-products

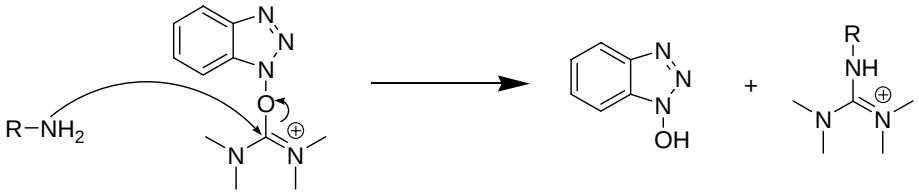

3.2 Optimized Synthesis of Diacid 112

Although the macrocycle synthesis has been proven successful, the overall yield was low. Therefore, an alternative synthesis was carried out to optimize the synthesis (Scheme 3.5). Thus, formation of the corresponding lithiate of **106** and quenching with diethyl 2, 6-pyridinedicarboxylate, resulted in the expected dibromide **120**. Refluxing of **120** with ethylene glycol in benzene in the presence of acid catalyst afforded the diketal **121** in high yield. The bromide was then substituted by cyanide groups by refluxing of **121** in pyridine in the presence of CuCN, and the resulting dicyanide **122** was hydrolyzed under acidic conditions to yield the diacid **112**. Vigorous hydrolysis conditions were employed in this reaction to ensure complete ketal to ketone conversion. The new synthesis of diacid **112** was two steps less than the initial synthesis with much higher yield of the desired product (the overall yield of synthesizing **112** is 43%, compared to a yield of 16% of the previous synthesis).

Scheme 3.5 Optimized synthesis of diacid **112**

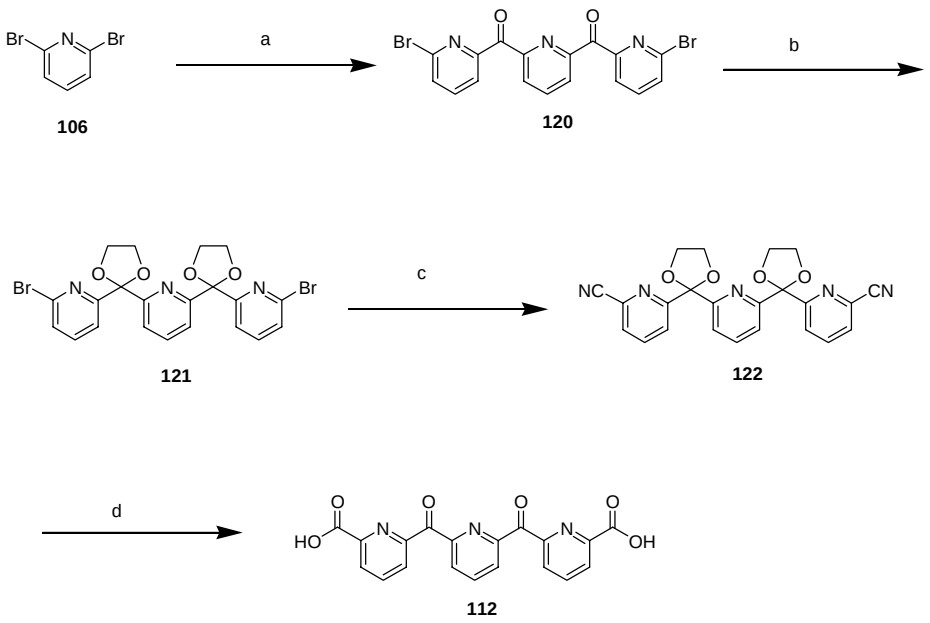

Key: a) *n*-BuLi, diethyl 2, 6-pyridinedicarboxylate, -78 °C, ether, 65%; b) TsOH, ethylene glycol, benzene, reflux, 2 days, 75%; c) CuCN, pyridine, reflux, 6 hours, 98%; d) Conc. HCl, reflux, 3 days, 90%.

3.3 Anion Binding Studies

The conformational behavior of macrocycle **105** in solution was investigated by NOESY experiment and FT-IT spectroscopy. The NOESY spectrum of **105** in DMSO-d_6 exhibits the cross-peaks between H_1-H_2, H_1-H_3 (Figure 3.4). Both NH groups also possess NOE effects with the glycine methylene. The IR spectrum (see experimental section) of a 1 mM solution of **105** in $CDCl_3$ shows a single NH stretching band around 3400 cm^{-1}. Those data suggest that macrocycle **105** does not form a β-turn. Rather, along with the information from CPK model, the two amide planes are perpendicular to each other.

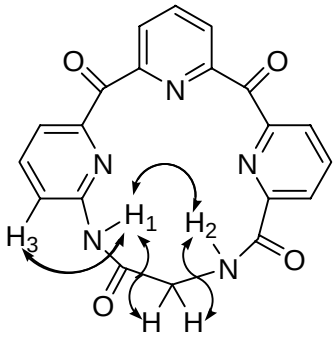

Figure 3.4 Noesy signals of receptor **105**

Preliminary NMR titration experiments were carried out to determine the anion binding properties of **105**. To minimize the possible effects of ion-pair formation, anions were added as their tetrabutylammonium (TBA) salts. The low-competiting, bulky tetrabutylammonium ion is expected to have the minimal interaction with **105** which possesses a relatively small complexation site. Addition of aliquots of the anions caused

a significant downfield shift of two amide signals of **105** on NMR spectra, indicating both amides involved in anion binding (Figure 3.5).

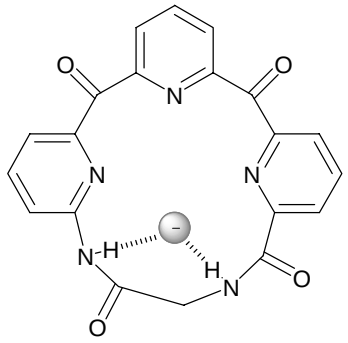

Figure 3.5 Proposed binding model of receptor **105** with anions

On the other hand, no obvious changes were observed on the chemical shift of the pyridyl protons, indicating that the tetrabutylammonium cation interacts minimally with the host. An exceptional case is TBA-F, in which the pyridyl signals also underwent a small downfield shift (< 0.1 ppm). This can perhaps be attributed to complexation-induced conformational changes. For all the titrations, 1:1 binding isotherm were generated (Figure 3.6) and anion binding constants were calculated from the titration data using an iterative curve-fitting method.

The stoichiometry of the anion complex of **105** could also be determined by Job's method. The Job's plot (Figure 3.7) of the TBA-Br complex possesses a maximum at an equimolar ratio of host and guest, indicating a 1:1 complexation.

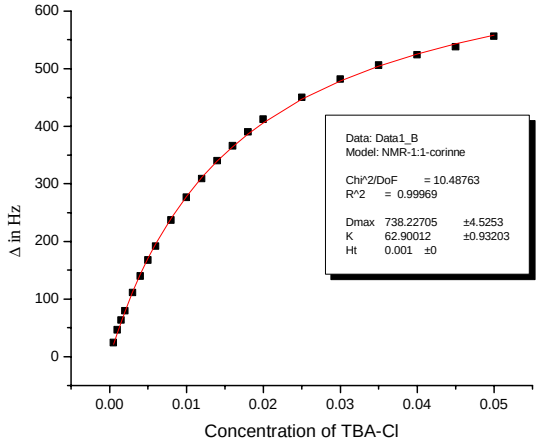

Figure 3.6 Binding isotherm for the complexation of macrocycle **105** and TBA-Cl

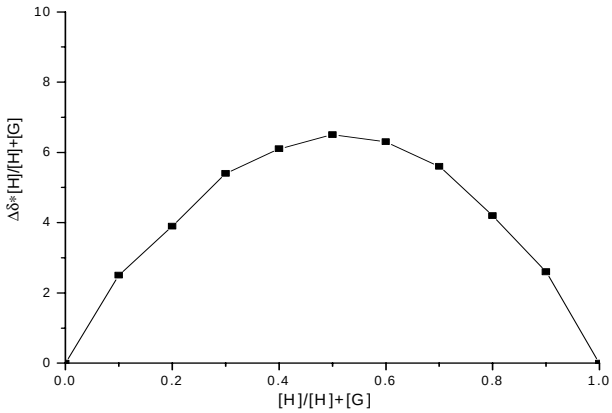

Figure 3.7 The Job's plot of macrocycle **105** with TBA-Br

The binding results, summarized in Table 3.2, reveal that macrocycle **105** binds anions, albeit rather weakly. Strongest binding was observed with small anions F^-, which is also the strongest hydrogen bond acceptor among the anions tested. In contrast, anion PF_6^-, a weak hydrogen bond acceptor, has no affinity with **105**. For all other anions, the binding constants exhibit an order that may be correlated to their ionic size. However, there are no significant differences.

Table 3.2 Associate constants[a] for macrocycle **105** with anions in $CDCl_3$.

Anion	K^b (M^{-1})	Radius (pm)[75]
F^-	110	133
NO_3^-	70	179
Cl^-	63	181
TFA^-	52	190
TsO^-	42	236
Br^-	40	196
I^-	32	220
PF_6^-	No binding	251

[a] At 25 °C, initial [**105**] = 1.0 mM; [b] K_a values are the average of three titrations, with error within 10%.

3.4 Primary Ammonium Salt Binding Studies

To determine the monoalkyl ammonium salt binding properties of macrocycle **105**, L-phenylalanine methyl ester **123** was chosen as the guest molecule with a systematic variation of the counteranion over a range of commonly employed anions (Figure 3.8).

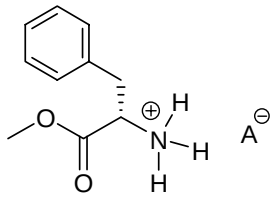

123

Figure 3.8 The structure of the guest molecule **123**

Addition of ammonium salt led to significant downfield shift of both amide signals (>0.5 ppm) and pyridyl signals (0.1-0.2 ppm) indicating that both amide and pyridyl moieties form hydrogen bonds with the guest. In all cases, 1:1 binding isotherms (Figure 3.9) were generated from the titration data and the 1:1 complexation was also confirmed by a Job's plot (Figure 3.10).

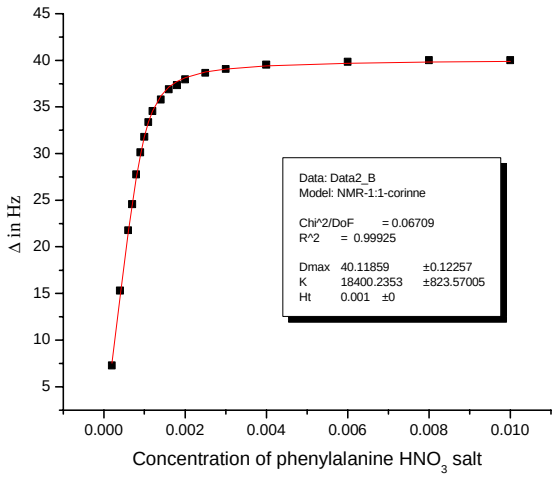

Figure 3.9 Binding isotherm for the complexation of macrocycle **105** and phenylalanine HNO_3 salt

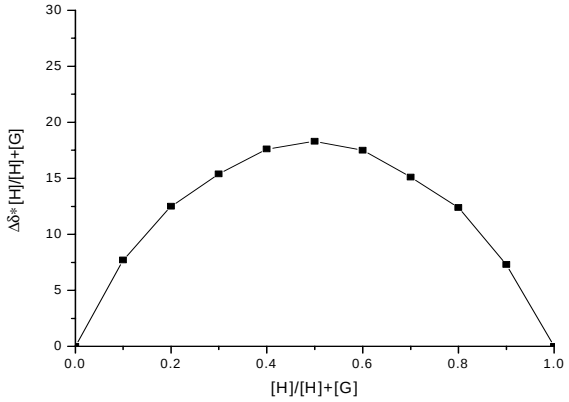

Figure 3.10 The Job's plot of macrocycle **105** with phenylalanine HBr salt

The binding constants (Table 3.3) calculated from the same method demonstrate that the counter anion does have a significant effect on ammonium cation binding. Strong bindings were observed with ammonium salts whose counter anions have relatively strong affinities with **105**. Thus, both HNO_3 and HCl salt gave high affinities with **105**. While the HI salt forms the least stable complex with receptor **105**.

The cooperativity factors[3d] are more illustructive (Table 3.3). A cooperativity factor is the K_a ratio of binding the primary and quaternary ammonium salts, which reflects complexation enhancement due to the ion-pair recognition. Strongly binding anions generally gave high degree of enhancement. Thus, NO_3^- leads to a highest cooperativity factor of 257, while weakly binding anions such as: I^-, Br^-, TsO^- result in cooperativity factors only ranging from 10-50.

Table 3.3. Associate constants[a] and cooperativity factors[c] for macrocycle **105** with various ammonium salts in $CDCl_3$.

$A^- \bullet NH_3^+$-phenylalanine- OMe	K (M^{-1})	Coorperativity factor[b]
F^-	- [c]	- [c]
NO_3^-	1.8×10^4	257
Cl^-	1.2×10^4	190
TFA^-	6.3×10^3	121
TsO^-	1.9×10^3	48
Br^-	1.5×10^3	36
I^-	4.2×10^2	13
PF_6^-	- [c]	- [c]

[a] At 25 °C, initial [**105**] = 1.0 mM; [b] Ratio of $K_{\text{TBA salt}}$ / $K_{\text{ammonium salt}}$; [c] Guest molecules are not soluble in $CDCl_3$.

A rationale of anion effects on the ammonium cation binding is not straightforward. While results obtained from salt binding studies may be related to the affinities of the corresponding anions with receptor **105**, this can hardly explain why small difference of anion affinities cause wide range of cooperativity factors. A tentative explanation could derive from two facts: 1) Anions that form small ion-pairs with ammonium cations

should sterically favor cation/host binding; 2) Although the model of binding is not clear, it is reasonable to hypothesize based on the structures of host and guest that the ammonium cation is bound to the pyridyl moiety of **105** and the counteranion of guest is captured by the amide moieties (Figure 3.11). Thus, high cooperativity factors are expected when small anions having high affinities with receptor **105** also form stable ion-pairs with ammonium cations.

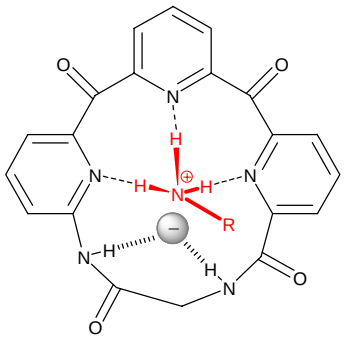

Figure 3.11 Proposed binding model of receptor **105** with ammonium salt

In summary, ditopic receptor **105** simultaneously binds monoalkyl ammonium cation and its counteranion in nonpolar solvent. The cation/host binding is strongly enhanced by the counteranion with the degree of enhancement depending on the nature of the counter anion.

IV Enantioselective Recognition of Amino Acid Derivatives by Chiral Ditopic Macrocycles

The design and synthesis of enantioselective artificial receptors continue to be of great interest in supramolecular chemistry. Such receptors selectively recognize one enantiomer over the other one through non-covalent attractive and repulsive interactions between chiral host and guest.[125-127] In addition to help understanding the enantioselective recognition processes in biological systems, investigations of these artificial receptors raise the opportunity of developing molecular devices in optical resolution,[155,156] chiral sensing,[180] membrane transportation,[136] and chiral catalysis.[181]

Amino acids are basic building blocks of biological molecules and possess a rich variety of side chains. Thus, study of the enantioselective recognition of amino acid and derivatives is particular important and intricit.[182-189] In the previous chapter, we described rigid *tris*(pyridyl) macrocyclic receptor **105** which has been proven to be able to simultaneously bind both a monoalkyl ammonium cation and its counteranion. The versatile synthesis of **105** has the advantage that, in principle, any amino acid can be incorporated into the marocyclic structure, to introduce extra functionality and chirality.

Herein, we synthesized two new chiral ditopic macrocycle **124** and **125** (Figure 4.1). Receptor **124** has a bulky phenylalanine residue incorporated into the macrocyclic structure to engender large steric interactions. Receptor **125** possesses a hydroxyl functionality providing an extra hydrogen bonding site. We anticipated that the macrocycles **124** and **125** would enantioselectively bind chiral monoalkyl ammonium cations. Furthermore, the ditopic properties of the macrocycles may also engender counter anion depended enantioselectivities.

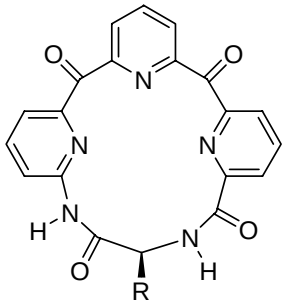

124 R = CH_2Ph
125 R = CH_2OH

Figure 4.1 The structures of macrocycles **124**, **125**.

4.1 Macrocycle Synthesis

The synthesis of receptors **124** and **125** is readily achieved by coupling of compound **116** with the respective N-Boc amino acids to give amino acid derivatives **126**, **127** (Scheme 4.1). Hydrolysis of the ester groups with 1 equivalent NaOH afforded carboxyl acid derivatives **128**, **129** in high yield. The Boc group of **128** was then removed in aqueous HCl solution to give the linear precursors for the cyclization step. Selective deprotection of Boc group of serine derivative **129** was accomplished with HCl/ethyl acetate. The product **131** precipitates in the solution during the reaction, thus preventing further deprotection of the *t*-butyl protected alcohol. The cyclization reactions were carried out under high dilution conditions using diphenylphosphoryl azide as a coupling reagent to give macrocycles **124** and **132**. Removal of the *t*-butyl group of **131** with formic acid gave macrocycle **125** in high yield.

Scheme 4.1 The synthesis of macrocycles **124, 125**

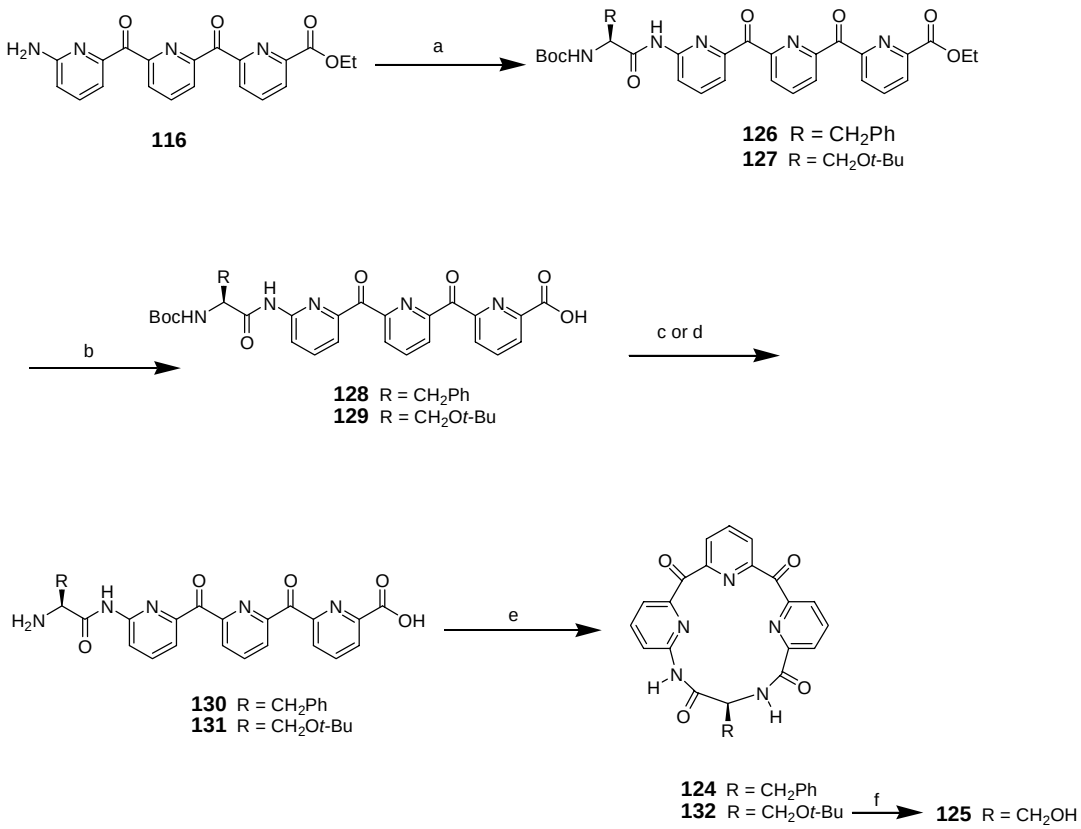

Key: a) HBTU, HOBt, respective *N*-Boc amino acid, 60-70%; b) 1.1 eq. NaOH, 85%; c) 10% HCl, 88%; d) HCl/ethyl acetate, 85%; e) DPPA / DMF, 37%; f) HCOOH, 65%.

4.2 Enantioselective Binding Studies of Macrocycles

Enantioselective recognition properties of receptors **124** and **125** were determined using NMR titrations in 40% $CD_3CN/CDCl_3$, a solvent system in which the exchange between free host and the complex is fast on the NMR time scale. The nitrate salts of amino acid methyl esters **133** (Figure 4.2) were chosen as guests since they afforded good solubility in organic solvents and formed relative stable complexes with macrocycle **105**.

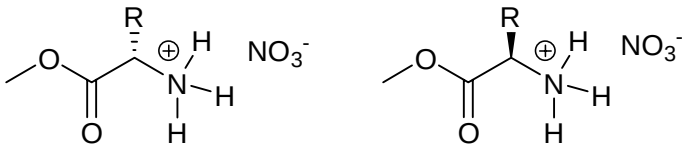

Figure 4.2 The structures of the guest molecules **133**

We have shown that the interactions between ammonium cation and receptor **105** caused a downfield shift of NMR signals of the receptor. The same effects were also observed upon adding guest to the solutions of **124** and **125**. The binding data could be readily fitted to 1:1 binding isotherms (Figure 4.3), and binding constants were obtained using the method previously described.

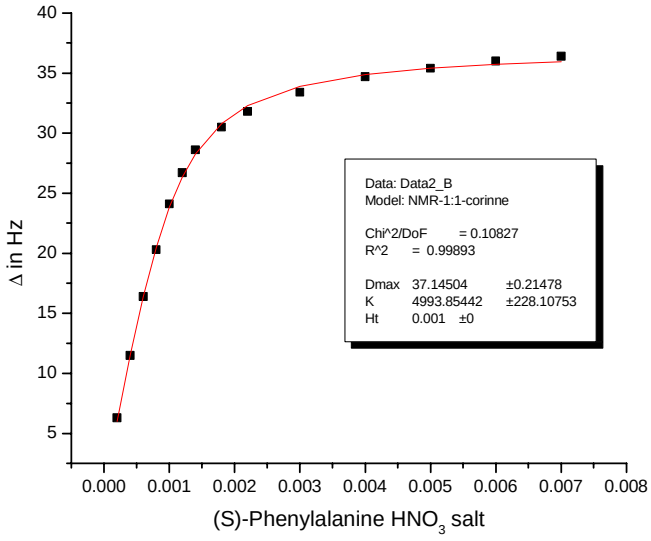

Figure 4.3 Binding isotherm for the complexation of macrocycle **124** and S-phenylalanine HNO_3 salt.

Our results (Table 4.1) demonstrate that the C_1 symmetric macrocycles **124** and **125** exhibit mild to high enantioselectivity for the enantiomers of various α-amino acid methyl ester nitrate salts. Thus, both receptors **124** and **125** form more stable complexes with S-isomers of amino acid derivatives than R-isomers. The extent of enantioselectivity highly depends on the nature of the chiral groups of both host and guest molecules. The bulky chiral groups cause large steric interactions upon complexing, resulting in good discrimination between the enantiomers. Thus, receptor **124**, with its bulky benzyl group, has better enantioselectivity than **125**. As for the effect of guests, both receptors gave highest degree of enantioselectivity toward the enantiomers of phenylglycine methyl esters, with K_S/K_R value of 3.0 and 2.6 respectively. On the other hand, the methyl group on alanine methyl ester provides insufficient interactions for enantioselective recognition. The rigidity of the chiral group also plays an important role in enantioselective recognition judging from the fact that the enantiomers of

phenylalanine methyl esters are less discriminated than those of phenylglycine methyl esters.

Although the steric interactions between the chiral groups result in a discrimination between the enantiomers of the guest molecules, it also destabilize the complexes. Thus, among the S-isomers, phenylglycine methyl ester forms the least stable complex due to the bulky and rigid α-phenyl group. By contrast, alanine methyl ester, with only a methyl group on the α-position, forms the most stable complex.

Table 4.1. Associate constants[a,b] for macrocycles **124** and **125** with nitrate salt of amino acid methyl esters.

Host	Guest[c]	$K_{S\text{-isomer}}$	$K_{R\text{-isomer}}$	K_S/K_R
124	NH_3^+-alanine-OMe	1.5×10^4	1.2×10^4	1.3
124	NH_3^+-valine-OMe	9.5×10^3	5.0×10^3	1.9
124	NH_3^+-phenylalanine-OMe	5.0×10^3	1.9×10^3	2.6
124	NH_3^+-phenylglycine-OMe	2.8×10^3	9.3×10^2	3.0
125	NH_3^+-alanine-OMe	8.5×10^3	7.3×10^3	1.2
125	NH_3^+-valine-OMe	4.8×10^3	3.2×10^3	1.5
125	NH_3^+-phenylalanine-OMe	2.9×10^3	1.5×10^3	1.9
125	NH_3^+-phenylglycine-OMe	2.1×10^3	8.0×10^2	2.6

[a] At 25 °C, initial [host] = 1.0 mM; [b] NMR titrations were carried out in 40% $CD_3CN/CDCl_3$; [c] Guests were added as nitrate salts.

It is unexpected that receptor **125** forms less stable complexes with ammonium cations than **124**, despite the extra hydrogen bonding site on **125**. The serine residue of

receptor **125** provides mild steric interactions. At the same time, the OH group can also possibly form two kinds of hydrogen bonds with opposite effects on the complex formation. There are an intermolecular hydrogen bond with the guest molecule and an intramolecular hydrogen bond with one pyridine N atom or one of the carbonyl groups. The first promotes the complex formation, while the second results in a decrease of complex stability by blocking one binding site of the receptor. The binding results suggest that intramolecular hydrogen bonding might be the case.

To test the effect of the functionalities on the guest molecules, we also examined threonine and methionine methyl esters. Threonine has a hydrogen bond donating group on its side chain, while methionine possesses a weak hydrogen bond accepting group. NMR titration results (Table 4.2) indicate that the hydrogen bond accepting group on the side chain of the guest has little effect on chiral discrimination as well as complex stability. However, the hydroxyl group of threonine stabilizes the complex, presumably by forming an extra hydrogen bond with the receptor. Interestingly, the chiral discrimination is also enhanced by the hydroxyl group, presumably resulting from the stereospecific hydrogen bonding of with one carbonyl group of the host.

Table 4.2 Associate constants[a,b] for macrocycles **124** and **125** with nitrate salts of methionine and threinine methyl esters.

Host	Guest[c]	$K_{S\text{-isomer}}$	$K_{R\text{-isomer}}$	K_S/K_R
124	NH_3^+-methionine-OMe	1.0×10^4	5.8×10^3	1.7
124	NH_3^+-threonine-OMe	1.8×10^4	6.4×10^3	2.8
125	NH_3^+-methionine-OMe	6.2×10^3	4.4×10^3	1.4
125	NH_3^+-threonine-OMe	1.1×10^4	4.7×10^3	2.3

[a] At 25 °C, initial [host] = 1.0 mM; [b] NMR titrations were carried out in 40% $CD_3CN/CDCl_3$; [c] Guests were added as nitrate salts.

4.3 Investigation of the Ditopic Properties of Macrocycles 124 and 125

In the previous chapter, we have shown that the associations between macrocycle **105** and monoalkyl ammonium cations highly depend on the nature of counter anions. To test the ditopic properties of macrocycles **124** and **125**, as well as to investigate the effect of the counter anion on enantioselectivity, we examined the binding properties of the enantiomers of phenylalanine methyl esters, with different counter anions. Results from NMR titration experiments demonstrate that macrocycle **124** has the similar ditopic properties to **105**. Thus, ammonium salts with small counter anions bind more strongly than those with large counter anion (Table 4.1, 4.3), a trend that has already been observed on macrocycle **105**.

Surprisingly however, although the counter anions significantly influence the complex stabilities, they do not affect the enantioselectivities. Thus, different enantio-pairs of phenylalanine methyl esters display essentially the same degree of chiral discrimination with macrocycle **124** (Table 4.1, 4.3). Similar results were obtained with

macrocycle **125**. Thus **125** forms less stable complexes with the chloride salts of phenylalanine methyl esters than the nitrate salts, but with the same enantioselectivies (Table 4.1, 4.3).

Table 4.3 Associate constants[a,b] for macrocycles **124** and **125** with various ammonium salts of phenylalanine methyl ester

Host	$A^- \bullet NH_3^+$-phenylalanine- OMe	$K_{S\text{-isomer}}$	$K_{R\text{-isomer}}$	K_S/K_R
124	Cl^-	4.4×10^3	1.7×10^3	2.6
124	Br^-	1.7×10^3	6.6×10^2	2.5
124	TsO^-	2.0×10^3	8.1×10^2	2.5
125	Cl^-	2.6×10^3	1.4×10^3	1.9

[a] At 25 °C, initial [host] = 1.0 mM; [b] NMR titrations were carried out in 40% $CD_3CN/CDCl_3$.

In conclusion, we have demonstrated the enantioselective recognition and ditopic properties of receptors **124** and **125**. ^1H NMR titration experiments toward a number of amino acid esters reveal that the enantioselectivity and complex stability highly depend on the nature of chiral groups on both host and guest. The bulky and rigid chiral group generally allows good enantioselectivity. The presence of extra hydrogen bond donating group on the guest also promotes the complex formation as well as chiral discrimination. However, the counter anions of the guest molecules have no effects on the enantioselectivies.

V Conclusions

Three generations of *tris*(2-pyridyl)methanol ligands were synthesized for Carbonic Anhydrase mimicry. Zinc binding studies revealed that the binding properties of the *tris*(2-pyridyl)methanol derivatives are closely related to the steric and electronic properties of the substituents, as well as the remote methyl group on tertiary alcohol. The electron-donating substituents or removal of the methyl group, both promote the zinc binding of the ligands. Our results demonstrated that the potentially active $[ZnL]^{2+}$ species can be obtained with limited steric shielding. However, no catalytic activities were observed of the $[ZnL]^{2+}$ complex for the hydrolysis of *p*-nitrophenyl acetate.

A novel macrocyclic *tris*-pyridyl receptor was synthesized, and its ditopic properties investigated. Binding studies toward a variety of monoalkyl ammonium salts revealed that the receptor simultaneously bound both ammonium cation and the counter anion. The cation/host association highly depends on the nature of the counter anion. Strong binding was observed when the counter anion was also a relatively strong binder.

The synthesis of chiral macrocycles has been described. The chiral receptors selectively bind S-isomers of amino acid methyl esters over R-isomers. Large chiral groups on both host and guest result in good enantioselectivity.

VI Experimental Section

6.1 General

All reagents were purchased from Novabiochem or Aldrich Chemical Company. Dimethylformamide (DMF) was stored over molecular sieves and degassed prior to use. Diethyl ether, tetrahydrofuran (THF) were dried by distillation from sodium benzophenone ketyl. *t*-BuOH was dried with CaH_2, and then distilled. Other reagents are used as received. All reactions were run under a nitrogen atmosphere.

Chromatography (silica gel 60Å. 200-400 mesh; Natland International) was used for product purification. ^{1}H NMR spectra were recorded on Varian Inova instruments (400 MHz or 500 MHz). MS analysis of the products was performed on Macromass Quattro-II, using the Electron Spray technique. All the samples were prepared in a mixture of MeOH and H_2O. Elemental analysis was performed by Atlantic Microlab Inc. Melting points are uncorrected.

6.2 Synthesized Compounds

General procedure for the formation of ligands 86-87

DMF was added to an oven-dried flask containing 0.20 g of *tris*-acid **85** and three equivs. of the corresponding amino acid methyl ester. With stirring, three equivs. of *O*-Benzotriazol-1-yl-*N,N,N′N′*-tetramethyluronium hexafluoro-phosphate (HBTU) followed

by 3.6 equivs. of Et_3N were then added. The mixture was stirred at rt for 4 h. After this time, the reaction mixture was poured into water and extracted three times with chloroform. The combined organic layer was washed with 5% K_2CO_3 solution, and then dried with anhydrous Na_2SO_4. Removal of the solvent under reduced pressure gave the crude product. Pure product was obtained with chromatography (see specific examples).

***Tris*-glycine 86**

The crude product was purified by (gravity) chromatography (mobile phase: 5% methanol in chloroform) to give 0.26 g (85% yield) of **86** as a white solid. mp 113-115 °C; ^{1}H NMR (DMSO-d_6) δ 3.20 (s, 3H), 3.65 (s, 9H), 4.05 (d, J = 4.8 Hz, 6H), 7.73 (d, J = 8.0 Hz, 3H), 8.22 (d, J = 8.4 Hz, 3H), 8.91 (s, 3H), 9.15 (t, J = 5.6 Hz, 3H); MS (ES^+) *m/z* (rel intens.) = 1267.1 (45) $[2M + Na]^+$, 956.3 (40) $[3M + 2Na]^{2+}$, 645.2 (100) $[M + Na]^+$; Anal. Calcd. for $C_{29}H_{30}N_6O_{10}$: C, 55.95; H, 4.86; Found: C, 55.90; H, 4.99.

***Tris*-serine 87**

The crude product was purified by (gravity) chromatography (mobile phase: 10% methanol in chloroform) to give 0.23 g (65% yield) of **87** as a white solid. mp 136-138 °C; ^{1}H NMR (acetone-d_6) δ 3.29 (s, 3H), 3.72 (s, 9H), 4.03 (m, 6H), 4.77 (m, 3H), 7.72 (d, J = 8.4 Hz, 3H), 8.04 (d, J = 8.8 Hz, 3H), 8.25 (d, J = 8.2 Hz, 3H), 8.99 (s, 3H); MS (ES^+) *m/z* (rel intens.) = 1447.0 (20) $[2M + Na]^+$, 1091.3 (30) $[3M + 2Na]^{2+}$, 735.3 (100) $[M + Na]^+$, 713.1 (15) $[M + H]^+$; Anal. Calcd. for $C_{32}H_{36}N_6O_{13} \cdot 2H_2O$: C, 51.28; H, 5.34; Found: C, 50.95; H, 5.03.

***Tris*-phenylalanine 88**

The crude product was purified by (gravity) chromatography (mobile phase 30% acetone in chloroform) to give 0.41 g (95% yield) of **88** as a white solid. mp 94-96 °C; ^{1}H NMR (acetone-d_6) δ 3.25 (s, 3H), 3.31 (m, 6H), 3.69 (s, 9H), 4.92 (m, 3H), 7.32 (m, 15H), 7.71 (d, *J* = 8.4 Hz, 3H), 8.11 (m, 6H), 8.83 (s, 3H); MS (ES^+) *m/z* (rel intens.) = 915.1 (100) $[M + Na]^+$, 893.1 (25) $[M + H]^+$; Anal. Calcd. for $C_{50}H_{48}N_6O_{10} \cdot H_2O$: C, 65.99; H, 5.49; Found: C, 66.12; H, 5.36.

Protected *tris*-methyl 89

Sodium hydride (60% dispersion in mineral oil, 2.0 g, 50 mmol) was washed twice with pentane and made up as a THF suspension (80 mL). To this was added **83** (3.1 g, 10 mmol) in 40 mL THF. MOMBr (4.2 mL, 50 mmol) was then added dropwise into the flask and the mixture was stirred at rt for 4 h. The reaction was then quenched with water, and partitioned between chloroform and water. The aqueous layer was washed twice with chloroform, and the organic layers were combined and dried with anhydrous Na_2SO_4. Removal of the solvent under reduced pressure gave the crude product. Flash chromatography (mobile phase: 10% acetone in hexane) gave 3.5 g (98% yield) of pure **89** as a white solid. mp 99-100 °C; ^{1}H NMR ($CDCl_3$) δ 2.29 (s, 9H), 3.22 (s, 3H), 4.97 (s, 2H), 7.46 (d, *J* = 8.2 Hz, 3H), 7.55 (d, *J* = 8.4 Hz, 3H), 8.37 (s, 3H); MS (ES^+) *m/z* (rel intens.) = 721.3 (100) $[2M + Na]^+$, 372.3 (75) $[M + Na]^+$, 350.0 (50) $[M + H]^+$; Anal. Calcd. for $C_{21}H_{23}N_3O_2$: C, 72.18; H, 6.63; Found: C, 72.26; H, 6.59.

***Tris*-acid 90 · 3HCl**

To a suspension of **89** (2.0 g, 5.7 mmol) in 80 mL water was added NaOH (2.3 g, 57 mmol) and $KMnO_4$ (9.0 g, 57 mmol). The mixture was stirred at 60 °C for 16 h and quenched with methanol. The MnO_2 precipitate was filtered off, and the filtrate acidified with concentrate HCl and stirred at rt for 1 h. Removal of water under reduced pressure gave the crude product as a yellow solid. The crude product was dry-loaded on a silica column and isolated with flash chromatography (mobile phase: 20% methanol in chloroform). Removal of the solvent under reduced pressure afforded 1.9 g (85% yield) of product as a white solid. mp > 250 °C; ^{1}H NMR (DMSO-d_6) δ 7.06 (s, 1H), 7.43 (d, J = 8.0 Hz, 3H), 8.04 (d, J = 8.2 Hz, 3H), 8.79 (s, 3H); MS (ES^+) *m/z* (rel intens.) = 396.3 (100) $[M + H]^+$, 366.3 (40); Anal. Calcd. for $C_{19}H_{13}N_3O_7 \cdot 2H_2O \cdot 3HCl$: C, 42.20; H, 3.73; Found: C, 42.08; H, 3.55.

General procedure for the formation of ligands 91-93

Replacing *tris*-acid **85** with **90**, a procedure similar to that used in the synthesis of ligands **86-88** yielded ligands **91-93**.

***Tris*-glycine 91**

The crude product was purified by (gravity) chromatography (mobile phase: 5% methanol in chloroform) to give 0.23 g (75% yield) of **91** as a white solid. mp 105-106 °C; ^{1}H NMR (acetone-d_6) δ 3.68 (s, 9H), 4.16 (d, J = 6.4 Hz, 6H), 7.17 (s, 1H), 7.85 (d, J = 8.4 Hz, 3H), 8.25 (d, J = 8.0 Hz, 3H), 8.30 (t, J = 5.6 Hz, 3H), 8.99 (s, 3H); MS (ES^+) *m/z* (rel intens.) = 1239.2 (25) $[2M + Na]^+$, 935.4 (40) $[3M + 2Na]^{2+}$, 631.2 (100) [M +

$Na]^+$, 609.2 (30) $[M + H]^+$; Anal. Calcd. for $C_{28}H_{28}N_6O_{10} \cdot H_2O$: C, 53.67; H, 4.79; Found: C, 53.43; H, 4.61.

***Tris*-serine 92**

The crude product was purified by (gravity) chromatography (mobile phase: 10% methanol in chloroform) to give 0.21 g (60%) of **92** as a white solid. mp 125-127 °C; ^{1}H NMR (acetone-d_6) δ 3.72 (s, 9H), 3.95 (m, 6H), 4.29 (t, J = 6.4 Hz, 3H), 4.78 (m, 3H), 7.17 (s, 1H), 7.87 (d, J = 8.4 Hz, 3H), 7.98 (d, J = 7.6 Hz, 3H), 8.30 (d, J = 8.6 Hz, 3H), 9.00 (s, 3H); MS (ES^+) *m/z* (rel intens.) = 1420.0 (20) $[2M + Na]^+$, 1070.3 (30) $[3M + 2Na]^{2+}$, 721.8 (100) $[M + Na]^+$, 699.2 (20) $[M + H]^+$; Anal. Calcd. for $C_{31}H_{34}N_6O_{13} \cdot 2H_2O$: C, 50.63; H, 5.17; Found: C, 50.27; H, 5.03.

***Tris*-phenylalanine 93**

The crude product was purified by (gravity) chromatography (mobile phase: 30% acetone in chloroform) to give 0.39 g (88% yield) of **93** as a white solid. mp 91-92 °C; ^{1}H NMR (acetone-d_6) δ 3.27 (m, 6H), 3.69 (s, 9H), 4.93 (m, 3H), 7.08 (s, 1H), 7.31 (m, 15H), 7.79 (d, J = 8.4 Hz, 3H), 8.07 (d, J = 8.0 Hz, 3H), 8.14 (d, J = 8.4 Hz, 3H), 8.83 (s, 3H); MS (ES^+) *m/z* (rel intens.) = 879.3 (100) $[M + H]^+$; Anal. Calcd. for $C_{49}H_{46}N_6O_{10} \cdot H_2O$: C, 65.62; H, 5.35; Found: C, 65.64; H, 5.34.

***Tris*-azide 94**

To a suspension of **90** (2.5 g, 6.3 mmol) in 40 mL dry THF was added diphenylphosphoryl azide (DPPA) (4.5 mL, 21 mmol) at rt. Triethylamine (4.1 mL, 29

mmol) was then added. After 2 h, the mixture was concentrated under reduced pressure and the product was isolated by flash chromatography (mobile phase: 20% ethyl acetate in hexanes). Removal of the solvent under reduced pressure gave 2.2 g (75% yield) of **94** as a white solid (caution: do not heat during isolation). mp 85-88 °C; ^{1}H NMR ($CDCl_3$) δ 7.19 (s, 1H), 7.90 (d, *J* = 8.4 Hz, 3H), 8.30 (d, *J* = 8.8 Hz, 3H), 9.10 (s, 3H); MS (ES^+) *m/z* (rel intens.) = 471.0 (65) $[M + H]^+$, 369.0 (100), 265.1 (80); Anal. Calcd. for $C_{19}H_{10}N_{12}O_4$: C, 48.52; H, 2.14; Found: C, 48.83; H, 1.94.

***Tris*-BOC 95**

A solution of **94** (2.0 g, 4.3 mmol) in 80 mL dry *t*-BuOH was refluxed for 8 h. The *t*-BuOH was removed under reduced pressure. Flash chromatography over silica gel (mobile phase: 20% acetone in chloroform) afforded 2.1 g (80% yield) of **95** as a white solid. mp 120-122 °C; ^{1}H NMR (DMSO-d_6) δ 1.47 (s, 27H), 6.74 (s, 1H), 7.41 (d, *J* = 8.8 Hz, 3H), 7.83 (d, *J* = 8.0 Hz, 3H), 8.44 (s, 3H), 9.53 (s, 3H); MS (ES^+) *m/z* (rel intens.) = 609 (100) $[M + H]^+$; Anal. Calcd. for $C_{31}H_{40}N_6O_7$: C, 61.17; H, 6.62; Found: C, 60.92; H, 6.64.

***Tris*-amine 96**

To a solution of **95** (1.5 g, 2.47 mmol) in 10 mL methanol was added 10 mL of 20% HCl solution. The mixture was stirred at rt for 16 h. The solvent was removed under reduced pressure and the yellow solid re-dissolved in methanol and precipitated with ether to afford 0.84 g (90% yield) of **96** · 2HCl as a white powder. mp 140-143 °C; ^{1}H NMR (D_2O) δ 7.31 (d, *J* = 8.8 Hz, 3H), 7.37 (d, *J* = 8.8 Hz, 3H), 7.87 (s, 3H); MS (ES^+)

m/z (rel intens.) = 323.1 (15), 309.1 (35) $[M + H]^+$, 291.1 (100); Anal. Calcd. for $C_{16}H_{16}N_6O \cdot 2H_2O \cdot 2HCl$: C, 46.25; H, 5.30; Found: C, 45.91; H, 5.24.

General procedure for the formation of ligands 97-99

DMF was added to an oven-dried flask containing 0.20 g of **96** and 3.3 equivs. of the corresponding N-Cbz amino acid. With stirring, 3.3 equivs. of both HBTU and *N*-hydroxybenzotriazole (HOBT) were then added. Finally 4.5 equivs. of Et_3N was added dropwise into the mixture. The reaction was stirred at 40 °C for 12 h. After this time, the reaction mixture was poured into water and extracted with ethyl acetate. The organic layer was washed with 5% K_2CO_3 solution, and then dried with anhydrous Na_2SO_4. Removal of the solvent under reduced pressure gave the crude product. Pure product was obtained with chromatography (see specific examples).

***Tris*-glycine 97**

The crude product was purified by flash chromatography (mobile phase: 5% methanol, 1% Et_3N in chloroform) to give 0.40 g (70% yield) of **97** as a white solid. mp 103-105 °C; ^1H NMR (acetone-d_6) δ 4.00 (d, J = 6.0 Hz, 6H), 5.10 (s, 6H), 6.67 (s, 3H), 6.94 (s, 1H), 7.38 (m, 15H), 7.66 (d, J = 8.8 Hz, 3H), 8.07 (d, J = 8.4 Hz, 3H), 8.67 (s, 3H), 9.44 (s, 3H); MS (ES^+) *m/z* (rel intens.) = 904.4 (25) $[M + Na]^+$, 882.1 (100) $[M + H]^+$; Anal. Calcd. for $C_{46}H_{43}N_9O_{10}$: C, 62.65; H, 4.91; Found: C, 62.80; H, 4.99.

***t*-Butyl protected *Tris*-serine 98**

The crude product was purified by flash chromatography (mobile phase: 3% methanol in chloroform) to give 0.55 g (75% yield) of **98** as a white solid. mp 119-122 °C; ^{1}H NMR (acetone-d_6) δ 1.15 (s, 27H), 3.79 (m, 6H), 4.39 (m, 3H), 5.13 (m, 6H), 6.45 (d, *J* = 6.8 Hz, 3H), 6.95 (s, 1H), 7.38 (m, 15H), 7.68 (d, *J* = 8.8 Hz, 3H), 8.09 (d, *J* = 8.4 Hz, 3H), 8.70 (s, 3H), 9.43 (s, 3H); MS (ES^+) *m/z* (rel intens.) = 1140.8 (100) $[M + H]^+$, 949.7 (50); Anal. Calcd. for $C_{61}H_{73}N_9O_{13} \cdot H_2O$: C, 63.25; H, 6.53; Found: C, 63.37; H, 6.53.

***Tris*-phenylalanine 99**

The crude product was purified by flash chromatography (mobile phase: 3% methanol in chloroform) to give 0.56 g (75% yield) of **99** as a white solid. mp 99-101 °C; ^{1}H NMR (acetone-d_6) δ 3.27 (m, 6H), 4.58 (m, 3H), 5.06 (m, 6H), 6.67 (d, *J* = 8.4 Hz, 3H), 6.96 (s, 1H), 7.31 (m, 15H), 7.66 (d, *J* = 8.4 Hz, 3H), 8.04 (d, *J* = 8.0 Hz, 3H), 8.65 (s, 3H), 9.50 (s, 3H); MS (ES^+) *m/z* (rel intens.) = 1152.6 (100) $[M + H]^+$; Anal. Calcd. for $C_{67}H_{61}N_9O_{10} \cdot H_2O$: C, 68.76; H, 5.43; Found: C, 69.15; H, 5.32.

General procedure for the synthesis of *tris*-acetate derivatives 100-102

A solution containing 1 equivalent of *tris*-Cbz derivatives **97-99** and 3.6 equivalents of acetic anhydride in methanol was hydrogenated for 2 h over 10% palladium on charcoal at rt and 1 atm. of H_2. The catalyst was removed by filtration through celite, and the solvent was removed under reduced pressure to afford the crude product. Pure product was obtained with chromatography (see specific examples)

***Tris*-glycine 100**

The product was purified by flash reverse phase chromatography (mobile phase: 20% methanol in water). Yield: 80%. mp 163-165 °C; ^{1}H NMR (D_2O) δ 1.89 (s, 9H), 3.88 (s, 6H), 7.24 (d, *J* = 8.8 Hz, 3H), 7.74 (d, *J* = 8.8 Hz, 3H), 8.36 (s, 3H); MS (ES^+) *m/z* (rel intens.) = 1210.7 (10) $[2M + H]^+$, 606.1 (100) $[M + H]^+$; Anal. Calcd. for $C_{28}H_{31}N_9O_7 \cdot 2H_2O$: C, 52.41; H, 5.50; Found: C, 52.41; H, 5.22.

***t*-Butyl protected *Tris*-serine 101**

The product was purified by flash chromatography (mobile phase: 5% methanol in chloroform). Yield: 80%. mp 144-147 °C; ^{1}H NMR (acetone-d_6) δ 1.14 (s, 27H), 1.96 (s, 9H), 3.75 (m, 6H), 4.61 (m, 3H), 6.95 (s, 1H), 7.33 (d, *J* = 8.0 Hz, 3H), 7.66 (d, *J* = 8.8 Hz, 3H), 8.06 (d, *J* = 8.4 Hz, 3H), 8.69 (s, 3H), 9.38 (s, 3H); MS (ES^+) *m/z* (rel intens.) = 864.3 (100) $[M + H]^+$; Anal. Calcd. for $C_{43}H_{61}N_9O_{10} \cdot H_2O$: C, 58.55; H, 7.20; Found: C, 58.59; H, 7.13.

***Tris*-phenylalanine 102**

The product was purified by flash chromatography (mobile phase: 5% methanol in chloroform). Yield: 80%. mp 145-148 °C; ^{1}H NMR (acetone-d_6) δ 1.89 (s, 9H), 3.21 (m, 6H), 4.78 (m, 3H), 6.92 (s, 1H), 7.26 (m, 15H), 7.45 (s, 3H), 7.63 (d, *J* = 8.4 Hz, 3H), 7.99 (d, *J* = 8.0 Hz, 3H), 8.62 (s, 3H), 9.47 (s, 3H); MS (ES^+) *m/z* (rel intens.) = 876.2 (100) $[M + H]^+$; Anal. Calcd. for $C_{49}H_{49}N_9O_7 \cdot 3H_2O$: C, 63.28; H, 5.96; Found: C, 63.33; H, 5.62.

***Tris*-serine 103**

A solution of **102** (300 mg, 0.35 mmol) in 3 mL trifluoroacetc acid was stirred at rt for 16 h. The solvent was removed under reduced pressure and the yellow solid was basified with 5% K_2CO_3 solution. The product was isolated by flash reverse phase chromatography (mobile phase: 20% methanol in water). Removal of the solvent under reduced pressure gave 157 mg (65% yield) of **103** as a white solid. mp 169-172 °C; ^{1}H NMR (D_2O) δ 1.91 (s, 9H), 3.77 (m, 6H), 4.38 (t, *J* = 5.2 Hz, 3H), 7.31 (d, *J* = 8.8 Hz, 3H), 7.81 (d, *J* = 8.8 Hz, 3H), 8.40 (s, 3H); MS (ES^+) *m/z* (rel intens.) = 696.0 (100) [M + H]$^+$; Anal. Calcd. for $C_{31}H_{37}N_9O_{10} \cdot 3H_2O$: C, 49.66; H, 5.78; Found: C, 49.89; H, 6.14.

***Tris*-acetate 104**

A solution containing **96** (200 mg, 0.65 mmol), *N*,*N*-dimethylaminopyridine (DMAP) (24 mg, 0.19 mmol), acetic anhydride (0.22 mL, 2.34 mmol) and Et_3N (0.4 mL, 2.9 mmol) in 2 mL DMF was stirred at rt for 4 h. After this time, the solvent was removed under reduced pressure. The residue was chromatographed (mobile phase: 10% methanol in chloroform) to afford 169 mg (60% yield) of **104** as a white solid. mp 134-137 °C; ^{1}H NMR (D_2O) δ 2.01 (s, 9H), 7.29 (d, *J* = 8.8 Hz, 3H), 7.78 (d, *J* = 8.8 Hz, 3H), 8.37 (s, 3H); MS (ES^+) *m/z* (rel intens.) = 869.0 (15) [2M + H]$^+$, 435.1 (100) [M + H]$^+$; Anal. Calcd. for $C_{22}H_{22}N_6O_4 \cdot H_2O$: C, 59.40; H, 5.35; Found: C, 59.41; H, 5.14.

DiMOM 110

A solution of **109** (10 g, 41 mmol) in 150 mL dry ether was cooled to -78 °C. To this solution was added *n*-butyllithium (18.5 mL of a 2.2 M in hexanes) dropwise over a period of 30 minutes. Then a solution of ethyl 2,6-pyridinedicarboxylate (4.8 g, 20 mmol) in 50 mL dry ether was added dropwise to the solution. The temperature was maintained at -78 °C for 2 h. After this time, the solution was warmed up slowly to ca. -20 °C and quenched with water. The mixture was then extracted three times with ether. The combined organic phase was dried with anhydrous Na_2SO_4 and salts filtered off. The product was isolated by flash phase chromatography (mobile phase: 20% ethyl acetate in hexanes). Removal of the solvent under reduced pressure gave 2.8 g (35% yield) of **110** as a white solid. mp 72-74 °C; ^{1}H NMR ($CDCl_3$) δ 1.21 (t, J = 5.8 Hz, 6H), 3.58 (t, J = 6.0 Hz, 4H), 4.70 (s, 4H), 4.82 (s, 4H), 7.62 (d, J = 7.6 Hz, 2H), 7.98 (t, J = 7.6 Hz, 2H), 8.05 (d, , J = 7.6 Hz, 2H), 8.10 (t, , J = 8.4 Hz, 1H), 8.30 (d, , J = 7.6 Hz, 2H); MS (ES^+) *m/z* (rel intens.) = 467.2 (100) $[M + H]^+$; Anal. Calcd. for $C_{25}H_{27}N_3O_6$: C, 64.37; H, 6.05; Found: C, 64.41; H, 6.14.

Dihydroxide 111

To a solution of **110** (2.0 g, 4.4 mmol) in 50 mL THF was added 30 mL 10% HCl solution. The mixture was stirred at rt for 16 h. After this time, the solution was basified with 10% K_2CO_3 solution and extracted with chloroform three times. The combined organic phase was dried with anhydrous Na_2SO_4 and the salts filtered off. The product was isolated by flash phase chromatography (mobile phase: 20% acetone in chloroform). Removal of the solvent under reduced pressure gave 1.5 g (95% yield) of **111** as a white

solid. mp 84-86 °C; ^{1}H NMR ($CDCl_3$) δ 4.78 (s, 4H), 7.46 (d, *J* = 7.6 Hz, 2H), 7.82 (t, *J* = 7.6 Hz, 2H), 8.02 (d, *J* = 7.6 Hz, 2H), 8.13 (t, , *J* = 8.4 Hz, 1H), 8.25 (d, , *J* = 7.6 Hz, 2H); MS (ES^+) *m/z* (rel intens.) = 350.4 (100) $[M + H]^+$; Anal. Calcd. for $C_{19}H_{15}N_3O_4 \cdot H_2O$: C, 62.12; H, 4.66; Found: C, 62.15; H, 4.64.

Diacid 112 (Procedure 1)

To a solution of **111** (2.0 g, 5.5 mmol) in 40 mL acetone was added $KMnO_4$ (4.3 g, 27 mmol) in 40 mL water. The mixture was stirred at rt for 16 h. After this time, the reaction was quenched with methanol and the precipitate filtered off. The filtrate was concentrated to ca. 20 mL and acidified with concentrated HCl solution. The product was collected by filtration as a white solid (2.1 g, 90% yield). mp 133-135 °C; ^{1}H NMR (DMSO-*d6*) δ 8.00 (t, *J* = 8.0 Hz, 2H), 8.27 (m, 4H), 8.38 (s, 3H), 13.5 (s, 2H); MS (ES^-) *m/z* (rel intens.) = 376.2 (100) $[M - H]^-$; Anal. Calcd. for $C_{19}H_{11}N_3O_6 \cdot 1/2H_2O$: C, 59.07; H, 3.11; Found: C, 58.70; H, 3.00.

Diacid 112 (Procedure 2)

A suspension of **122** (5.0 g, 12 mmol) in 100 mL concentrated HCl solution was refluxed for 3 d. After this time, the solvent was removed under reduced pressure. The residue was dissolved in 10% NaOH solution, and then acidified with concentrated HCl solution. The precipitate was collected by filtration and dried in vacuum to afford 4.0 g (90% yield) of **112** as a white solid.

Diester 113

A solution of **112** (5.0 g, 13.3 mmol) in 80 mL saturated HCl / EtOH was stirred at rt for 1 d. The solvent was removed at rt under reduced pressure and the residue was partitioned between chloroform and 5% aqueous K_2CO_3 solution three times. The combined organic layer was dried with anhydrous Na_2SO_4 and salts filtered off. Removal of the solvent under reduced pressure gave yellowish residue which was crystallized in acetone / hexanes to afford 4.3 g (75% yield) of **113** as a white solid. mp 69-71 °C; ^{1}H NMR ($CDCl_3$) δ 1.40 (t, J = 7.2 Hz, 6H), 4.46 (t, J = 6.8 Hz, 4H), 7.82 (t, J = 8.0 Hz, 2H), 7.81 (t, J = 8.0 Hz, 1H), 8.23 (d, J = 7.6 Hz, 2H), 8.26 (d, J = 7.6 Hz, 2H), 8.46 (d, J = 7.6 Hz, 2H); MS (ES^+) *m/z* (rel intens.) = 434.3 (100) $[M + H]^+$; Anal. Calcd. for $C_{23}H_{19}N_3O_6 \cdot H_2O$: C, 61.47; H, 4.68; Found: C, 61.41; H, 4.69.

Monoester 114

To a solution of **113** (4 g, 9.2 mmol) in 100 mL 40% aqueous THF was added dropwise a solution of NaOH (0.37 g, 9.2 mmol) in 10 mL water. The mixture was stirred at rt for 1 d. After this time, the mixture was partitioned between water and ethyl acetate, and the water phase was concentrated and acidified with concentrated HCl solution. The product was collected by filtration as a white solid. Yield: 65%. mp 120-122 °C; ^{1}H NMR (acetone-*d6*) δ 1.34 (t, J = 7.2 Hz, 3H), 4.40 (t, J = 6.8 Hz, 2H), 8.07 (m, 2H), 8.21 (d, J = 7.6 Hz, 1H), 8.25 (d, J = 8.0 Hz, 1H), 8.29 (d, J = 7.6 Hz, 1H), 8.33 (d, J = 8.0 Hz, 1H), 8.43 (m, 3H). MS (ES^-) *m/z* (rel intens.) = 404.1 (100) $[M - H]^-$. Anal. Calcd. for $C_{21}H_{15}N_3O_6 \cdot 2HCl$: C, 52.74; H, 3.58; Found: C, 52.50; H, 3.61.

Boc-amine 115

To a suspension of **114** (5.0 g, 12.3 mmol) in 80 mL dry *t*-BuOH was added DPPA (2.9 mL, 13.5 mmol) at rt. Triethylamine (2.3 mL, 18.5 mmol) was then added. The mixture was stirred at rt for 4 h, and then refluxed for 6 h. After this time, the solvent was removed under reduced pressure and the residue was partitioned between chloroform and 5% aqueous K_2CO_3 solution three times. The combined organic layer was dried with anhydrous Na_2SO_4 and salts filtered off. Removal of the solvent under reduced pressure gave yellowish residue which was flash chromatographied (mobile phase: 30% ethyl acetate in hexanes) to afford 3.5 g (60% yield) of **115** as a white solid. mp 83-85 °C; ^{1}H NMR ($CDCl_3$) δ 1.40 (t, J = 7.2 Hz, 3H), 1.50 (s, 9H), 4.46 (t, J = 6.8 Hz, 2H), 7.33 (s, 1H), 7.61 (t, J = 7.6 Hz, 1H), 7.87 (d, J = 7.6 Hz, 1H), 7.94 (t, J = 7.6 Hz, 1H), 8.09 (d, J = 8.4 Hz, 1H), 8.13 (t, J = 8.0 Hz, 1H), 8.23 (d, J = 8.0 Hz, 1H), 8.28 (d, J = 7.6 Hz, 1H), 8.31 (d, J = 8.0 Hz, 1H), 8.42 (d, J = 8.0 Hz, 1H). MS (ES^+) *m/z* (rel intens.) = 477.3 (100) $[M + H]^+$, 509.3 (80) $[M + MeOH + H]^+$; Anal. Calcd. for $C_{25}H_{24}N_4O_6$: C, 63.02; H, 5.08; Found: C, 63.13; H, 5.13.

Free amine 116

Boc-amine **115** (2.0 g, 4.2 mmol) was dissolved in 10 mL CH_2Cl_2. To this solution was added 4 mL trifluoroacetc acid (TFA). The mixture was stirred at rt for 1 day. After this time, the solvent and TFA were removed under reduced pressure. The residue was partitioned between chloroform and 5% K_2CO_3 aqueous solution three times. The combined organic layer was dried and evaporated under reduced pressure. The residue was recrystallized in acetone / hexanes to give 1.4 g (90% yield) of **116** as a yellow solid.

mp 78-80 °C; ^{1}H NMR ($CDCl_3$) δ 1.40 (t, *J* = 7.2 Hz, 3H), 4.46 (t, *J* = 6.8 Hz, 2H), 5.02 (s, 2H), 6.71 (d, *J* = 8.4 Hz, 1H), 7.37 (t, *J* = 8.4 Hz, 1H), 7.60 (d, *J* = 7.6 Hz, 1H), 7.99 (t, *J* = 8.0 Hz, 1H), 8.11 (t, *J* = 8.0 Hz, 1H), 8.27 (m, 3H), 8.41 (d, *J* = 7.6 Hz, 1H). MS (ES^+) *m/z* (rel intens.) = 377.2 (100) $[M + H]^+$; Anal. Calcd. for $C_{20}H_{16}N_4O_4$: C, 63.82; H, 4.28; Found: C, 63.90; H, 4.29.

Glycine Derivative 117

To a solution of **116** (0.5 g, 1.33 mmol) in 2 mL DMF was added Boc-glycine-OH (0.35 g, 2.0 mmol), HBTU (0.76 g, 2.0 mmol) and HOBT (0.27 g, 2.0 mmol). Triethylamine (0.5 mL, 4.0 mmol) was then added, and the mixture was stirred at 40 °C for 1 d. After this time, the mixture was partitioned between chloroform and 5% aqueous K_2CO_3 solution three times. The combined organic layer was dried and evaporated at reduced pressure. The product was isolated by a flash chromatography (mobile phase: 10% acetone in chloroform). Removal of the solvent under reduced pressure gave 0.43 g (60% yield) of **117** as a white solid. mp 117- 119 °C; ^{1}H NMR (acetone-d_6) δ 1.35 (t, *J* = 7.2 Hz, 3H), 1.40 (s, 9H), 4.05 (d, *J* = 6.2 Hz, 2H), 4.42 (t, *J* = 6.8 Hz, 2H), 6.37 (s, 1H), 7.75 (d, *J* = 8.4 Hz, 1H), 7.83 (t, *J* = 8.4 Hz, 1H), 8.12 (t, *J* = 7.6 Hz, 1H), 8.20 (d, *J* = 8.0 Hz, 1H), 8.25 (d, *J* = 8.0 Hz, 1H), 8.29 (d, *J* = 7.6 Hz, 1H), 8.32 (m, 2H), 8.41 (d, *J* = 7.6 Hz, 1H), 9.61 (s, 1H); MS (ES^+) *m/z* (rel intens.) = 534.3 (100) $[M + H]^+$, 556.3 (20) $[M + Na]^+$, 566.3 (30) $[M + MeOH + H]^+$; Anal. Calcd. for $C_{27}H_{27}N_5O_7 \cdot 1/2H_2O$: C, 59.89; H, 5.22; Found: C, 59.82; H, 5.58.

Glycine Carboxyl Acid Derivatives 118

To a solution of **117** (0.6 g, 1.1 mmol) in 30 mL 40% aqueous THF was added dropwise a solution of NaOH (42 mg, 1.2 mmol) in 5 mL water. The mixture was stirred at rt for 1 d. After this time, the mixture was partitioned between water and ethyl acetate three times. The combined water phase was concentrated to ca. 20 mL and was poured into 50 mL chloroform. The mixture was acidified with concentrated HCl solution and the white precipitate was extracted into chloroform immediately by shaking the mixture. The organic phase was dried and evaporated at reduced pressure to give acid derivative **118** (0.49 g, 85% yield) as a white solid. mp 122-124 °C; ^{1}H NMR (DMSO-d_6) δ 1.40 (s, 9H), 3.80 (d, J = 6.2 Hz, 2H), 7.21 (s, 1H), 7.80 (d, J = 8.4 Hz, 1H), 7.86 (t, J = 8.4 Hz, 1H), 7.95 (m, 2H), 8.01 (d, J = 8.0 Hz, 1H), 8.30 (t, J = 8.0 Hz, 1H), 8.24 (m, 3H), 10.74 (s, 1H); MS (ES^+) *m/z* (rel intens.) = 504.2 (100) $[M - H]^-$; Anal. Calcd. for $C_{25}H_{23}N_5O_7 \cdot 1/2H_2O$: C, 58.48; H, 4.68; Found: C, 58.44; H, 4.58.

Glycine Amine Derivatives 119

Compound **118** (0.50 g, 1.0 mmol) was suspended in 10 mL water. The mixture was acidified with 2 mL concentrated HCl solution and stirred at rt until homogeneous (ca. 20 min). The solvent was then removed under reduced pressure to give yellowish crude product, which was then redissolved in 2 mL methanol, and precipitated out with ether. The product **119** was isolated by filtration as a white solid (0.42 g, 90% yield). mp 140-142 °C; ^{1}H NMR (DMSO-d_6) δ 3.82 (s, 2H), 7.80 (d, J = 8.4 Hz, 1H), 7.88 (t, J = 8.4 Hz, 1H), 8.13 (m, 5H), 8.32 (d, J = 7.6 Hz, 1H), 8.36 (d, J = 7.6 Hz, 1H), 11.18 (s,

1H); MS (ES^+) *m/z* (rel intens.) = 404.2 (100) $[M - H]^-$; Anal. Calcd. for $C_{20}H_{15}N_5O_5 \cdot 2H_2O \cdot 2HCl$: C, 46.69; H, 4.08; Found: C, 46.57; H, 4.07.

Glycine Macrocycle 105

To a solution of **119** (0.2 g, 0.5 mmol) in 250 mL DMF was added triethylamine (0.25 mL, 2.0 mmol). A solution of DPPA (0.22 mL, 1.0 mmol) in 10 mL DMF was added dropwise over a period of 5 h. The mixture was stirred at rt for 2 d. Removal of the solvent under reduced pressure afforded yellowish residue which was partitioned between chloroform and water three times. The combined organic layer was dried and evaporated under reduced pressure. Flash chromatography (mobile phase: 20% acetone in chloroform) gave the crude product **105** as a white solid, which was further purified by washing the solid with acetone (70 mg, 35% yield). mp 189-191 °C; ^1H NMR ($CDCl_3$) 4.46 (d, *J* = 5.2 Hz, 2H), 7.02 (d, *J* = 8.0 Hz, 1H), 7.19 (d, *J* = 8.0 Hz, 1H), 7.67 (t, *J* = 8.0 Hz, 1H), 7.89 (s, 1H), 8.03 (t, *J* = 8.0 Hz, 1H), 8.19 (t, *J* = 8.0 Hz, 1H), 8.26 (m, 3H), 8.41 (m, 2H); MS (ES^+) *m/z* (rel intens.) = 388.2 (100) $[M + H]^+$; 406.2 (50) $[M + H_2O + H]^+$; 420.2 (60) $[M + MeOH + H]^+$; Anal. Calcd. for $C_{20}H_{13}N_5O_4 \cdot H_2O$: C, 59.21; H, 3.70; Found: C, 59.09; H, 3.31.

Dibromoketone 120

A solution of 2,6-dibromopyridine **106** (10 g, 42.2 mmol) in 150 mL dry ether was cooled to -78 °C. To this solution was added *n*-butyllithium (21.1 mL of a 2.2 M in hexanes) dropwise over a period of 30 min. Then a solution of ethyl 2,6-pyridinedicarboxylate (5.2 g, 21.1 mmol) in 50 mL dry ether was added dropwise to the

solution. The temperature was maintained at -78 °C for 2 h. After this time, the solution was warmed up slowly to ca. -20 °C and quenched with 10% HCl solution. The mixture was acidified with 10% HCl solution and then basified with 10% K_2CO_3 solution, extract with ether three times. The combined organic phase was dried with anhydrous Na_2SO_4 and salts filtered off. Removal of solvent under reduced pressure gave crude product as a yellowish solid. Crystallization from acetone / hexane afforded 6.6 g (70% yield) of product **120** as a white solid. ^{1}H NMR ($CDCl_3$) δ 7.69 (d, *J* = 8.1 Hz, 2H), 7.78 (t, *J* = 7.8 Hz, 2H), 8.16 (d, *J* = 7.5 Hz, 2H), 8.18 (t, *J* = 8.1 Hz, 1H), 8.40 (d, *J* = 7.5 Hz, 2H).

DiBromoacetal 121

To a suspension of **120** (5.0 g, 11.2 mmol) in 80 mL benzene was added *p*-toluenesulfonyl acid (2.14 g, 11.2 mmol) and 10 mL ethylene glycol. The mixture was refluxed with a Dean-Stark trap for 2 d. After this time, benzene was removed under reduced pressure, and the residue was partitioned between chloroform and water three times. The combined organic layer was dried with anhydrous Na_2SO_4 and salts filtered off. The solvent was removed under reduced pressure. The obtained white solid[190] was recrystallized in acetone/ hexanes to afford 5.9 g (75% yield) product **121**. ^{1}H NMR ($CDCl_3$) δ 4.11 (m, 8H), 7.35 (d, *J* = 8.0 Hz, 2H), 7.46 (t, *J* = 7.5 Hz, 2H), 7.53 (d, *J* = 8.0 Hz, 2H), 7.70 (d, *J* = 7.5 Hz, 2H), 7.76 (s, *J* = 7.5 Hz, 1H).

***Di*-Cyanide 122**

To a suspension of **121** (5.0 g, 9.3 mmol) in 80 mL pyridine was added CuCN (4.3 g, 46.5 mmol). The mixture was refluxed (ca. 140 °C) under nitrogen for 10 h. After this

time, the pyridine was removed under reduced pressure and the residue was partitioned between chloroform and 10% aqueous ammonia solution four times. The combined organic layer was washed with water, dried with anhydrous Na_2SO_4 and salts filtered off. The solvent was removed under reduced pressure and the residue was crystallized in acetone / hexanes to afford 3.8 g (96% yield) of dicyanide **122** as a white solid. mp 105-107 °C; ^{1}H NMR ($CDCl_3$) δ 4.03 (m, 4H), 4.18 (m, 4H), 7.74 (m, 4H), 7.81 (d, *J* = 7.5 Hz, 2H), 7.95 (m, 3H); MS (ES^+) *m/z* (rel intens.) = 428.2 (100) $[M + H]^+$, 450.2 (35) $[M + Na]^+$; Anal. Calcd. for $C_{23}H_{17}N_5O_4$: C, 64.63; H, 4.01; Found: C, 64.37; H, 3.93.

Boc-phenylalanine 126

To a solution of **116** (0.5 g, 1.33 mmol) in 2 mL DMF was added Boc-phenylalanine-OH (0.35 g, 2.0 mmol), HBTU (0.76 g, 2.0 mmol) and HOBT (0.27 g, 2.0 mmol). Triethylamine (0.5 mL, 4.0 mmol) was then added, and the mixture was stirred at 40 °C for 1 d. After this time, the mixture was partitioned between chloroform and 5% aqueous K_2CO_3 solution. The combined organic layer was dried and evaporated at reduced pressure. The product was isolated by a flash chromatography (mobile phase: 6% acetone in chloroform). Removal of the solvent under reduced pressure gave 0.56 g (60% yield) of **126** as a white solid. mp 115-117 °C; ^{1}H NMR (acetone-d_6) 1.31 (s, 9H), 1.34 (t, *J* = 7.2 Hz, 3H), 3.28 (m, 2H), 4.40 (t, *J* = 6.80 Hz, 2H), 4.67 (m, 1H), 6.29 (d, *J* = 8.0 Hz, 1H), 7.20 (t, *J* = 7.5 Hz, 1H), 7.26 (t, *J* = 7.5 Hz, 2H), 7.34 (d, *J* = 7.5 Hz, 2H), 7.78 (d, *J* = 7.5 Hz, 1H), 7.83 (t, *J* = 7.5 Hz, 1H), 8.09 (t, *J* = 8.0 Hz, 1H), 8.22 (d, *J* = 8.0 Hz, 1H), 8.24 (d, *J* = 8.0 Hz, 1H), 8.34 (d, *J* = 8.4 Hz, 1H), 8.35 (d, *J* = 7.5 Hz, 1H), 8.38 (t, *J* = 6.0 Hz, 1H), 8.42 (d, *J* = 7.0 Hz, 1H), 9.77 (s, 1H); MS (ES^+) *m/z* (rel intens.) =

624.2 (100) $[M + H]^+$; 656.2 (20) $[M + MeOH + H]^+$; Anal. Calcd. for $C_{34}H_{33}N_5O_7 \cdot H_2O$: C, 63.71; H, 5.51; Found: C, 63.90; H, 5.81.

Boc-Serine 127

To a solution of **116** (0.5 g, 1.33 mmol) in 2 mL DMF was added Boc-serine(*t*-Bu)-OH (0.34 g, 2.0 mmol), HBTU (0.76 g, 2.0 mmol) and HOBT (0.27 g, 2.0 mmol). Triethylamine (0.5 mL, 4.0 mmol) was then added, and the mixture was stirred at 40 °C for 1 d. After this time, the mixture was partitioned between chloroform and 5% aqueous K_2CO_3 solution. The combined organic layer was dried and evaporated at reduced pressure. The product was isolated by a flash chromatography (mobile phase: 6% acetone in chloroform). Removal of the solvent under reduced pressure gave 0.43 g (65% yield) of the product **127** as a white solid. mp 110-111 °C; ^{1}H NMR (acetone-d_6) 1.13 (s, 9H), 1.35 (t, J = 7.2 Hz, 3H), 1.41 (s, 9H), 3.81 (m, 2H), 4.43 (m, 3H), 6.16 (s, 1H), 7.80 (d, J = 7.0 Hz, 1H), 7.88 (t, J = 7.5 Hz, 1H), 8.11 (t, J = 8.0 Hz, 1H), 8.22 (d, J = 8.0 Hz, 1H), 8.26 (d, J = 7.5 Hz, 1H), 8.31 (d, J = 8.0 Hz, 1H), 8.36 (t, J = 8.0 Hz, 2H), 8.44 (t, J = 8.0 Hz, 1H), 9.67 (s, 1H); MS (ES^+) *m/z* (rel intens.) = 620.2 (100) $[M + H]^+$; Anal. Calcd. for $C_{32}H_{37}N_5O_8$: C, 62.02; H, 6.02; Found: C, 61.79; H, 6.16.

Phenylalanine Carboxyl Acid Derivatives 128

To a solution of **126** (0.75 g, 1.2 mmol) in 30 mL 30% aqueous THF was added dropwise a solution of NaOH (42 mg, 1.2 mmol) in 5 mL water. The mixture was stirred at rt for 1 d. After this time, the mixture was partitioned between water and ethyl acetate, and extracted with water three times. The water phase was combined and concentrated to

ca. 20 mL. 50 mL chloroform was poured into the aqueous solution, and the mixture was acidified with concentrated HCl solution. The product precipitated out as a white solid which was extracted by chloroform immediately. Removal of the solvent under reduced pressure gave the acid derivatives **128** as a white solid. Yield: 85%. mp 120-121 °C; ^{1}H NMR (DMSO-d_6) 1.28 (s, 9H), 3.02 (m, 2H), 4.45 (m, 1H), 7.16 (t, J = 7.6 Hz, 1H), 7.25 (t, J = 7.2 Hz, 2H), 7.36 (d, J = 7.6 Hz, 2H), 7.73 (d, J = 7.6 Hz, 1H), 7.86 (t, J = 8.0 Hz, 1H), 8.10 (t, J = 7.6 Hz, 1H), 8.20 (d, J = 6.8 Hz, 2H), 8.29 (m, 2H), 8.36 (m, 2H), 11.0 (s, 1H); MS (ES$^-$) *m/z* (rel intens.) = 594.3 (100) [M - H]$^-$; Anal. Calcd. for $C_{32}H_{29}N_5O_7 \cdot H_2O$: C, 62.70; H, 5.06; Found: C, 62.97; H, 5.05.

Serine Carboxyl Acid Derivatives 129

To a solution of **127** (0.60 g, 1.0 mmol) in 30 mL 30% aqueous THF was added dropwise a solution of NaOH (40 mg, 1.0 mmol) in 5 mL water. The mixture was stirred at rt for 1 d. After this time, the mixture was partitioned between water and ethyl acetate, and the water phase was concentrated and extracted three times with water. The water phase was combined and concentrated to ca. 20 mL. 50 mL chloroform was poured into the aqueous solution, and the mixture was acidified with concentrated HCl solution. The product precipitated as a white solid which was extracted by chloroform immediately. Removal of the solvent under reduced pressure gave acid derivatives **129** as a white solid. Yield: 85%. mp 116-117 °C; ^{1}H NMR (DMSO-d_6) 1.05 (s, 9H), 1.36 (s, 9H), 3.54 (m, 2H), 4.35 (m, 1H), 6.83 (d, J = 8.4 Hz, 1H), 7.82 (t, J = 8.0 Hz, 2H), 7.93 (d, J = 7.6 Hz, 1H), 7.97 (t, J = 8.0 Hz, 2H), 8.25 (m, 3H), 8.30 (t, J = 7.6 Hz, 1H), 10.74 (s, 1H); MS

(ES$^-$) *m/z* (rel intens.) = 590.3 (100) [M - H]$^-$; Anal. Calcd. for $C_{30}H_{33}N_5O_8 \cdot 1/2H_2O$: C, 59.99; H, 5.71; Found: C, 60.16; H, 5.68.

Phenylalanine Amine Derivatives 130

To a suspension of **128** (0.5 g, 0.99 mmol) in 10 mL water was added 2 mL of concentrated HCl solution. The mixture was stirred at rt until homogeneous (ca. 20 min). The solvent was removed under reduced pressure. The crude product was redissolved in methanol, and precipitated with ether. The product **130** was isolated by filtration as a white solid. Yield: 90%. mp 140-141 °C; ^{1}H NMR (DMSO-d_6) 3.17 (m, 2H), 4.31 (m, 1H), 7.30 (m, 5H), 7.81 (d, *J* = 7.2 Hz, 1H), 7.87 (d, *J* = 7.6 Hz, 1H), 8.13 (t, *J* = 7.6 Hz, 1H), 8.19 (d, *J* = 8.0 Hz, 1H), 8.23 (m, 2H), 8.34 (m, 3H), 8.39 (s, 2H), 11.29 (s, 1H); MS (ES$^-$) *m/z* (rel intens.) = 494.2 (100) [M - H]$^-$; Anal. Calcd. for $C_{27}H_{21}N_5O_5 \cdot 1/2H_2O$: C, 64.28; H, 4.36; Found: C, 64.13; H, 4.00.

Serine Amine Derivatives 131

To a suspension of **129** (0.5 g, 0.99 mmol) in 50 mL saturated HCl / ethyl acetate was sonicated and stirred at rt for 24 h. At this time, the suspension was dissolved slowly and a white precipitate appeared after ca. 2 h. The product **131** was isolated by filtration as a white solid. Yield: 85%. mp 135-136 °C; ^{1}H NMR (DMSO-d_6) 1.09 (s, 9H), 4.12 (m, 2H), 5.52 (m, 1H), 7.80 (t, *J* = 7.6 Hz, 1H), 7.89 (t, *J* = 7.6 Hz, 1H), 7.93 (d, *J* = 7.6 Hz, 1H), 8.11 (t, *J* = 8.0 Hz, 1H), 8.20 (d, *J* = 8.0 Hz, 1H), 8.24 (m, 3H), 8.35 (m, 2H), 11.26 (s, 1H), 13.76 (s, 1H); MS (ES$^-$) *m/z* (rel intens.) = 490.3 (100) [M - H]$^-$; Anal. Calcd. for $C_{25}H_{25}N_5O_6 \cdot 3HCl \cdot H_2O$: C, 49.36; H, 4.56; Found: C, 49.26; H, 4.88.

Cyclic-phenylalanine 124

To a solution of **130** (0.26 g, 0.5 mmol) in 250 mL DMF was added triethylamine (0.25 mL, 2.0 mmol). A solution of DPPA (0.22 mL, 1.0 mmol) in 10 mL DMF was added dropwise over a period of 5 h. The mixture was stirred at rt for 2 d. Removal of the solvent under reduced pressure afforded yellowish residue which was partitioned between chloroform and water. The organic layer was dried and evaporated under reduced pressure. Flash chromatography (mobile phase: 10% acetone in chloroform) gave crude product **124** as a white solid, which was further purified by washing the solid with 1:1 mixture of hexanes/acetone. Yield: 35%. mp 187-188 °C; ^{1}H NMR (acetonitrile-d_3) 3.60 (m, 2H), 4.92 (m, 1H), 7.20 (m, 5H), 7.42 (d, J = 8.0 Hz, 1H), 7.52 (d, J = 8.0 Hz, 1H), 7.84 (t, J = 8.0 Hz, 1H), 8.20 (m, 3H), 8.28 (d, J = 8.0 Hz, 1H), 8.40 (s, 3H), 8.63 (s, 1H), 8.68 (d, J = 6.8 Hz, 1H), 9.78 (s, 1H); MS (ES^+) *m/z* (rel intens.) = 478.2 (60) $[M + H]^+$; 496.2 (100) $[M + H_2O + H]^+$; 510.2 (30) $[M + MeOH + H]^+$; Anal. Calcd. for $C_{27}H_{19}N_5O_4 \cdot H_2O$: C, 64.41; H, 4.37; Found: C, 64.45; H, 4.06.

Cyclic-serine(*t*-Bu) 132

To a solution of **131** (0.2 g, 0.5 mmol) in 250 mL DMF was added triethylamine (0.25 mL, 2.0 mmol). A solution of DPPA (0.22 mL, 1.0 mmol) in 10 mL DMF was added dropwise over a period of 5 h. The mixture was stirred at rt for 20 h. Removal of the solvent under reduced pressure afforded yellowish residue which was partitioned between chloroform and water. The organic layer was dried and evaporated under reduced pressure. Flash chromatography (mobile phase: 6% acetone in chloroform) gave

crude product **132** as a white solid, which was further purified by washing the solid with 1:1 mixture of hexanes / acetone. Yield: 35%. mp 180-182 °C; ^{1}H NMR (acetone-d_6) 1.12 (s, 9H), 4.00 (m, 2H), 4.66 (m, 1H), 7.62 (d, *J* = 8.0 Hz, 1H), 7.67 (d, *J* = 8.0 Hz, 1H), 7.84 (t, *J* = 7.6 Hz, 1H), 8.10 (d, *J* = 8.0 Hz, 1H), 8.15 (m, 2H), 8.18 (t, *J* = 7.6 Hz, 1H), 8.35 (m, 2H), 8.50 (d, *J* = 8.0 Hz, 1H), 9.02 (s, 1H); MS (ES$^+$) *m/z* (rel intens.) = 474.3 (100) $[M + H]^+$; 492.3 (80) $[M + H_2O + H]^+$; Anal. Calcd. for $C_{25}H_{23}N_5O_5 \cdot H_2O$: C, 62.24; H, 5.01; Found: C, 62.63; H, 4.87.

Cyclic-serine 125

A solution of **132** (50 mg) in 4 mL formic acid was stirred at rt for 12 hours. After this time, the acid was removed at reduced pressure. The residue was re-dissolved in 5 mL acetone, basified with 20 mL 2% K_2CO_3 solution. The mixture was extracted three times with chloroform. The combined organic layer was dried with anhydrous Na_2SO_4 and the salts filtered off. Removal of the solvent under reduced pressure gave white solid which was crystallized in acetone/hexanes to give 65% product **125** as white solid. mp > 250 °C; ^{1}H NMR (acetone-d_6) 4.12 (m, 2H), 4.37 (s, 1H), 4.73 (m, 1H), 7.57 (d, *J* = 7.6 Hz, 1H), 7.63 (d, *J* = 7.6 Hz, 1H), 7.86 (t, *J* = 8.4 Hz, 1H), 8.10 (d, *J* = 7.6 Hz, 1H), 8.14 (d, *J* = 7.6 Hz, 1H), 8.20 (m, 2H), 8.37 (t, *J* = 6.4 Hz, 1H), 8.40 (d, *J* = 6.8 Hz, 1H), 8.63 (d, *J* = 6.8 Hz, 1H), 9.10 (s, 1H); MS (ES$^+$) *m/z* (rel intens.) = 436.2 (100) $[M + H_2O + H]^+$; Anal. Calcd. for $C_{21}H_{15}N_5O_5$: C, 60.43; H, 3.62; Found: C, 60.59; H, 3.61.

6.3 Zinc Binding Studies of *Tris*(2-pyridyl)methanol Derivatives

Analytical grade $Zn(ClO_4)_2 \cdot 6H_2O$ was used to make stock solutions (ca. 20 mM) in deutarated solvents. To determine the concentration, amounts of stock solution were transferred into 100 mL volumetric flasks and diluted to ca. 1 ppm, 5 ppm and 10 ppm with 1% aqueous HCl solution. The accurate concentrations of these diluted solutions were determined by Atomic Absorption Spectroscopy. All stock solutions of ligands were prepared with the concentration of 5 mM except for ligands **83, 84**, which were prepared as 1 mM solutions because of solubility limits.

In a typical experiment, 0.2 mL stock solutions of ligand and 1 equivalent of zinc perchlorate were mixed in a NMR tube, and the solution diluted to 1 mM. The NMR spectra were then recorded and the intergrations of the peaks in the aromatic region were used to calculate the percentage of each species. All quoted percentages were the average of at least three measurements (starting from fresh stock solutions). A typical NMR spectrum is shown in Figure 6.1.

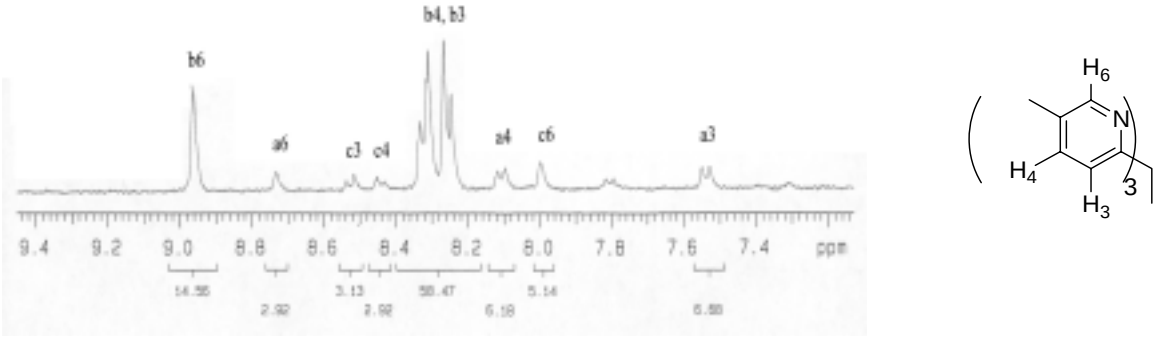

Figure 6.1 ^{1}H NMR of a 1:1 mixture of ligand **91** and zinc perchlorate in D_2O. The labeled signals correspond to free ligand (a), $[ZnL]^{2+}$ (b), and $[ZnL_2]^{2+}$ (c).

6.4 Kinetic Studies of Zinc Complexes of *Tris*(2-pyridyl)methanol Derivatives in D_2O

The stock solutions of ligands and zinc perchlorate were prepared in the same way as those used for zinc binding studies. In a typical experiment, after ligand and zinc perchlorate were mixed in a NMR tube (1 mM each), the NMR spectra was recorded immediately to determine the percentages of each species. The NMR spectra were recorded every 20-30 minutes in the first 2-3 hours and recorded every 2-4 hours after this time, and were followed until there were no changes in the NMR spectra.

The changes of the percentages of $[ZnL]^{2+}$ and $[ZnL_2]^{2+}$ complexes are shown in Figures 6.2-6.5.

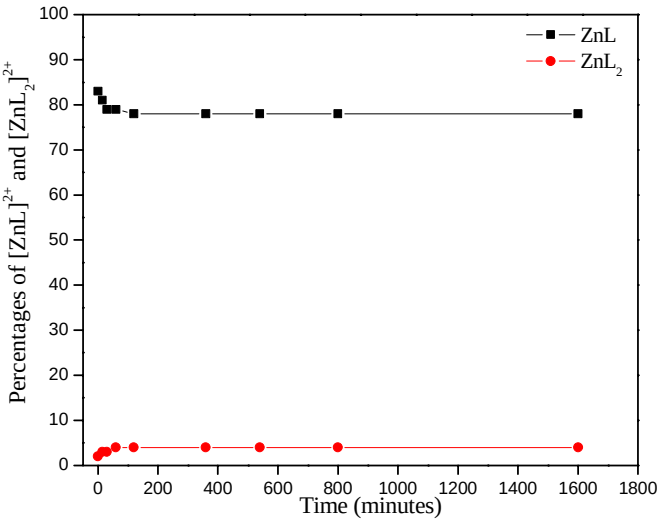

Figure 6.2 Change of the percentages of $[ZnL]^{2+}$ and $[ZnL_2]^{2+}$ of ligand **91** as a function of time.

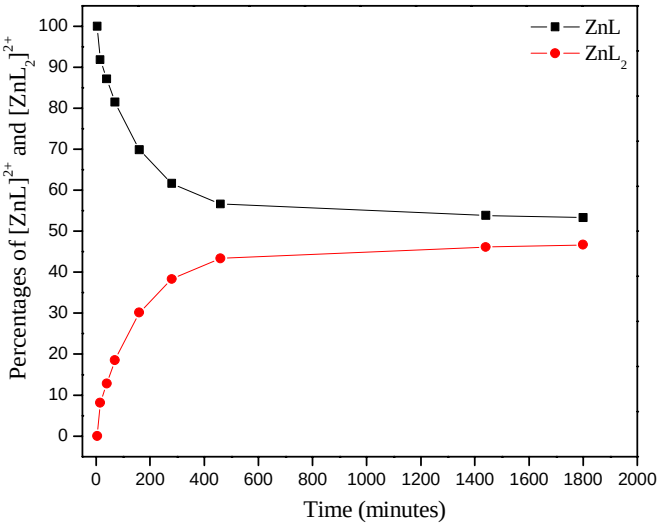

Figure 6.3 Change of the percentages of $[ZnL]^{2+}$ and $[ZnL_2]^{2+}$ of ligand **100** as a function of time.

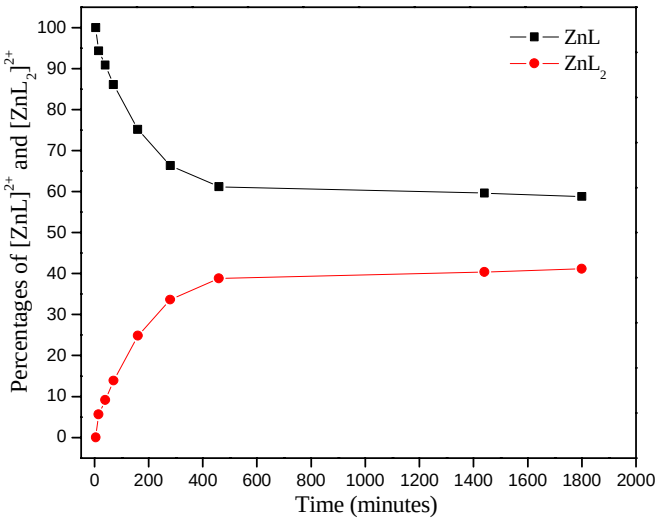

Figure 6.4 Change of the percentages of $[ZnL]^{2+}$ and $[ZnL_2]^{2+}$ of ligand **103** as a function of time.

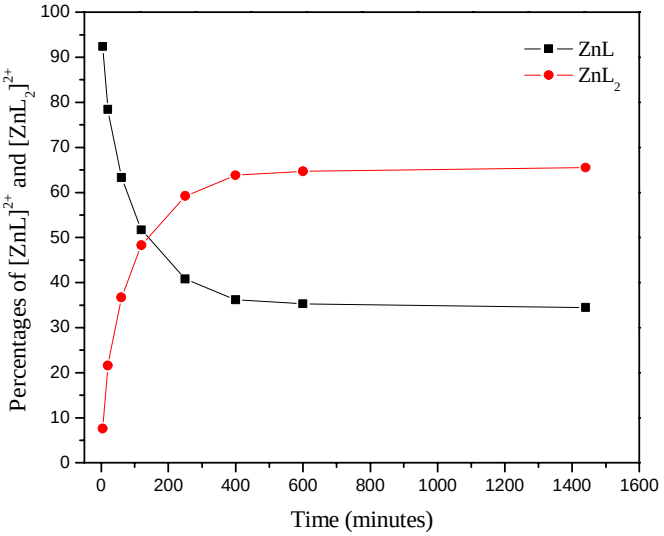

Figure 6.5 Change of the percentages of $[ZnL]^{2+}$ and $[ZnL_2]^{2+}$ of ligand **104** as a function of time.

6.5 Kinetics of *p*-nitrophenyl Acetate Hydrolysis

The hydrolysis of *p*-nitrophenyl acetate was measured at 25^{o}C by an initial slope method following the increase in the 400 nm absorption on UV-spectra. The ionic strength was adjusted to 0.1 with $NaClO_4$ (0.1M). Three buffers were used: HEPES, pH = 7.4; EPPS, pH = 7.9; TAPS, pH = 8.4. The pH of the buffer solution was determined by pH-meter.

In a typical experiment, after *p*-nitrophenyl acetate and complex were mixed in an aqueous solution with 10% acetonitrile in appropriate pH, the UV absorption at 400 nm was recorded immediately. The UV absorption was recorded every 2 minutes and was followed until about 2% decay of the substrate. The concentration of the product *p*-nitrophenate was calculated according to the following equations:

$$c = A / \lambda \qquad \text{(eq. 6.1)}$$

where:

c: concentration of *p*-nitrophenate

A: UV absorption

λ: absorption constant of *p*-nitrophenate ($\log \lambda = 4.34$)

In all cases, plots of the product concentration as a function of time gives a straight line, indicating first order kinetics. When $C < 2\% C_0$, the first-order rate constant was determined from slope of the line according to the following equation:

$$\frac{c}{c_0} = kt \qquad \text{(eq. 6.2)}$$

Where:

k: first-order rate constant

c: concentration of *p*-nitrophenate

c_0: initial concentration of *p*-nitrophenyl acetate

t: reaction time

The kinetics of *p*-nitrophenyl acetate hydrolysis is shown in Figure 6.6-6.8.

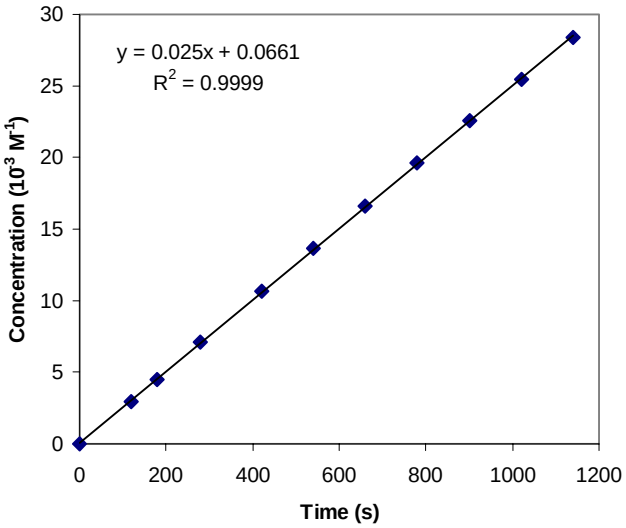

Figure 6.6 The kinetics of *p*-nitrophenyl acetate hydrolysis in the presence of 1 mM zinc complex of ligand **100** at 298 K and pH = 8.4 ($k = 2.5 \times 10^{-5}$ s^{-1}).

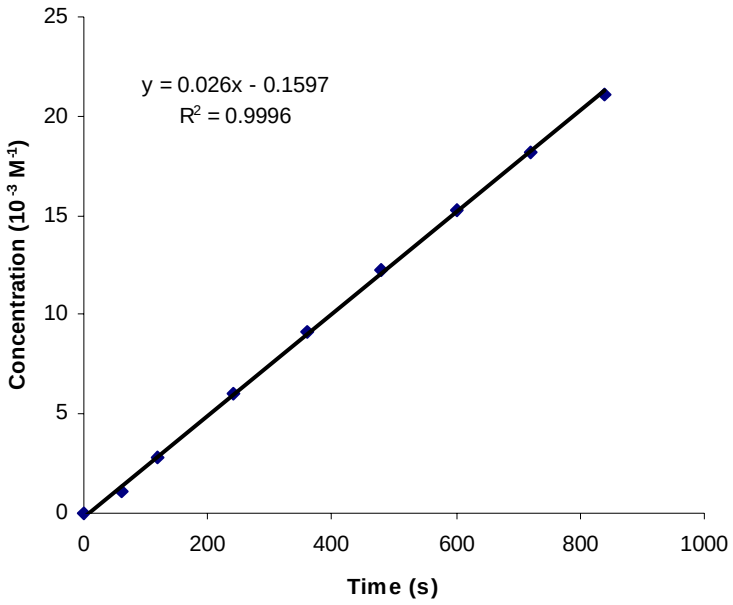

Figure 6.7 The kinetics of *p*-nitrophenyl acetate hydrolysis in the presence of 2 mM zinc complex of ligand **100** at 298 K and pH = 8.4 ($k = 2.55 \times 10^{-5}$ s^{-1}).

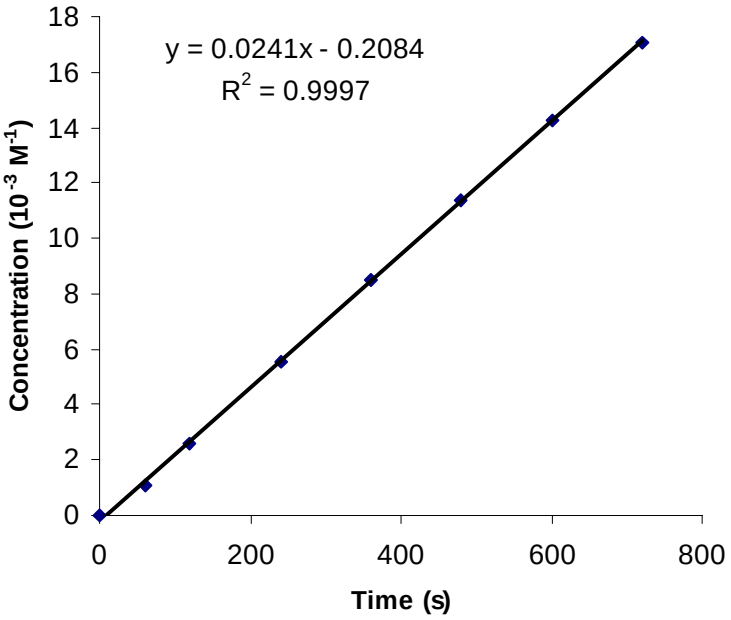

Figure 6.8 The kinetics of *p*-nitrophenyl acetate hydrolysis in absence complexes at 298 K and pH = 8.4 ($k = 2.4 \times 10^{-5}$ s^{-1}).

6.6 COSY and NOESY ^{1}H NMR of Macrocycle 105

The ^{1}H NMR COSY and NOESY spectra of macrocycle **105** are shown in Figure 6.11 and 6.13 respectively. For a comparison, the same region of the corresponding 1D NMR is shown in Figure 6.10 and 6.12 respectively.

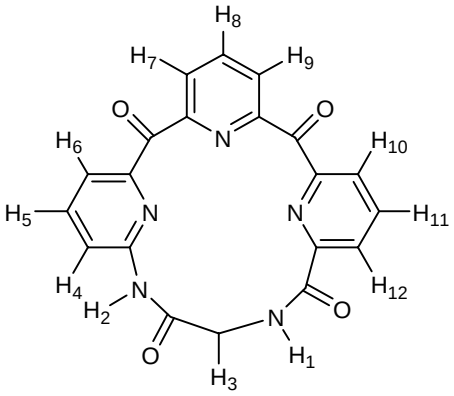

Figure 6.9 The structure of the macrocycle **105**

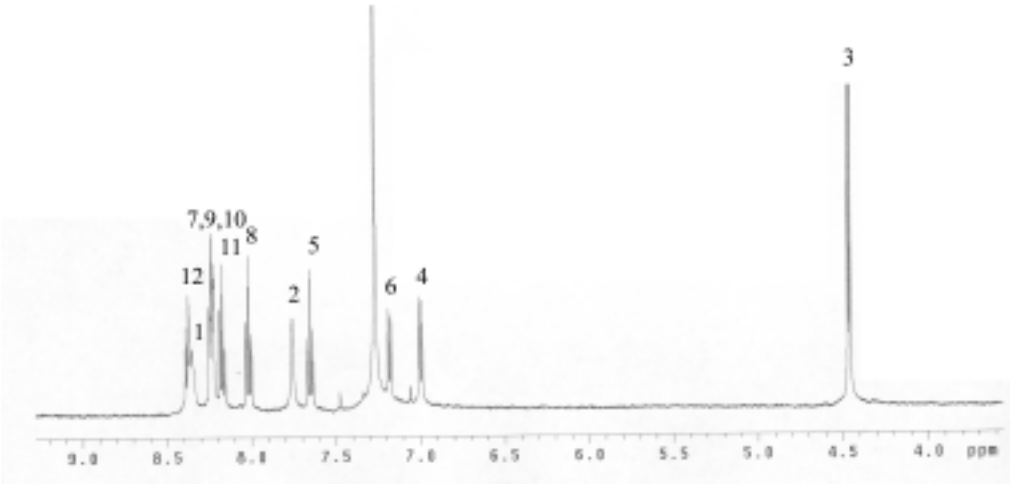

Figure 6.10 ^{1}H NMR of macrocycle **105** in $CDCl_3$.

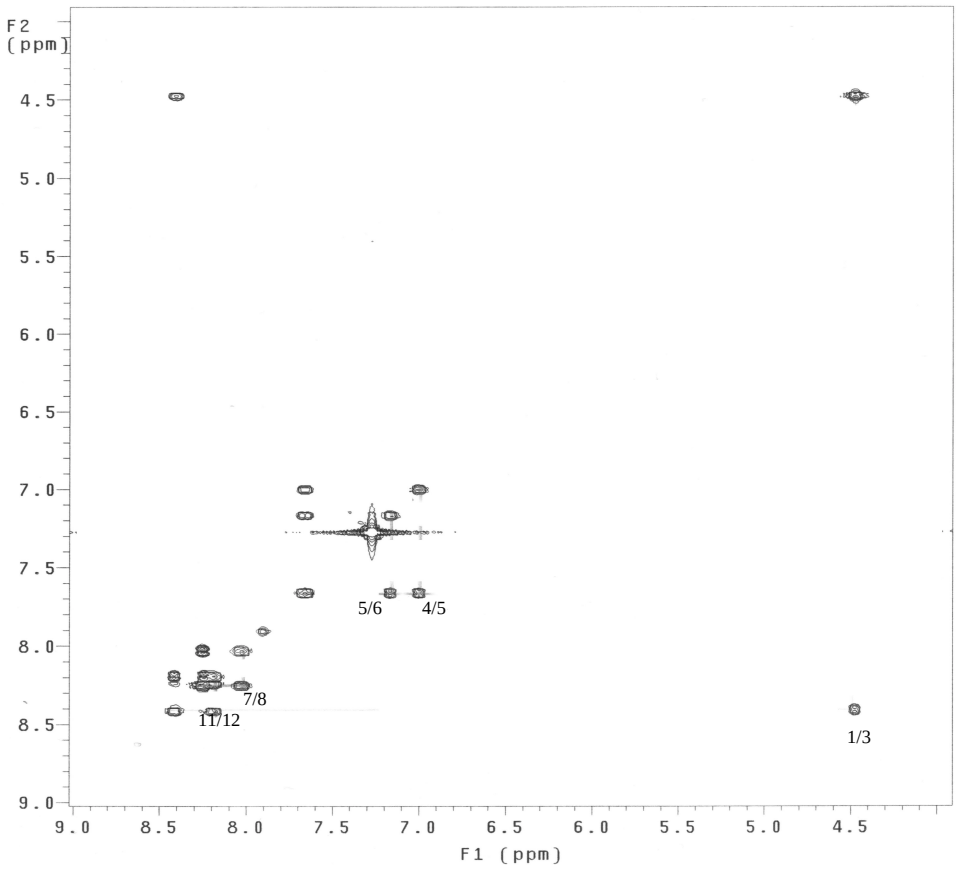

Figure 6.11 ^{1}H NMR COSY spectrum of macrocycle **105** in $CDCl_3$. The labeled cross peaks correspond to the interactions between numbered protons in **105**

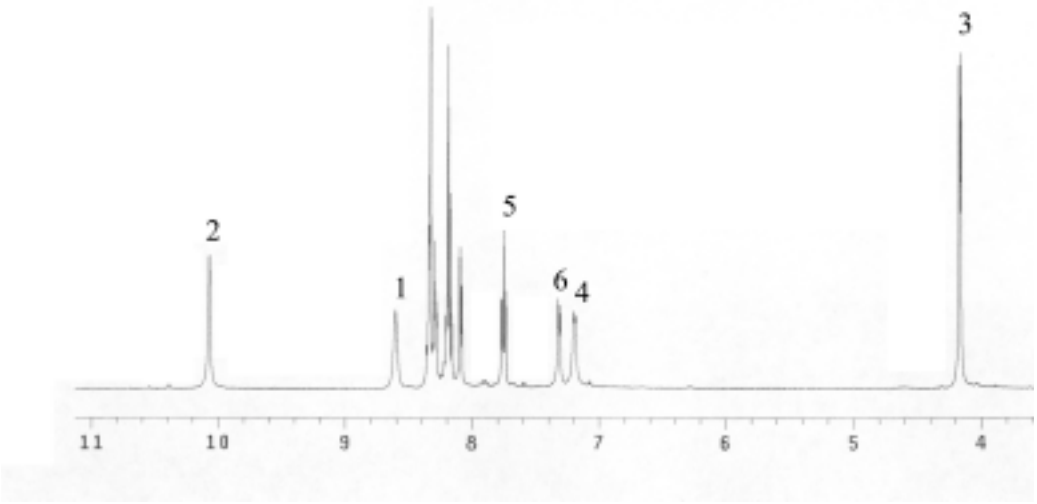

Figure 6.12 ^{1}H NMR of macrocycle **105** in DMSO.

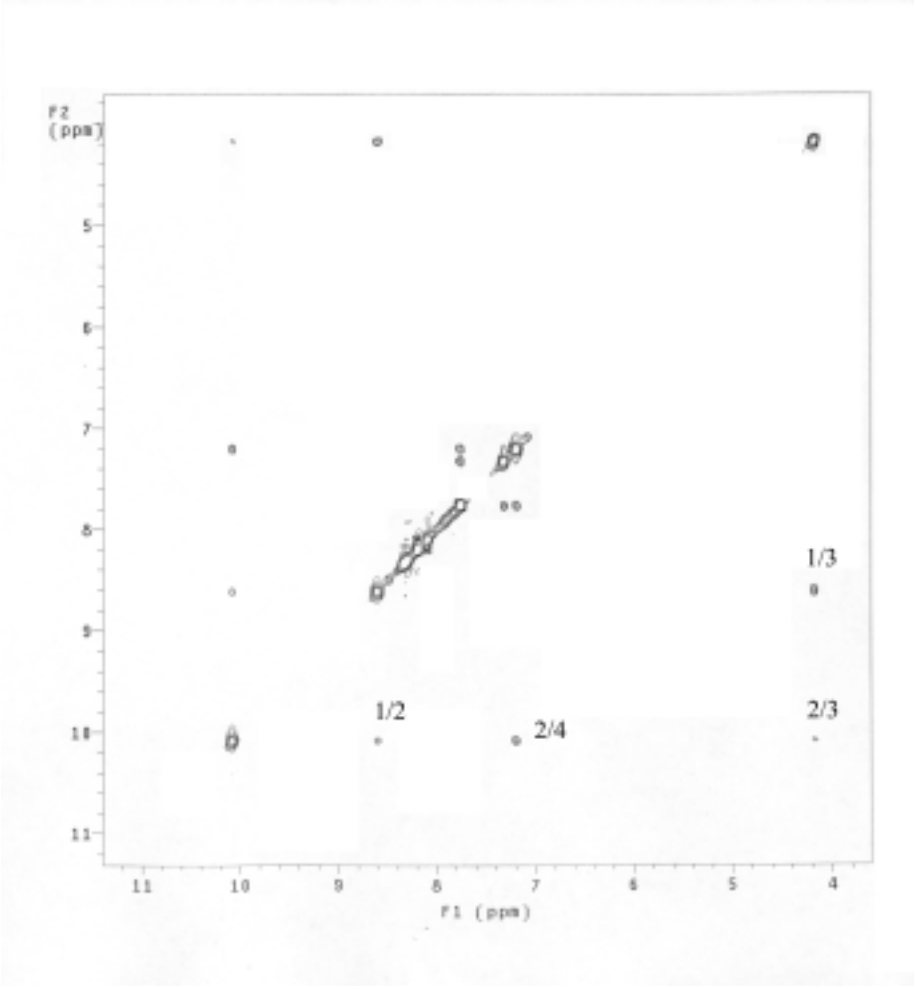

Figure 6.13 ^{1}H NMR NOESY spectrum of macrocycle **105** in DMSO. The labeled cross peaks correspond to the interactions between numbered protons in **105**

6.7 IR Study

All IR spectra were obtained with a Perkin-Elmer 2000 spectrometer. Samples were run as $CDCl_3$ solutions at 1 mM concentration. A background spectrum of the $CDCl_3$ was substracted from sample spectrum. The IR spectrum of macrocycle **105** at NH stretching region is shown in Figure S6.

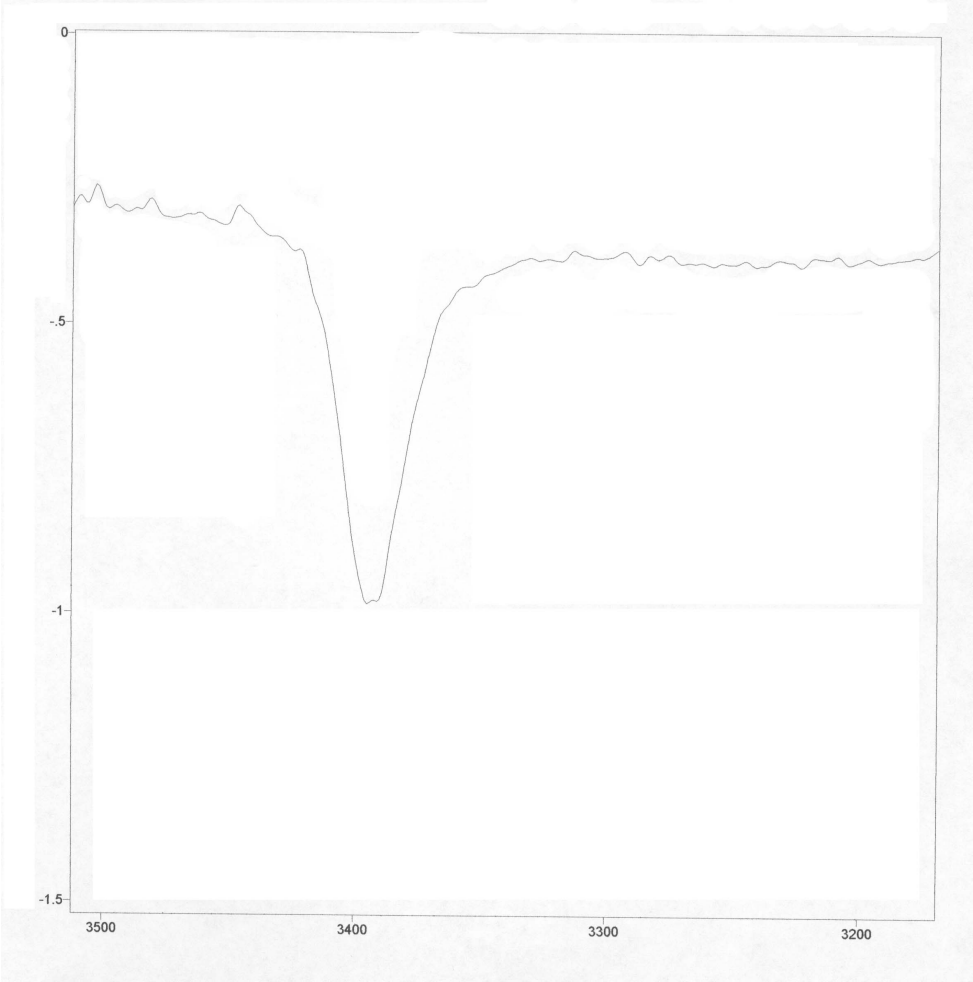

Figure 6.14 NH stretching region of the FT-IR spectra of macrocycle **105** in $CDCl_3$

6.8 ^{1}H NMR Titration Experiments of Macrocycle 105 with Tetrabutyl Ammonium (TBA) Salts and Monoalkyl Ammonium Salts

All quoted association constants were the average of three titrations. For each experiment a 1.0 mM stock solution of macrocycle **105** in $CDCl_3$ was prepared. A 0.5 mL of the stock solution was then measured into an NMR tube and its spectra recorded (500 MHz NMR, 298 K). Small aliquots of guest solution prepared in the range of 20 mM-50 mM (high concentrations were used for the TBA salts) were measured into the tube and the spectra recorded after each addition. The chemical shift of proton H-2 (Figure 6.9) or H-5 (in case when the peak of H-2 is too broad to measure) was used to generate the binding isotherm.

An iterative curve-fitting method using Origin 6.1 (Aston Scientific Ltd.) was used to generate the association constants according to the following equation:

$$y = (D_{max}/(2/(K*x-1-K*Ht+((1-K*x+K*Ht)^2+4*K*x)^0.5)+1)) \quad \text{(eq. 6.3)}$$

Where:

y: chemical shift

D_{max}: maximum chemical shift

K: binding constant

Ht: concentration of the host

x: total concentration of the guest

Typical binding isotherms are shown in Figure 6.14-6.24.

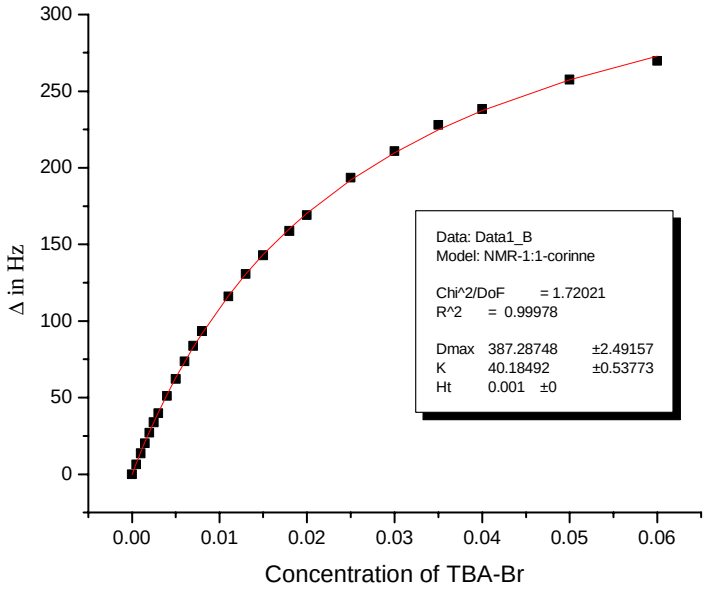

Figure 6.15 Binding isotherm for the complexation of macrocycle **105** and TBA-Br.

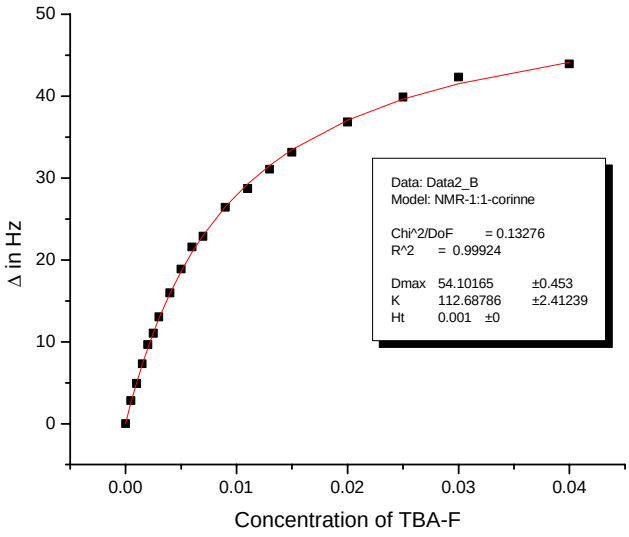

Figure 6.16 Binding isotherm for the complexation of macrocycle **105** and TBA-F.

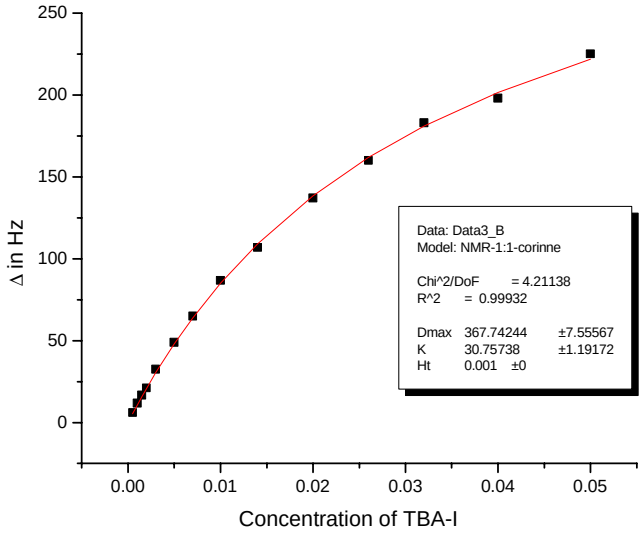

Figure 6.17 Binding isotherm for the complexation of macrocycle **105** and TBA-I.

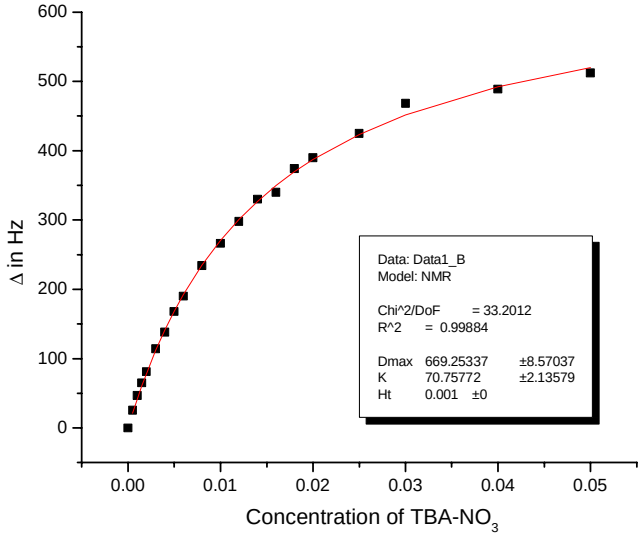

Figure 6.18 Binding isotherm for the complexation of macrocycle **105** and TBA-NO_3.

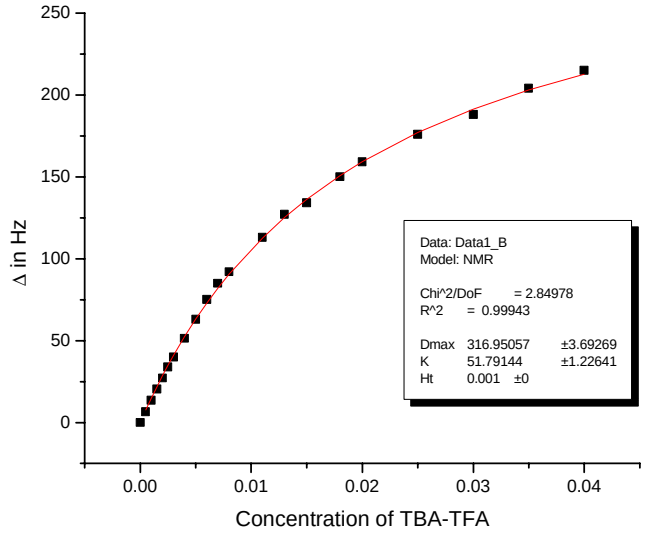

Figure 6.19 Binding isotherm for the complexation of macrocycle **105** and TBA-TFA.

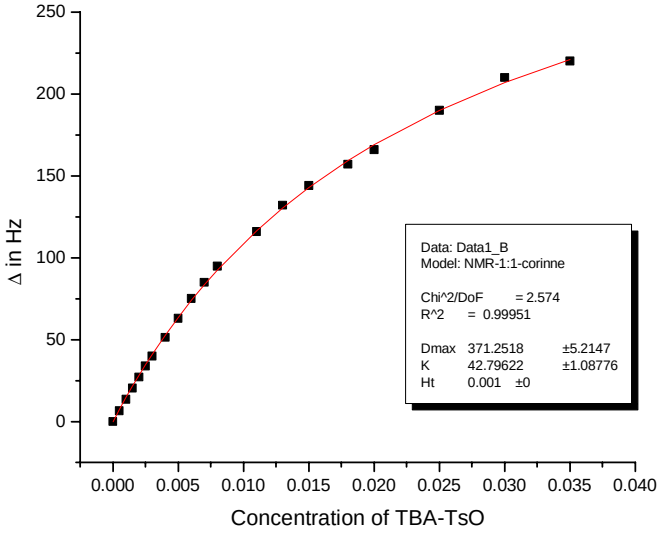

Figure 6.20 Binding isotherm for the complexation of macrocycle **105** and TBA-TsO.

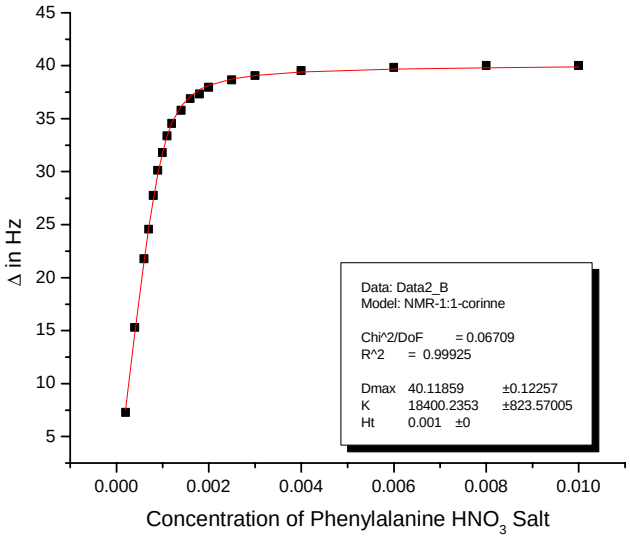

Figure 6.21 Binding isotherm for the complexation of macrocycle **105** and phenylalanine HNO_3 salt.

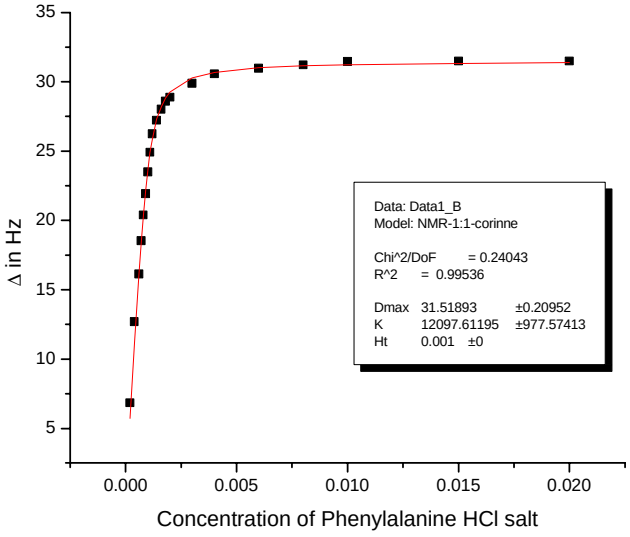

Figure 6.22 Binding isotherm for the complexation of macrocycle **105** and phenylalanine HCl salt.

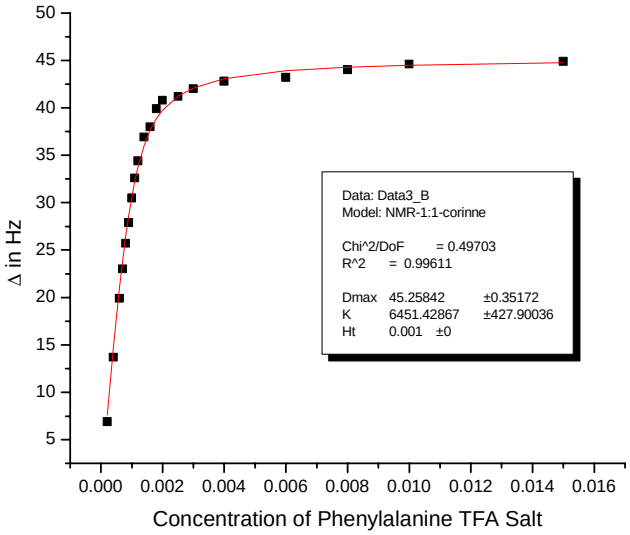

Figure 6.23 Binding isotherm for the complexation of macrocycle **105** and phenylalanine TFA salt.

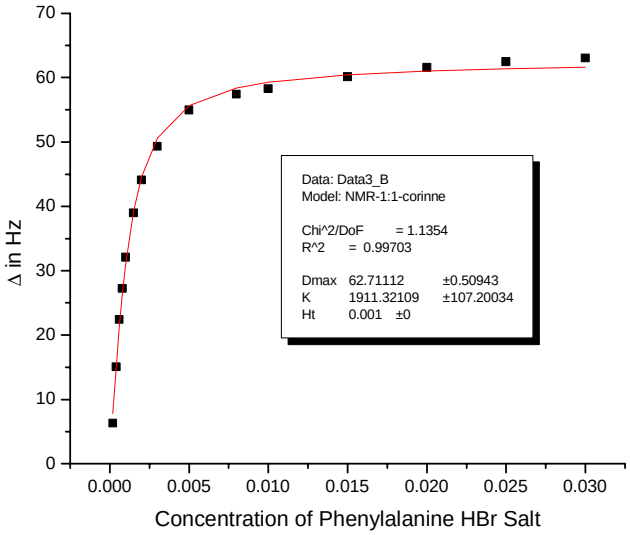

Figure 6.24 Binding isotherm for the complexation of macrocycle **105** and phenylalanine HBr salt.

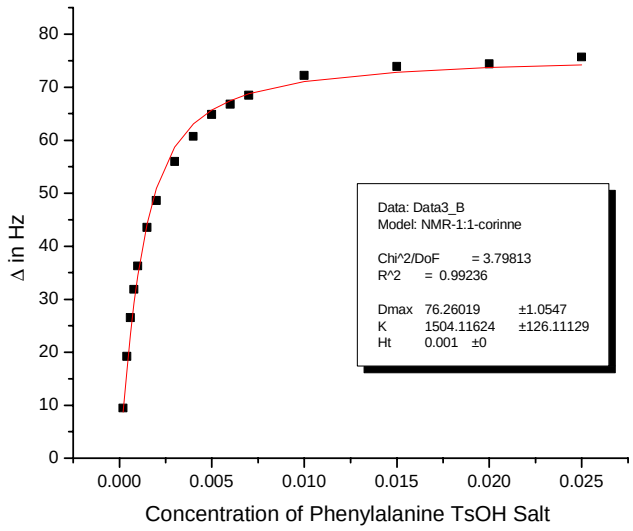

Figure 6.25 Binding isotherm for the complexation of macrocycle **105** and phenylalanine TsOH salt.

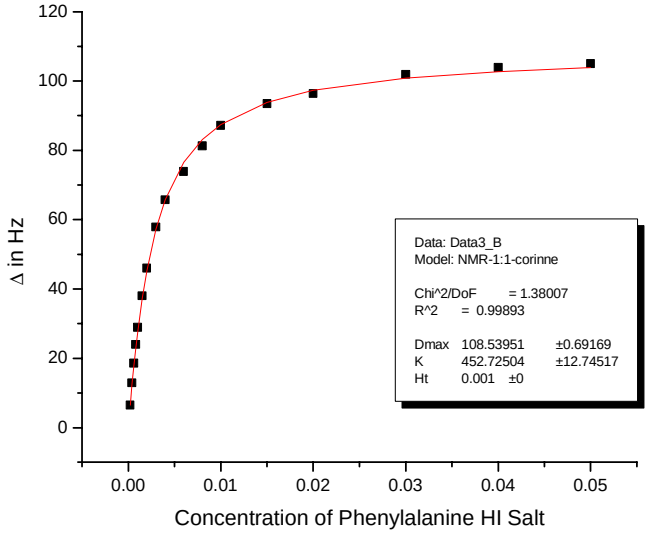

Figure 6.26 Binding isotherm for the complexation of macrocycle **105** and phenylalanine HI salt.

6.9 Job's Plots of Macrocycle 105

Stock solutions (2 mM) of macrocycle **105** and guest were prepared and were measured into NMR tubes with the following host:guest ratios: 10:0; 9:1; 8:2; 7:3; 6:4; 5:5; 4:6; 3:7; 2:8; 1:9. ^{1}H NMR spectra of all these solutions were recorded, and the chemical shifts of H-5 or H-2 were analyzed (Figure 6.25, 6.26).

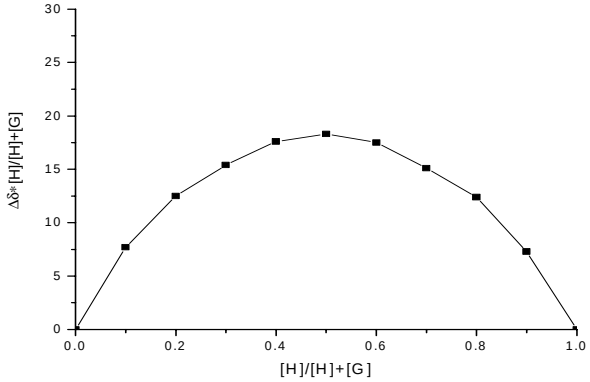

Figure 6.27 The Job's plot of macrocycle **105** with phenylalanine HBr salt, the chemical shifts of H-5 were analyzed

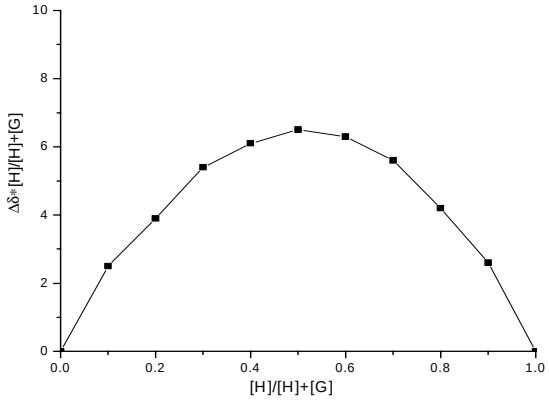

Figure 6.28 The Job's plot of macrocycle **105** with TBA-Br, the chemical shifts of H-2 were analyzed

6.10 ^{1}H NMR Titration Experiments of Macrocycles 124 and 125 with Enantiomers of Amino Acid Methyl Ester HNO_3 Salts

All quoted association constants were the average of three titrations. All titrations were carried out in 40% $CH_3CN/CDCl_3$. For each experiment a 1 mM stock solution of macrocycle was prepared. A 0.5 mL of the stock solution was then measured into an NMR tube and its spectra recorded (500 MHz NMR, 298 K). Small aliquots of guest solution prepared in the range of 20 mM - 50 mM (high concentrations were used for the weakest binding) were measured into the tube and the spectra recorded after each addition. The chemical shift of proton H-5 (Figure 6.27) was used to generate the binding isotherms.

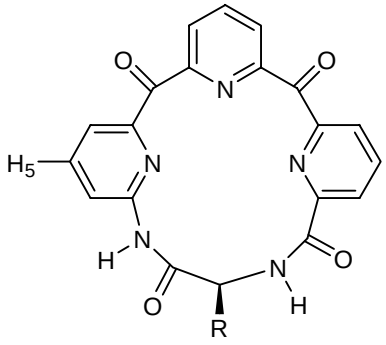

124 R = CH_2Ph
125 R = CH_2OH

Figure 6.29 The structure of macrocycle **124** and **125**.

Typical binding isotherms are shown in Figure 6.28-6.51.

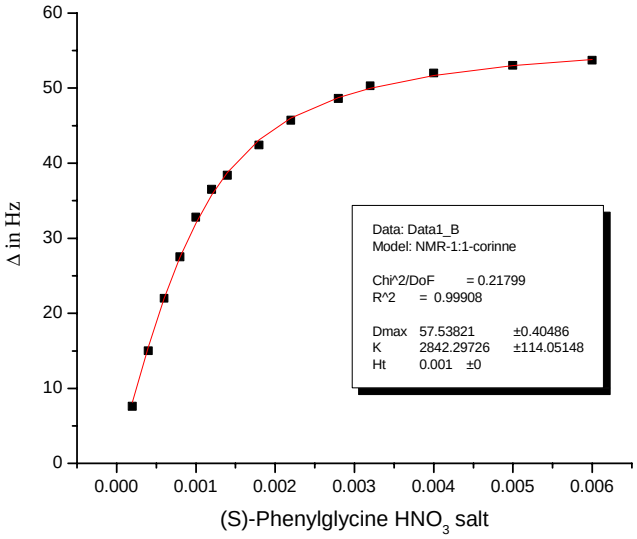

Figure 6.30 Binding isotherm for the complexation of macrocycle **124** and S-phenylglycine HNO_3 salt.

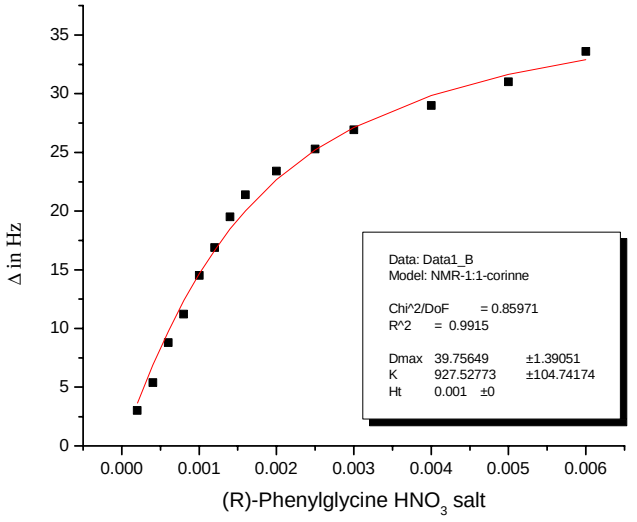

Figure 6.31 Binding isotherm for the complexation of macrocycle **124** and R-phenylglycine HNO_3 salt.

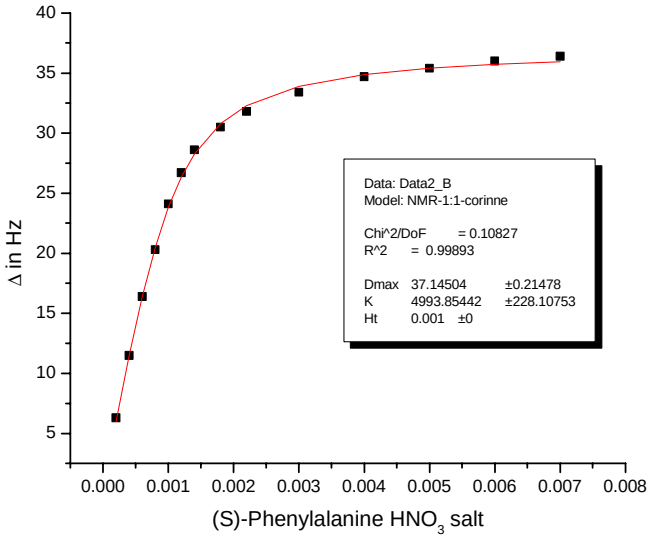

Figure 6.32 Binding isotherm for the complexation of macrocycle **124** and S-phenylalanine HNO_3 salt.

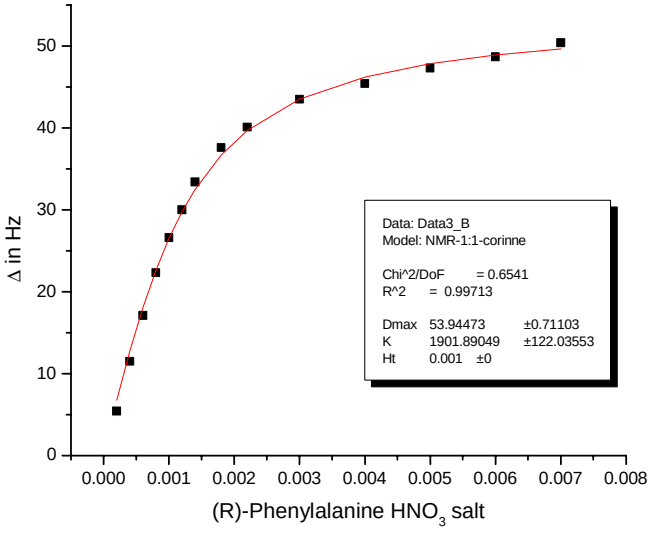

Figure 6.33 Binding isotherm for the complexation of macrocycle **124** and R-phenylalanine HNO_3 salt.

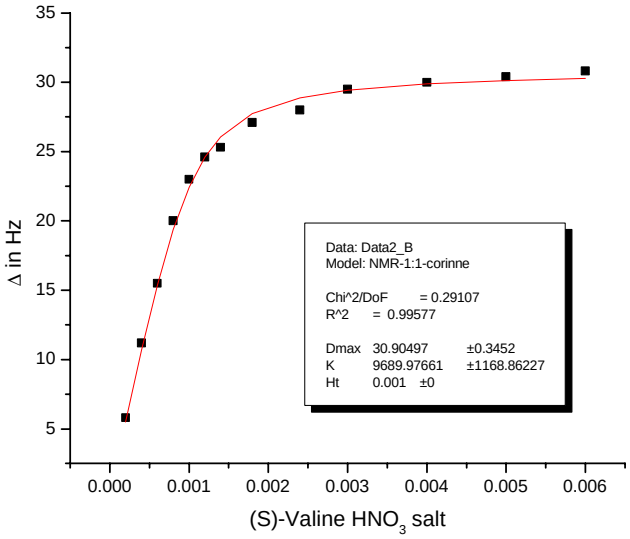

Figure 6.34 Binding isotherm for the complexation of macrocycle **124** and S-Valine HNO_3 salt.

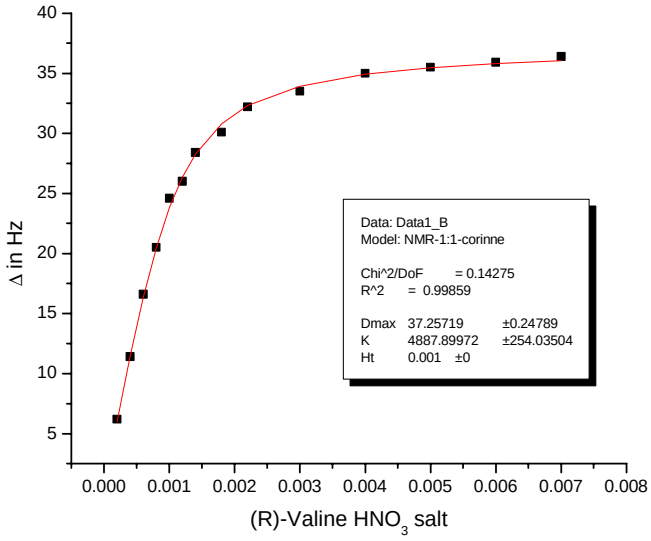

Figure6.35 Binding isotherm for the complexation of macrocycle **124** and R-Valine HNO_3 salt.

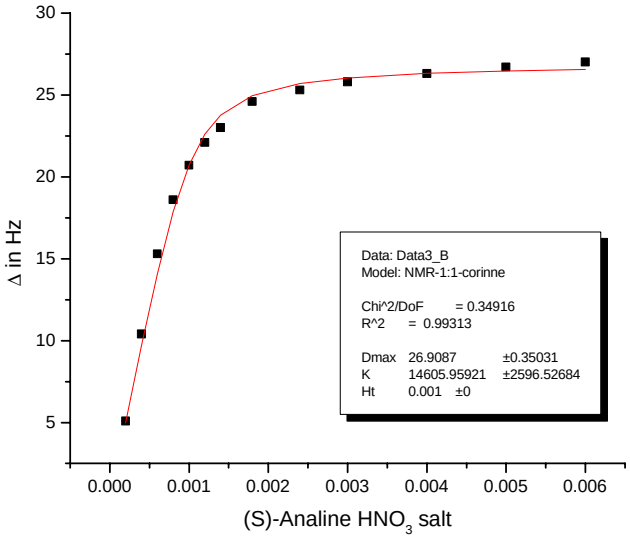

Figure 6.36 Binding isotherm for the complexation of macrocycle **124** and S-Analine HNO_3 salt.

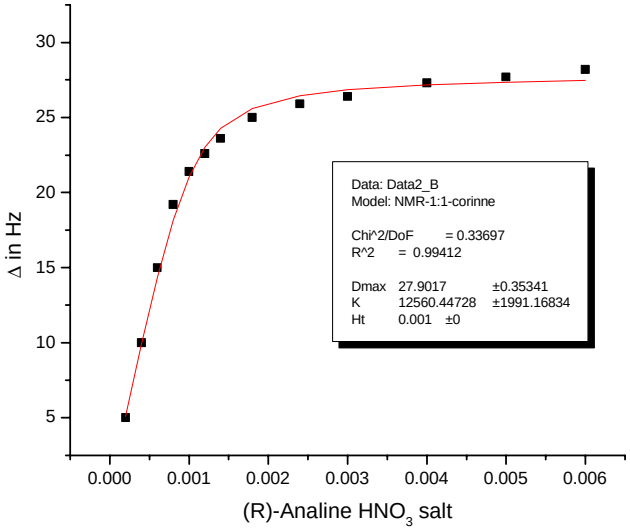

Figure 6.37 Binding isotherm for the complexation of macrocycle **124** and R-analine HNO_3 salt.

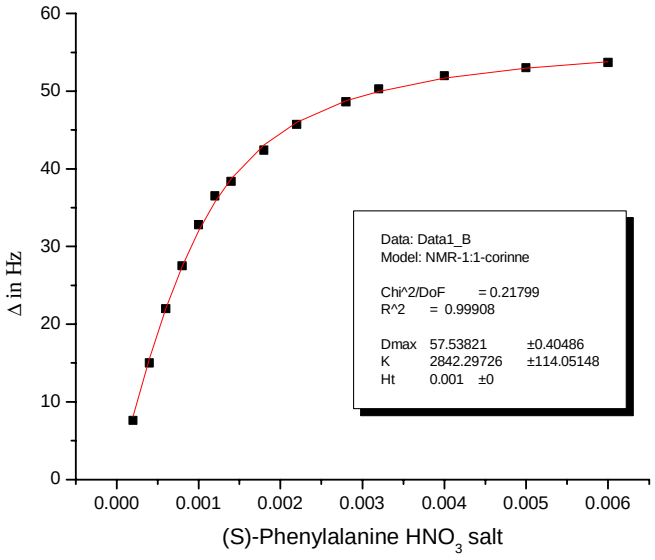

Figure 6.38 Binding isotherm for the complexation of macrocycle **125** and S-phenylalanine HNO_3 salt.

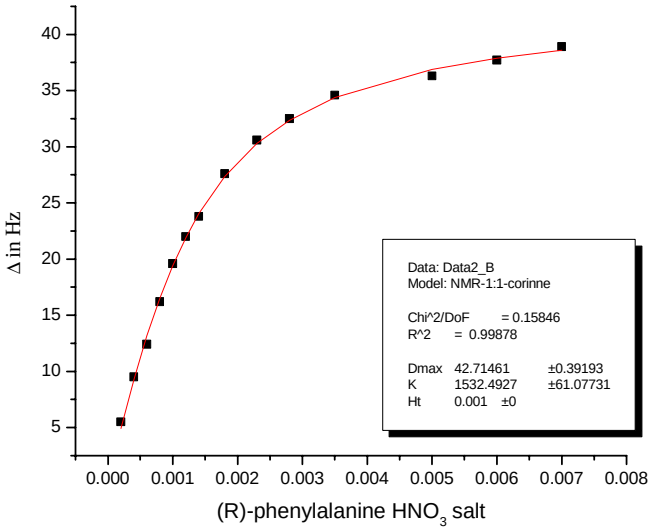

Figure 6.39 Binding isotherm for the complexation of macrocycle **125** and R-phenylalanine HNO_3 salt.

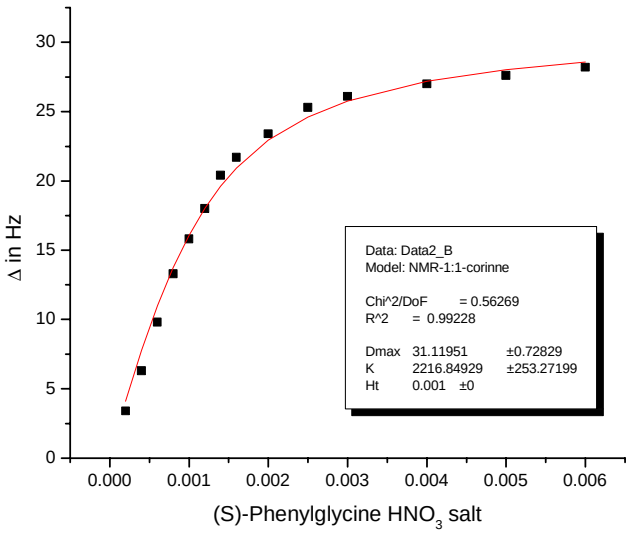

Figure 6.40 Binding isotherm for the complexation of macrocycle **125** and S-phenylglycine HNO_3 salt.

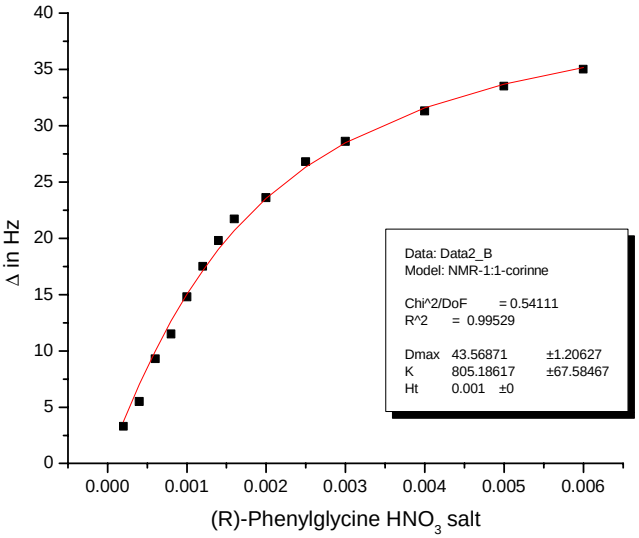

Figure 6.41 Binding isotherm for the complexation of macrocycle **125** and R-phenylglycine HNO_3 salt.

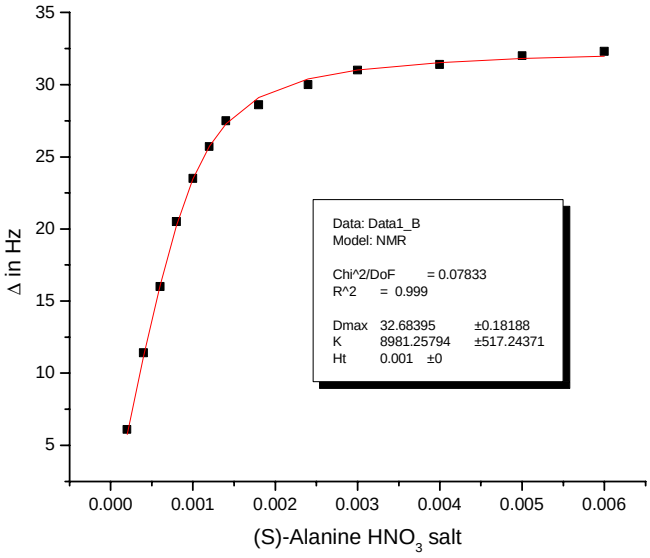

Figure 6.42 Binding isotherm for the complexation of macrocycle **125** and S-alanine HNO_3 salt.

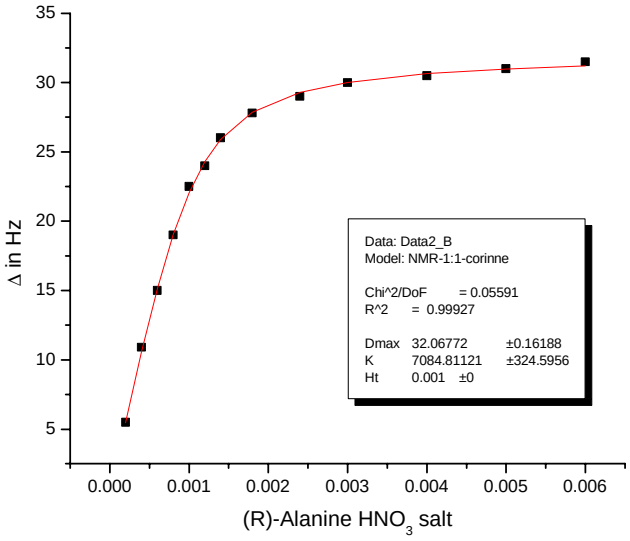

Figure 6.43 Binding isotherm for the complexation of macrocycle **125** and R-alanine HNO_3 salt.

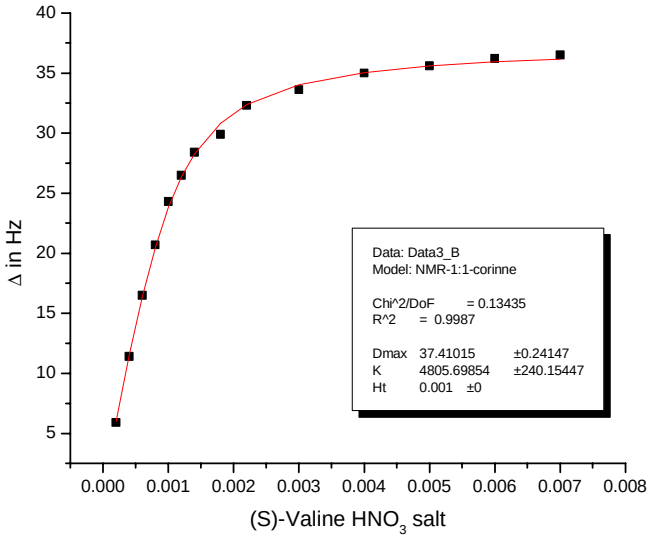

Figure 6.44 Binding isotherm for the complexation of macrocycle **125** and S-valine HNO_3 salt.

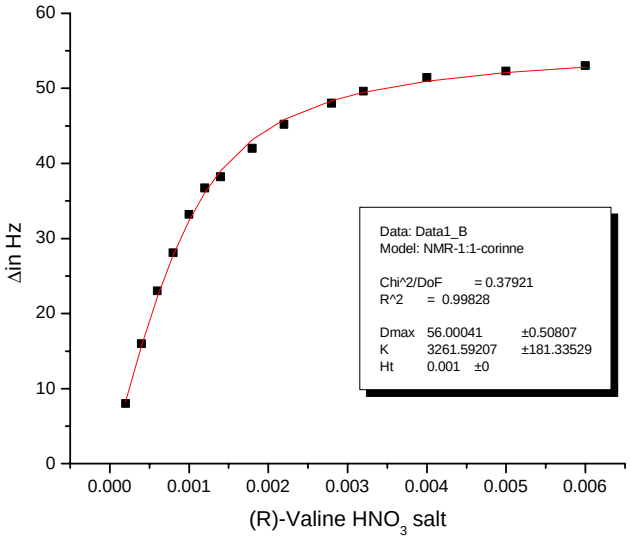

Figure 6.45 Binding isotherm for the complexation of macrocycle **125** and R-valine HNO_3 salt.

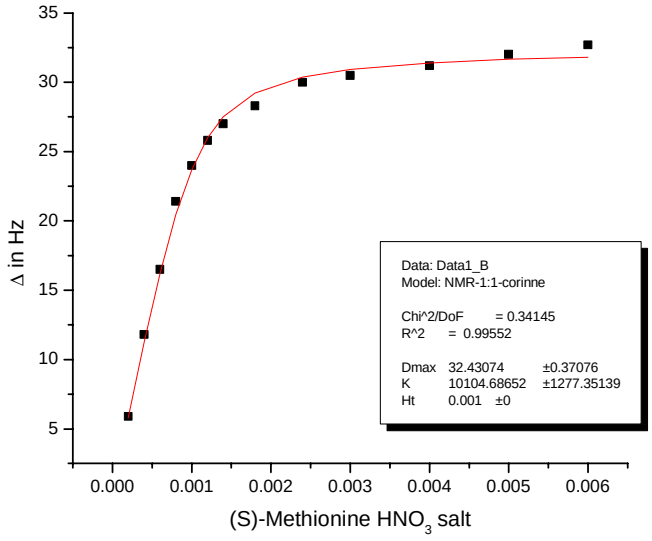

Figure 6.46 Binding isotherm for the complexation of macrocycle **124** and S-methionine HNO_3 salt.

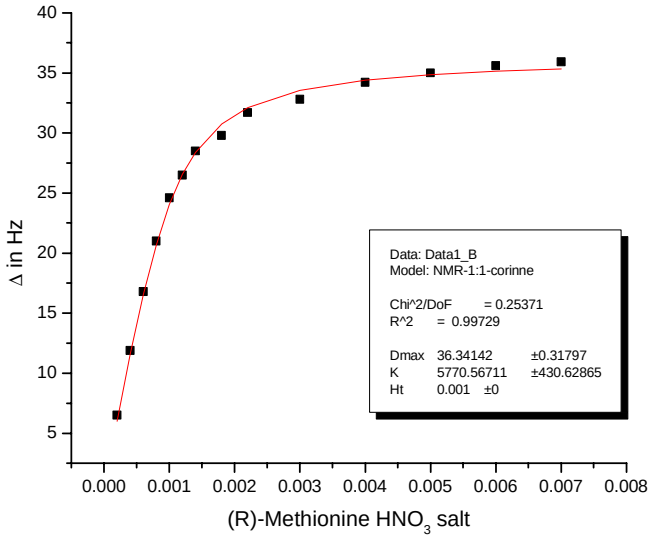

Figure 6.47 Binding isotherm for the complexation of macrocycle **124** and R-methionine HNO_3 salt.

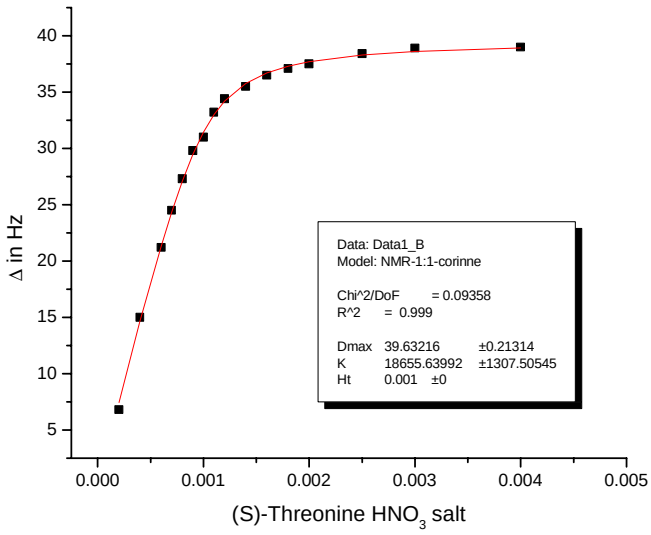

Figure 6.48 Binding isotherm for the complexation of macrocycle **124** and S-threonine HNO_3 salt.

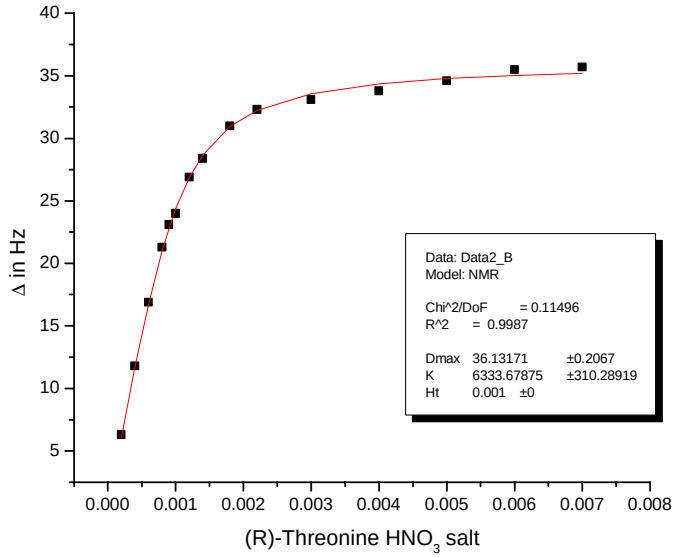

Figure 6.49 Binding isotherm for the complexation of macrocycle **124** and R-threonine HNO_3 salt.

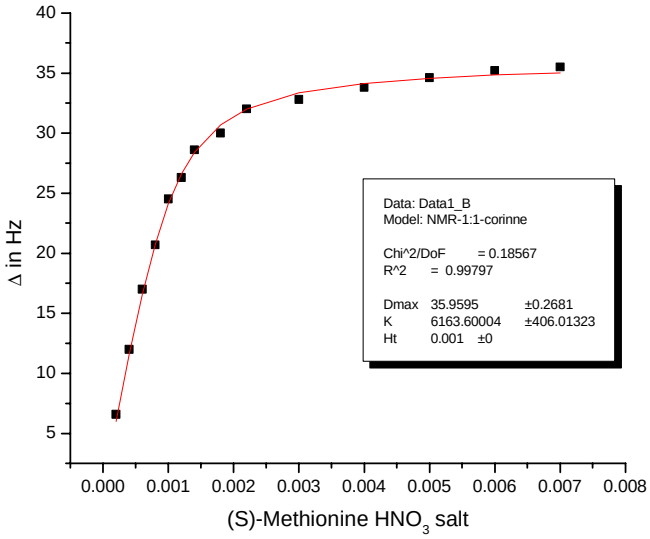

Figure 6.50 Binding isotherm for the complexation of macrocycle **125** and S-methionine HNO_3 salt.

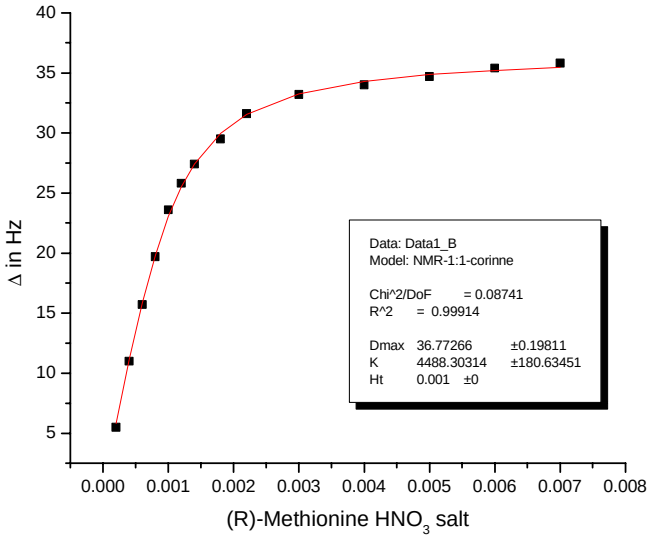

Figure 6.51 Binding isotherm for the complexation of macrocycle **125** and R-methionine HNO_3 salt.

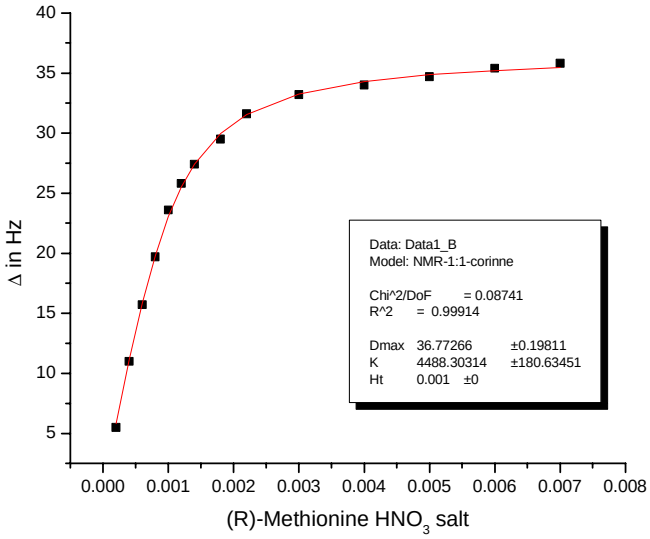

Figure 6.52 Binding isotherm for the complexation of macrocycle **125** and S-threonine HNO_3 salt.

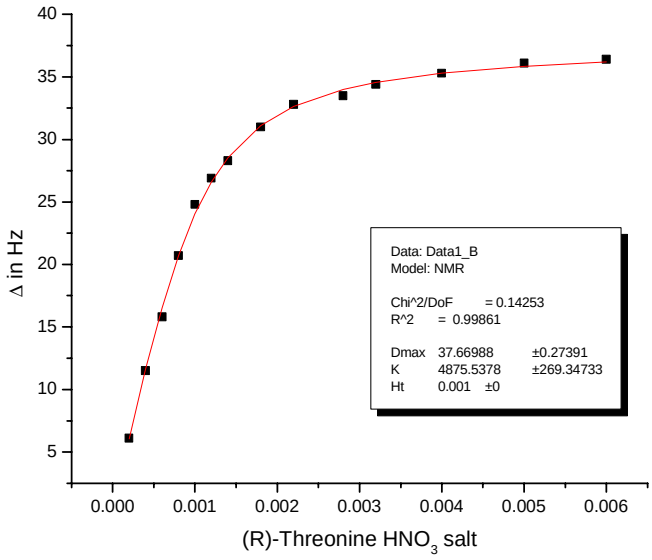

Figure 6.53 Binding isotherm for the complexation of macrocycle **125** and R-threonine HNO_3 salt.

VII References

1. Steed, J. W.; Arwood, J. L. *Supramolecular Chemistry*, John Wiley & Sons, Ltd., **2000**.

2. Lehn, J. M. *Supramolecular Chemistry: Concepts and Perspectives, WILEY-VCH,* Weinheim, **1995**.

3. Fischner, E. *Ber. Dt. Chem*. Ges. **1994**, 27, 2985-2993.

4. Lehn, J. M. *Angew. Chem., Int. Ed.* **1988**, 27, 89-91.

5. Vahrenkamp, H. *Acc. Chem. Res*. **1999**, 32, 589-596.

6. Berg, J. M.; Shi, Y. G. *Science* **1996**, 271, 1081-1085

7. Parkin, G. *Chem. Commun*. **2000**, 197-1985

8. Parkin, G. *Chem. Rev*. **2004**, 104, 699-767

9. Supuran, C. T.; Olar, R.; Marinescu, D.; Brezeanu, M. *Roumaniun Chem. Quart. Rev*. **1993**, 1, 193-209

10. Christianson, D. W.; Fierke, C. A. *Acc. Chem. Res*. **1996**, 29, 331-339

11. Xu. X.; Lajmi, A. R.; Canary, J. W. *Chem. Commun*. **1998**, 2701-2702

12. Krebs, J. F.; Ippolito, J. A.; Christianson, D.W.; Fierke, C.A. *J. Biol. Chem*. **1993**, 268, 27458-27466.

13. Dluhy, R. A.; Fierke, C. A. *Biochem.* **1993**, 32, 4496-4505.

14. Kiefer, L. L.; Fierke, C. A. *Biochem*. **1994**, 33, 15233-15240.

15. Liljas, A.; Kannan, K. K.; Bergsten, P.-C.; Waara, I.; Fridborg, K.; Strandberg, B.; Carlbom, U.; Jarup, L.; Lovgren, S.; Petef, M. *Nature New Biol*. **1972**, 235, 131-137.

16. Pocker, Y.; Stone, J. T. *J. Am. Chem. Soc*. **1965**, 87, 5497-5498.

17. Pocker, Y.; Sarkanen, S. *Adv. Enzymol*. **1987**, 47, 149-155.

18. Kiefer, L. L.; Paterno, S. A.; Fierke, C. A. *J. Am. Chem. Soc*. **1995**, 117, 6831-6837.

19. Lesburg, C. A.; Christianson, D. W. *J. Am. Chem. Soc*. **1995**, 117, 6838-6844.

20. Wooley, P. *Nature* **1975**, 258, 677-679

21. Wooley, P. *J. Am. Chem. Soc., Perkin Trans*. **1977**, 318-321

22. Tang, C. C.; Davalian, D.; Huang, P.; Breslow, R. *J. Am. Chem. Soc.* **1978**, *100*, 3918-3922.

23. Breslow, R.; Hunt, J.; Smiley, R.; Tarnowski, T., *J. Am. Chem. Soc.* **1983**, *105*, 5337-5341.

24. Slebocka-Tilk, H.; Cocho, J. L.; Frakman, Z.; Brown, R. S. *J. Am. Chem. Soc.* **1984**, *106*, 2421-2431.

25. Brown, R. S.; Huguet, J. *Can. J. Chem.* **1980**, *58*, 889-901.

26. Brown, R. S.; Curtius, N. J.; Huguet, J. *J. Am. Chem. Soc.* **1981,** *103*, 6947-6952.

27. Kimblin, C.; Murphy, J. V.; Hascall, T.; Bridgewater, M. B.; Bonanno, B. J.; Parkin, G. *Inorg. Chem.* **2000**, *39*, 967-974.

28. Bridgewater, B.; Parkin, G. *J. Am. Chem. Soc.* **2000**, *122*, 7140-7141.

29. Berquist, C.; Parkin, G. *J. Am. Chem. Soc.* **1999**, *121*, 6322-6323.

30. Alsfasser, R.; Ruf, M.; Trofimenko, S.; Vahrenkamp, H. *Chem. Ber*. **1993**, *126*, 703-710.

31. Alsfasser, R.; Powell, A.; Vahrenkamp, H. *Angew. Chem., Int. Ed. Engl*. **1990**, *29*, 898-901.

32. Looney, A.; Han, B.; Mcueil, K.; Parkin, G. *J. Am. Chem. Soc.* **1993**, *115*, 4690-4697.

33. Gelinsky, M.; Vogler, R.; Vahrenkamp, H. *Inorg. Chem*. **2003**, 41, 2560-2564.

34. Sénèque, O.; Rager, M. N.; Giorgi, M.; Reinaud, O. *J. Am. Chem.* Soc. **2000**, 122, 6183-6189

35. Sénèque, O.; Rager, M.-N.; Giorgi, M.; Reinaud, O. *J. Am. Chem. Soc.* **2001**, *123*, 8442-8443.

36. Cronin, L.; Walton, P. H. *Chem. Commun*. **2003**, 1572-1573

37. Greener, B.; Moore, M. H.; Walton, P. H. *Chem. Commun*. **1996**, 27-28.

38. Szalda, D. J.; Keene, F. R. *Inorg. Chem*. **1996**, 25, 2795-2799.

39. Hannon, M. J.; Mayers, P. C.; Taylor, P. C. *J. Chem. Soc., Parkin Trans. 1* **2000**, 1881-1887.

40. Hannon, M. J.; Mayers, P. C.; Taylor, P. C. *Angew. Chem., Int. Ed. Engl.* **2001**, *40*, 1081-1084.

41. Kimura, E. *Tetrahedron*, **1992**, 48, 6175-6217.

42. Kimura, E. *Acc. Chem. Res*. **2001**, 34, 171-179.

43. Kimura, E.; Shiota, T.; Koike, T.; Shiro, M.; Kodama, M. *J. Am. Chem. Soc*. **1990**, 112, 5805-5811.

44. Kimura, E.; Nakamura, I.; Shionoya, M.; Kodama, Y.; Ikeda, T.; Shiro, M. *J. Am. Chem. Soc*. **1994**, 116, 4764-4771.

45. Sakurai, M.; Furuki, T.; Inoue, Y. *J. Phys. Chem***. 1995,** 99**,** 17789-17794.

46. Pedersen, C. J. *J. Am. Chem. Soc*., **1967**, 89, 7017-7036.

47. Illuminati, G.; Mandolini, L.; Masci, B. *J. Am. Chem. Soc*. **1983**, 105, 555-563.

48. Mandolini, L.; Masci, B. *J. Am. Chem. Soc*. **1984**, 106, 168-174.

49. Izatt, R. M.; Terry, R. E.; Haymore, B. L.; Hanson, L. D.; Dalley, N. K.; Avondet, A. G.; Christenson, J. J. *J. Am. Chem. Soc*. **1976**, 99, 7620-7626.

50. Izatt, R. M.; Nelsen, D. P.; Rytting, J. H.; Haynoe B. L.; Christenson, J. J. *J. Am. Chem. Soc*. **1971**, 93, 1619-1623.

51. Ikeda, I.; Emmra, H.; Yamamura, S.; Okahara, M. *J. Org. Chem*. **1982**, 47, 5150-5153

52. Arnaud-Neu, F.; Spiess, B.; Schwing-Weill, M. J. *J. Am. Chem. Soc*. **1982**, 104, 5641-5645.

53. Lamb, J. D.; Izatt, R. M.; Swain, S. W.; Christenson, J. J. *J. Am. Chem. Soc.* **1980**, 102, 475-479.

54. Izatt, R. M.; Lamb, J. D.; Mass, G. E.; Asay, R. E.; Bradsaw, J. S., Christenson, J. J. *J. Am. Chem. Soc*. **1977**, 99, 2365-2366.

55. Izatt, R. M.; Rytting, J. H.; Nelsen, D. P.; Haynore B. L.; Christenson, J. J. *Science* **1969**, 164, 443-444.

56. Ishizu. K.; Kohana, H.; Mukai, K. *Chem. Lett*. **1978**, 227-230.

57. Frensdorf, H. K. *J. Am. Chem. Soc*. **1971**, 93, 600-606.

58. Clarke, P.; Gulbis, J. M.; Lincoln, S. F.; Tiekink, E. R. T. *Inorg. Chem*. **1992**, 31, 3398-3404.

59. Clarke, P.; Lincoln, S. F.; Tiekink, E. R. T. *Inorg. Chem*. **1991**, 30, 2747-2751.

60. Salmon, M.; Hefter, G. T. *Pure Appl. Chem*. **1993**, 65, 1533-1540

61. Lincoln, S. F.; Stenphens, A. K. W. *Inrog. Chem*. **1992**, 31, 5067-5071

62. Benini, A.; Bianchi, A.; Bazzocalupi, C.; Ciampolini, M.; Dapporto, P.; Fusi, V.; Micheloni, M.; Nardi, N.; Paoli, P.; Valtancoli, B. *J. Chem. Soc., Perkin Trans. 2* **1993**, 115-120.

63. Benini, A.; Bianchi, A.; Bazzocalupi, C.; Ciampolini, M.; Dapporto, P.; Fusi, V.; Micheloni, M.; Nardi, N.; Paoli, P.; Valtancoli, B. *J. Chem. Soc., Perkin Trans. 2* **1993**, 715-720.

64. Benini, A.; Bianchi, A.; Chimichi, S.; Ciampolini, M.; Dapporto, P.; Carcia, E.; Micheloni, M.; Nardi, N.; Paoli, P.; Valtancoli, B. *Inorg. Chem*. **1991**, 30, 3687-3691.

65. Daley, N. K.; Jiang, W.; Wu, G.; Bradshaw, J. S.; An, H.; Krakowiak, K. E.; Izatt, R. M. *J. Inclusion Phenom. Mol. Recogn. Chem*. **1992**, 12, 333-339.

66. Krakowiak, K. E.; Bradshaw, J. S.; Dalley, N. K.; Zhu, G.; Yi, G.; Curtis, J. C.; Li, D.; Izatt, R. M. *J. Org. Chem*. **1992**, 57, 3166-3173.

67. An, H.; Bradshaw, J. S.; Krakowiak, K. E.; Tarbet, B. J.; Dalley, N. K.; Kou, X.; Zhu, G.; Izatt, R. M. *J. Org. Chem*. **1993**, 58, 7694-7697

68. An, H.; Bradshaw, J. S.; Krakowiak, K. E.; Dalley, N. K.; Kou, X.; Zhu, G.; Izatt, R. M. *J. Org. Chem*. **1992**, 57, 4958-5005.

69. Bott, S. G.; Coleman, A. W.; Atwood, J. L. *J. Am. Chem. Soc*. **1988**, 110, 60-611

70. Araki, K.; Iwamoto, K.; Shinkai, S.; Matsnda, T. *Bull. Chem. Soc. Jpn*. **1990**, 63, 3480-3485.

71. Arnaud-Neu, F.; Barrett, G.; Harris, S. J.; Owens, M.; Mckervey, M. A.; Schwing-Weill, M. J.; Schwinte, P. *Inorg. Chem*. **1993**, 32, 2644-2650.

72. Barrett, G.; Mckervey, M. A.; Malone, J. F.; Walker, A.; Arnaud-Neu, F.; Guerra, L.; Scwing-Weill, M. J.; Gutche, C. D.; Stewart, D. R. *J. Chem. Soc., Perkin Trans. 2* **1993**, 1475-1479.

73. Arnaud-Neu, F.; Gremin, S.; Cunningham, D.; Harris, S. J.; Mcardle, P.; mckervey, M. A.; Mcmanus, M.; Schwing-Weill, M. J.; Ziat, K. *J. Inclusion, Phenom. Mol. Recogn. Chem*. **1991**, 10, 329-39.

74. Seangprasertkij, R.; Asfari, Z.; Arnaud-Neu, F. Weiss, J.; Vicens, J. *J. Inclusion Phenom. Mol. Recogn. Chem*. **1993**, 14, 141-147.

75. Schimidtchen, F. P.; Berger, M. *Chem. Rev*. **1997**, 97, 1609-1646.

76. Choi, K.; Hamilton, A. D. *Coord. Chem*. *Rev*. **2003**, 240, 101-110.

77. Schneider, H. J.; Schneider, U. *J. Inclu. Phenom. Mol. Recogn. Chem*. **1994**, 19, 67-83.

78. Hartley, J. H.; James, T. D.; Ward, C. J. *J. Chem. Soc., Perkin Trans. 1* **2000**, 3155-3184

79. Antonisse, M. G.; Reinhoudt, D. N. *Chem. Commun*. **1998**, 443-444.

80. Park, C. H.; Simmons, H. E. *J. Am. Chem. Soc*. **1968**, 90, 2429-2430.

81. Park, C. H.; Simmons, H. E. *J. Am. Chem. Soc*. **1968**, 90, 2431-2432.

82. Kise, N.; Oike, H.; Okazaki, E.; Yoshimoto, M.; Shono, T. *J. Org. Chem*. **1995**, 60, 3984-3988.

83. Searle, M. S.; Westwell, M. S.; Williams, D. H. *J. Chem. Soc., Perkin Trans. 2*, **1995**, 141-146.

84. Dietrich, B.; Hosseini, M. W.; Lehn, J. M.; Sessions, R. B. *Helv. Chim. Acta* **1983**, 66, 1262-1265.

85. Graf. E.; Lehn, J. M. *J. Am. Chem. Soc*. **1976**, 98, 6403-6406.

86. Graf. E.; Lehn, J. M. *J. Am. Chem. Soc*. **1975**, 97, 5022-5023

87. Choi, K.; Hamlton, A. D. *J. Am. Chem. Soc*. **2001**, 123, 2456-2464.

88. Kang, S. O.; Linares, J. M.; Powell, D.; Vandervelde, D.; Bowman-James, K. *J. Am. Chem. Soc*. **2003**, 125, 10152-10153.

89. Kubik, S. *J. Am. Chem. Soc*. **1999**, 121, 5846-5852.

90. Kubik, S.; Kirchner, R.; Nolting D.; Seiel, J. *J. Am. Chem. Soc*. **2002**, 124, 12752-12756.

91. Bucher, C.; Zimmerman, R. S.; Lynch, V.; Kral, V.; Sesslor, J. L. *J. Am. Chem. Soc*. **2001**, 123, 9716-9717..

92. Sessler, J. L.; An, D.; Cho, W.; Lynch, V. *Angew. Chem., Int. Ed. Engl*. **2003**, 42, 2278-2281.

93. Lee, C. H.; Sessler, J. L. *J. Am. Chem. Soc*. **2003**, 125, 7301-7306.

94. Gunnlaugasson, T.; Davis, A. P. *Chem. Commun*. **2001**, 2566-2557.

95. Lee, D. H.; Lee, H. Y.; Lee, K. H.; Hon, J. I. *Chem. Commun*. **2001**, 1188-1189.

96. Lee, K. H.; Hong, J. I. *Tetrahedral Lett*. **2002**, 41, 6083-6086.

97. Beer, P. D.; Gale, P. A. *Angew. Chem., Int. Ed*. **2001**, 40, 486-516.

98. Kirkovits, G. J.; Shriver, J. A.; Gale, P. A.; Sessler, J. L. *J. Inclusion Phenom. Macrocyclic Chem*. **2001**, 41, 69-75;

99. Gale, P. A. *Coord. Chem. Rev*. **2003**, 240, 191-221.

100. Reetz, M. T. "*Simultaneous Binding of Cations and Anions*" in *Comprehensive Supramolecular Chemistry*, ed. Atwood, J. L.; Davies, J. E. D.; Mcnicole, D. D.; Vogtle F., Pergamon, Oxford, **1996**, Vol. 2, pp 553-562.

101. Beer, P. D.; Cooper, J. B. "*Calixarence Based Anion Receptors*" in *Calixarences in Action*, ed. L. Mandolini and R. Ungaro, Imperial College Press, London, **2000**, pp 111-143.

102. Mahoney, J. M.; Reetz, M. T.; Niemeyer, C. M.; Harms K. *Angew. Chem., Int. Ed*. **1991**, 30, 1472-1474

103. Reetz, M. T.; Johnson, B. M.; Harms, K. *Tetrahedron Lett*. **1994**, 35, 2525-2527.

104. Beer, P. D.; Dent, S. W. *Chem. Comm*. **1998**, 825-826.

105. Beer, P. D.; Hopkins, P. K.; Mckinney, J. D. *Chem. Comm*. **1999**, 1253-1254.

106. Cooper, J. B.; Drew, M. G. B.; Beer, P. D. *J. Chem. Soc., Dalton Trans*. **2001**, 392-401.

107. Beer, P. D.; Drew, M. G.; Knubley, R. J.; Ogden, M. I. *J. Am. Chem. Soc., Dalton Trans*. **1995**, 3117-3120.

108. Schreeder, J.; Duyuhoven, J. P.; Reinhoudt, D. N. *Angew. Chem., Int. Ed. Engl*. **1996**, 35, 1090-1092.

109. Webber, P. R. A.; Beer, P. D. *J. Chem. Soc., Dalton Trans*. **2003**, 2249-2252.

110. Deetz, M. J.; Shang, M.; Smith, B. D. *J. Am. Chem. Soc*. **2000**, 122**,** 6201-6207.

111. Beatty, A. M.; Smith, B. D. *J. Am. Chem. Soc*. **2001**, 123, 5847-5848.

112. Echavarren, A.; Galan, A.; Mendoza, J.; Salmeron, A.; Lehn, J. M. *J. Am. Chem. Soc*. **1989**, 111, 4994-4998.

113. Galan, A.; Andreu, D.; Echavarren, A.; Prados, P.; Mendoza, J. *J. Am. Chem. Soc*. **1992**, 114, 1151-1152.

114. Sessler, J. C.; Andrievsky, A. *Chem. Commun*. **1996**, 1119-1120.

115. Kral, V.; Andrievsky, A.; Sessler, J. C. *J. Am. Chem. Soc*. **1995**, 117, 2953-2960.

116. Kral, V.; Andrievsky, A.; Sessler, J. C. *Chem. Commun*. **1995**, 2349-2350.

117. Kubik, S.; Goddard, R. *J. Org. Chem*. **1999**, 64, 9475-9486.

118. Kubik, S.; Goddard, R.; *Chem. Comm*. **2000**, 633-634.

119. Böhmer, V. A.; Cort, D.; Mandolini, L. *J. Org. Chem*. **2001**, 66, 1900-1908.

120. Mansikkamaki, H.; Nissinen, M.; Rissanen, K. *Chem. Comm*. **2002**, 1902-1903.

121. Shivanyuk, A.; Paulus, E. F.; Rissanen, K.; Kolehmainen, E.; Bohmer, V. *Chem. Eur. J*. **2001**, 7, 1994-1997.

122. Cametti, M.; Nissinen, M.; Dalla Cort, A.; Luigi, L.; Rissanen, K. *Chem. Comm*. **2003**, 2420-2421.

123. Kubik, S. *J. Am. Chem. Soc*. **1999**, 121, 5846-5855.

124. Bartoli, S.; Roelens, S. *J. Am. Chem. Soc*. **1999**, 121, 11908-11909.

125. Zhang, X.; Bradshaw, J. S.; Izatt, R. M. *Chem. Rev*. **1997**, 97, 3313-3361.

126. Webb, T. H.; Wilex, C. S. *Chem. Soc. Rev*. **1993**, 382-395.

127. Pu, L. *Chem. Rev*. **2004**, 104, 1687-1716.

128. Pernia, G. J.; Kilburn, J. D.; Rowley, M. *Chem. Commun*. **1995**, 305-306.

129. Bang, E.; Jung, J. W.; Lee, W.; Lee, D. W.; Lee, W. *J. Chem. Soc., Perkin Trans. 2* **2001**, 1685-1692.

130. Gasparrini, F.; Misiti, D.; Pierini, M.; Villani, C. *Org. Lett*. **2002**, 4, 3993-3996.

131. Metzger, A.; Gloe, K.; Stephen, H.; Schmidtchen, F. *J. Org. Chem*. **1996**, 61, 2051-2055

132. Hayashida, O.; Sebo, L.; Rebek, J. Jr. *J. Org. Chem*. **2002**, 67, 8291-8298.

133. Rivesa, J. M.; Martin, T.; Rebek, J. Jr. *J. Am. Chem. Soc*. **2001**, 123, 5213-5220.

134. Ito, K.; Noike, M.; Kida, A.; Ohba, Y. *J. Org. Chem*. **2002**, 67, 7519-7522.

135. Heintichs, G.; Vial, L.; Lacour, J.; Kubik, S. *Chem. Commun*. **2003**, 1252-1253.

136. Breccia, P.; Gool, M. V.; Fernandez, R.; Santamaria, S.; Gago, F.; Prados, P.; Mendoza, J. *J. Am. Chem. Soc*. **2003**, 125, 8270-8284.

137. Botta, B.; Botta, M.; Filippi, A.; Tafi, A.; Monache, G. D.; Speranza, M. *J. Am. Chem. Soc*. **2002**, 124, 7658-7659.

138. Grawe, T.; Schroder, T.; Finocchiaro, P.; Conaiglio, G.; Failla, S. *Org. Lett.* **2001**, 3, 1597-1600.

139. Hiroshi, T.; Uenishi, J.; Kanatani, T.; Itoh, H.; Yonemitsu, O. *Chem, Commun*. **1996**, 477-478.

140. You, J. S.; Yu, X. Q.; Zhang, G. C.; Xiang, Q. X.; Lam, J. B.; Xie, R. G. *Chem. Commun*. **2001**, 1816-1817.

141. Hellier, P. C.; Bradshaw, J. S.; Young, J. J.; Zhang, X.; Izatt, R. M. *J. Org. Chem*. **1996**, 61, 7270-7275.

142. Bradshaw, J. S.; Huszthy, P.; Mcdaniel, C. W.; Zhu, C. Y.; Dalley, N. K.; Izatt, R. M. *J. Org. Chem*. **1990**, 55, 3129-3137.

143. Araki, K.; Inada, K.; Sjinkai, S. *Angew. Chem., Int. Ed. Engl*. **1996**, 108, 92-94.

144. Kyba, E. P.; Siegel, M. G.; Sousa, L. R.; Sogah, G. D. Y.; Cram, D. J. *J. Am. Chem. Soc*. **1973**, 95, 2691-2695.

145. Cram, D. J.; Helgeson, R. C.; Peacock, S. C.; Kaplan, C. J.; Domeier, L. A.; Moreau, P.; Koga, K.; Mayer, J. M.; Chao, Y.; Siegel, M. G.; Hoffman, D. H.; Sogah, G. D. Y. *J. Org. Chem*. **1978**, 43, 1930-1936.

146. Newcomb, M.; Gokel, G. W.; Cram, D. J. *J. Am. Chem. Soc*. **1974**, 96, 6810-6811.

147. Dejong, F.; Siegel, M. G.; Cram, D. J. *Chem. Commun*. **1975**, 51-52.

148. Helgeson, R. C.; Weisman, G. R.; Toner, J. L.; Tarnowski, T. L.; Chaw, Y.; Mayer, J. M.; Cram, D. J. *J. Am. Chem. Soc*. **1979**, 101, 4928-4933.

149. Dietrich, B.; Lehn, J. M.; Simon, J. *Angew. Chem., Int. Ed. Engl*. **1974**, 13, 406-409.

150. Curtis, W. D.; Kin, R. M.; Stoddart, J. F.; Jones, G. H. *Chem. Commun*. **1976**, 284-285.

151. Wong, W. L.; Huang, K. H.; Teng, P. F.; Lee, C. S.; Kwong, H. L. *Chem. Commun*. **2004**, 384-385.

152. Kim, S. G.; Kim, K. H.; Kim, Y. K.; Shin, S. K.; Ahn, K. H. *J. Am. Chem. Soc*. **2003**, 125, 13819-3824.

153. Fitamaurice, R.; Kyne, G. M.; Douheret, D.; Kilburn, J. D. *J. Chem. Soc., Parkin Trans. 1* **2002**, 841-864.

154. Linton, B.; Hamilton, A. D. *Tetrahedron* **1999**, 55, 6027-6035.

155. Lawless, L. J.; Brackburn, A. G.; Ayling, A.; Perez-Payan, N.; Davis, A. P. *J. Chem. Soc. Perkin Trans. 1* **2001**, 1329-1341.

156. Siracusa, L.; Hurley, F. M.; Dresen, S.; Lawless, L.; Perez-Payan, N.; Davis, A. P. *Org. Lett*. **2002**, 4, 4639-4642.

157. Davis, A. P.; Lawless, L. J. *Chem. Commun*. **1999**, 9-10.

158. Schmuck C. *Chem. Commun*. **1999**, 843-844.

159. Schmuck, C. *Chem. Eur. J*. **2000**, 6, 709-124.

160. Kyne, G. M.; Light, M. E.; Hursthouse, M. B.; Mendoza, J.; Kilburn, J. D. *J. Chem. Soc., Perkin Trans. 1* **2001**, 1258-1263.

161. Rossi, S.; Kyne, G. M.; Turner, D. L.; Wells, N. J.; Kilburn, J. D. *Angew. Chem., Int. Ed. Engl*. **2002**, 41, 4233-4236.

162. Metzger, A.; Gloe, K.; Stephen, H.; Schmidtchen, F. P. *J. Org. Chem*. **1996**, 61, 2051-2055.

163. Escuder, B.; Rowan, A. E.; Feiters, M. C.; Nolte, R. J. M. *Tetrahedron* **2004**, 60, 291-300.

164. Li, X.; Gibb, C. L. D.; Kuebel, M. E.; Gibb, B. C. *Tetrahedron* **2001**, 57, 1175-1182.

165. Wilbaut, J. P.; de Jonge, A. P.; Van der Voot, H. G. P.; Otto, H. L. *Recl. Trav. Chim. Pays-Bas*, **1951**, 70, 1054-1060.

166. Bertini, I.; Luchinat, C. *Acc. Chem. Res*. **1983**, 272-279.

167. Chin, J.; Banaszczyk, M. *J. Am. Chem. Soc*. **1989**, 111, 2724-2725.

168. Chin, J.; Jubian, V. *Chem. Commun*. **1989**, 839-840.

169. Panda, P. K.; Lee, C.-H. *Org. Lett*. **2004**, 6, 671-674.

170. Shukla, R.; Kida, T.; Smith, B. D. *Org. Lett*. **2000**, 2, 3099-3102.

171. Shi, X.; Fettinger, J. C.; Davis, J. T. *Angew. Chem., Int. Ed*. **2001**, 40, 2827-2831.

172. Tumcharern,G.; Tuntulani, T.; Coles,S. J.; Hursthouse, M. B.; Kilburn, J. D. *Org. Lett*. **2003**, 5, 4971-4974.

173. Barboiu,M. D.; Hovnanian, N. D.; Luca, C.; Cot, L. *Tetrahedron* **1999**, 55, 9221-9232.

174. Schmidtchen, F. P. *J. Org. Chem*. **1986**, 51, 5161-5168.

175. Metzger, A.; Gloe, K.; Stephan, H.; Schmidtchen, F. P. *J. Org. Chem*. **1996**, 61, 2051-2055.

176. Evans, A. J.; Beer, P. D. *J. Chem. Soc., Dalton Trans*. **2003**, 4451-4456.

177. Savage, P. B.; Holmgren, S. K.; Gellman, S. H. *J. Am. Chem. Soc*. **1994**, 116, 4069-4070;

178. Reetz, M. T.; Niemeyer, C. M.; Harms, K. *Angew. Chem., Int. Ed*. **1991**, 30, 1474-1476;

179. Mahoney, J. M.; Davis, J. P.; Beatty, A. M.; Smith, B. D. *J. Org. Chem*., **2003**, 68, 9819-9820.

180. Kubo, Y.; Maeda, S.; Tokita, S.; Kubo, M. *Nature* **1996**, 382, 522-524.

181. Murakami, Y.; Kikuchi, J.-I.; Hisaeda, Y.; Hayashida, O. *Chem. Rev*. **1996**, 96, 721-758.

182. Tsukube, H.; Uenishi, J.-I.; Kanatani, T.; Itoh, H.; Yonemitsu, O. *Chem. Commun*. **1996**, 477-478.

183. You, J.-S.; Yu, X.-Q.; Zhang, G.-L.; Xiang, Q.-X.; Lan, J.-B.; Xie, R.-G. *Chem. Commun*. **2001**, 1816-1817.

184. Bang, E.; Jung, J.-W.; Lee, W.; Lee, D. W. ; Lee, W. *J. Chem. Soc., Perkin Trans. 2* **2001**, 1685-1692.

185. Grawe, T.; Schrader, T.; Finocchiaro, P.; Consiglio, G.; Failla, S. *Org. Lett*. **2001**, 3, 1597-1600.

186. Hirose, K.; Ogasahara, K.; Nishioka, K.; Tobe, Y.; Naemura, K. *J. Chem. Soc., Perkin Trans. 2* **2000**, 1984-1993.

187. Oliva, A. I.; Simón, L.; Muñiz, F. M.; Sanz, F.; Morán, J. R. *Org. Lett*, **2004**, 6, 1155-1157.

188. Oliva, A. I.; Simón, L.; Hernández, J. V.; Muñiz, F. M.; Lithgow, A.; Jiménez, A.; Morán, J. R. *J. Chem. Soc., Perkin Trans. 2* **2002**, 1050-1055.

189. Sessler, J. L.; Andrievsky, A.; Král, V.; Lynch, V. *J. Am. Chem. Soc*. **1997**, 119, 9385-9386.

190. Newkome, G. R.; Nayak, A.; Sauer, J. D.; Mattschei, P. K.; Watkins, S. F.; Fronczek, F.; Benton, W. H. *J. Org. Chem*., **1979**, 44, 3816-3822.

VITA

The author was born in Zhejiang, China. In 1989, he began his undergraduate study in chemistry at Ningbo University, where he received a B.S. degree in 1993. He continued his graduate study in physical chemistry at Lanzhou Institute of Chemical Physics, Chinese Academy of Sciences and earned a M.S. degree in 1996. After graduate, he worked as a senior scientist at Shanghai Petrochemical Co. In 1999, he came to US to pursue his Ph.D. degree in organic chemistry at the University of New Orleans, under the supervision of Professor Bruce C. Gibb.